

# Using Wireless Communications To Enable Decentralized Analysis And Control of Smart Distribution Systems

by

Michael Ibrahim

A thesis  
presented to the University of Waterloo  
in fulfillment of the  
thesis requirement for the degree of  
Doctor of Philosophy  
in  
Electrical and Computer Engineering

Waterloo, Ontario, Canada, 2014

© Michael Ibrahim 2014



I hereby declare that I am the sole author of this thesis. This is a true copy of the thesis, including any required final revisions, as accepted by my examiners.

I understand that my thesis may be made electronically available to the public.

Michael Ibrahim



## Abstract

The smart grid is a multidisciplinary approach that aims to revolutionize the whole electricity supply chain including generation, transmission and distribution systems in order to overcome the multiple challenges currently facing the electric power grid.

The smart grid could be seen as a modern electrical power grid in which information as well as electricity flows among all nodes in the system, information is continuously collected, processed and hence used to control and coordinate the different system components such as distributed generation (DG) units, capacitor banks, voltage regulating transformers, etc. Therefore distributed intelligence and two-way data communication links are essential components in implementing the smart grid vision.

There are numerous research efforts that focus on implementing the smart grid vision in electrical power distribution systems, most of which only target one aspect of the distribution system control and operation, e.g. a control system for voltage control, another one for DG control, a third one for protection, etc. The coexistence of such control strategies in a distribution system raises some concerns about their overall performance, their interactions with the other control strategies, and whether these control systems can adapt to changes in distribution system connectivity.

In this PhD thesis we try to address these issues by proposing an implementation of the smart grid vision for distribution systems that provides an integrated design of power systems, communication systems and control strategies. A unified and flexible framework that incorporates all the different aspects of distribution system control and operation is proposed.

Distributed processing units equipped with wireless communication capabilities are used to continuously process the local data along with the data received from other nodes and forward the results to neighboring nodes in the system, which in turn process the received data and share the results with their neighbors. Consequently, changes in any of the system components (load values, status of DG etc.) are taken into account in the calculations as soon as they occur, and the results are forwarded to relevant nodes in the systems. This way the information “propagates” throughout the system resulting in a seamless control and coordination among all the system components.

Simulation of the electrical power distribution and the communication systems reveal the effectiveness of the proposed framework to control and coordinate multiple capacitor banks, DG units and voltage regulating transformers with changing load levels. It also reveals the potential of the proposed framework to operate in real-time by combining the real-time measured quantities with computer analysis in order to control the different

system components within the time frame of normal non-emergency operating conditions. An experimental setup is built and used as a test bed for the proposed framework in order to assess the performance of the different ideas and techniques proposed in this thesis.

## **Acknowledgements**

I would like to thank Prof. M. M. A. Salama for his continuous support and guidance during the long journey of my Ph.D.

I also would like to thank the members of my examining committee for their time and effort in reading my Ph.D. thesis and for their insightful comments.

Last but not least, I would like to express my deep gratitude for my family, I wouldn't have completed this Ph.D. without their love, support, and encouragement.





## **Dedication**

*To the memory of my Father ...*

*To my Mother ...*



# Table of Contents

List of Tables	xvii
List of Figures	xix
<b>1 Introduction</b>	<b>1</b>
1.1 Introduction to The Smart Grid . . . . .	1
1.2 Motivation . . . . .	2
1.2.1 Decentralized Approach . . . . .	2
1.2.2 Unified and Flexible Approach . . . . .	3
1.3 Research Objectives . . . . .	4
1.4 Thesis Outline . . . . .	5
<b>2 Literature Review</b>	<b>7</b>
2.1 The Smart Grid . . . . .	7
2.2 Electrical Power Distribution Systems . . . . .	11
2.2.1 Distribution Systems [10, 11] . . . . .	11
2.2.2 Power Flow Analysis for Distribution Systems . . . . .	12
2.2.3 Smart Distribution Systems . . . . .	16
2.3 State of the Art in Smart Distribution Systems Research . . . . .	17
2.3.1 Centralized vs. Decentralized Control . . . . .	17
2.3.2 Real-Time Analysis . . . . .	19

2.3.3	Distributed Power Flow Analysis . . . . .	20
2.3.4	Distributed Generation . . . . .	20
2.3.5	The Role of Communication Systems . . . . .	22
2.3.6	The Proposed Decentralized/Distributed Analysis and Control Framework . . . . .	23
2.4	Wireless Communication Technology . . . . .	24
2.4.1	WiMAX [63, 64] . . . . .	25
2.4.2	LTE: [64, 66] . . . . .	29
2.4.3	WiMAX vs. LTE . . . . .	31
2.5	The Network Simulator NS-3 . . . . .	32
2.6	Summary . . . . .	33
<b>3</b>	<b>Decentralized/Distributed Power Flow Analysis for Distribution Systems</b>	<b>35</b>
3.1	Introduction . . . . .	35
3.2	System Model and Assumptions . . . . .	37
3.2.1	Node . . . . .	37
3.2.2	Connectivity Matrix . . . . .	41
3.2.3	Zone Control Unit (ZCU) . . . . .	42
3.3	Execution of the Decentralized/Distributed Power Flow Analysis . . . . .	43
3.4	NS-3 Implementation of the Decentralized / Distributed Power Flow Analysis	46
3.4.1	Data Connectivity . . . . .	46
3.4.2	<i>BuildNetworkTopology</i> Class . . . . .	48
3.4.3	<i>DspfaApp</i> Class . . . . .	50
3.4.4	<i>ZcuApp</i> Class . . . . .	51
3.5	Simulation Results . . . . .	52
3.5.1	18-Bus Distribution System . . . . .	52
3.5.2	34-Bus Distribution System . . . . .	57

3.5.3	69-Bus Distribution System . . . . .	60
3.5.4	Communication Network Performance Evaluation . . . . .	63
3.6	Summary . . . . .	67
<b>4</b>	<b>Decentralized/Distributed Control Techniques for Distribution Systems</b>	<b>69</b>
4.1	Introduction . . . . .	69
4.2	Multiple Switched Capacitor Banks Control and Coordination . . . . .	72
4.2.1	Introduction . . . . .	72
4.2.2	The Proposed Control Algorithm . . . . .	73
4.3	Multiple DG Units Control and Coordination . . . . .	76
4.3.1	Introduction . . . . .	76
4.3.2	The Proposed Control Algorithm . . . . .	76
4.4	Simulation Methodology . . . . .	77
4.4.1	Exhaustive Search . . . . .	78
4.4.2	Percentile Rank . . . . .	78
4.4.3	Performance Evaluation . . . . .	78
4.4.4	Wireless Communication System Simulation . . . . .	79
4.4.5	Simulation Parameters . . . . .	79
4.5	Multiple Switched Capacitor Banks Control and Coordination - Simulation Results . . . . .	79
4.5.1	31-Bus Distribution System . . . . .	80
4.5.2	69-Bus Distribution System . . . . .	82
4.6	Multiple DG Units Control and Coordination - Simulation Results . . . . .	84
4.6.1	31-Bus Distribution System . . . . .	85
4.6.2	69-Bus Distribution System . . . . .	86
4.7	Multiple Capacitor Banks and DG Units Control and Coordination . . . . .	89
4.7.1	Seamless Coordination . . . . .	89
4.7.2	31-Bus Distribution System . . . . .	89

4.8	Real-Time Operation . . . . .	91
4.8.1	69-Bus Distribution System . . . . .	92
4.9	Summary . . . . .	97
<b>5</b>	<b>Smart Volt/VAR Control Using the Analysis and Control Framework</b>	<b>99</b>
5.1	Introduction . . . . .	99
5.2	Smart Volt/VAR Control . . . . .	102
5.2.1	OLTC Control in The Smart Grid Environment . . . . .	103
5.2.2	Limiting The Number of Switching Operations . . . . .	105
5.3	GNU-Octave Simulation Results of the Smart VVC Technique . . . . .	106
5.3.1	IEEE 13-Node Test Feeder . . . . .	107
5.3.2	31-Node Feeder . . . . .	110
5.3.3	PG&E 69-Node Feeder . . . . .	112
5.3.4	Comments on the Simulation results . . . . .	114
5.4	NS-3 Simulation Results of the Smart VVC Technique . . . . .	115
5.5	Summary . . . . .	117
<b>6</b>	<b>A Test Bed to Examine the Analysis and Control Framework</b>	<b>119</b>
6.1	Introduction . . . . .	119
6.2	Raspberry PI Computer . . . . .	121
6.3	Socket Programming . . . . .	124
6.3.1	Client/Server Communication Model . . . . .	125
6.3.2	C/C++ Socket Programming - Data Structures and Linux System Calls . . . . .	127
6.4	The Test Bed . . . . .	128
6.4.1	Hardware . . . . .	128
6.4.2	Software . . . . .	131
6.4.3	Test Bed Operation . . . . .	133
6.5	15-Node Distribution Feeder Results . . . . .	136
6.6	Conclusion . . . . .	153

<b>7 Conclusion and Future Work</b>	<b>159</b>
7.1 Summary and Conclusion . . . . .	159
7.2 Future Work . . . . .	161
<b>APPENDICES</b>	<b>163</b>
<b>A Random Search Algorithms</b>	<b>165</b>
A.1 Generic Random Search . . . . .	165
A.1.1 Generating Candidate Points . . . . .	167
A.1.2 Updating the Current Iterate . . . . .	168
A.1.3 Stopping Criteria . . . . .	169
A.1.4 Convergence in Probability . . . . .	169
<b>References</b>	<b>171</b>





# List of Tables

3.1	WiMAX and LTE performance comparison - NS-3 simulation of the 18-bus system . . . . .	55
3.2	WiMAX and LTE performance comparison - NS-3 simulation of the 18-bus system with automatic voltage regulator . . . . .	55
3.3	WiMAX and LTE performance comparison - NS-3 simulation of the 34-bus system . . . . .	60
3.4	WiMAX and LTE performance comparison - NS-3 simulation of the 69-bus system . . . . .	62
3.5	Maximum voltage differences for the 18-bus, 34-bus, and the 69-bus systems	63
4.1	A 31-bus distribution system with five capacitor banks and no voltage regulator - GNU-Octave simulation results . . . . .	81
4.2	A 31-bus distribution system with five capacitor banks and no voltage regulator - NS-3 simulation results . . . . .	81
4.3	A 31-bus distribution system with five capacitor banks and a voltage regulator ( $V_{sec} = 1.05$ p.u.) - GNU-Octave simulation results . . . . .	82
4.4	A 31-bus distribution system with five capacitor banks and a voltage regulator ( $V_{sec} = 1.05$ ) - NS-3 simulation results . . . . .	83
4.5	A 69-bus distribution system with four capacitor banks - GNU-Octave simulation results . . . . .	83
4.6	A 69-bus distribution system with four capacitor banks - NS-3 simulation results . . . . .	84
4.7	A 31-bus distribution system with three DG - GNU-Octave simulation results	85

4.8	A 31-bus distribution system with three DG units - NS-3 simulation results	86
4.9	A 31-bus distribution system with three DG and a voltage regulator ( $V_{sec} = 1.05$ p.u.) - GNU-Octave simulation results . . . . .	87
4.10	A 31-bus distribution system with three DG units and a voltage regulator ( $V_{sec} = 1.05$ p.u.) - NS-3 simulation results . . . . .	87
4.11	A 69-bus distribution system with four DG units - GNU-Octave simulation results . . . . .	88
4.12	A 69-bus distribution system with four DG units - NS-3 simulation results	88
4.13	A 31-bus distribution system with three capacitor banks, two DG units and a voltage regulator ( $V_{sec} = 1.05$ p.u.) - GNU-Octave simulation results . . .	90
4.14	A 31-bus distribution system with three capacitor banks, two DG units and a voltage regulator ( $V_{sec} = 1.05$ p.u.) - NS-3 simulation results . . . . .	91
4.15	Total system losses for the simulated time period (31 days of January 2000)	93
5.1	IEEE 13-node test feeder: test case-2 - The proposed smart VVC - 100-run results - (Two capacitors & one OLTC) . . . . .	110
5.2	Switched capacitor banks information for the 31-node feeder . . . . .	110
5.3	31-node test feeder - The proposed smart VVC - 100-run results - (Six capacitors & an OLTC) . . . . .	112
5.4	PG&E 69-node feeder - The proposed smart VVC - 100-run results - (Ten capacitors) . . . . .	114
5.5	31-node test feeder - Smart VVC results - Dispatch table obtained from NS-3 simulation . . . . .	116
5.6	NS-3 simulation results of the 31-node feeder for WiMAX and LTE . . . . .	117
6.1	15-node radial distribution system data . . . . .	137
6.2	Optimal state vs. the state obtained from the test bed for the 15-node system with three switched capacitor banks (test case 1) . . . . .	140
6.3	Optimal state vs. the state Obtained from the test bed for the 15-node system with two DG units (test case 2) . . . . .	143
6.4	Optimal state vs. the state obtained from the test bed for the 15-node system with three switched capacitor banks and two DG units (test case 3)	147

# List of Figures

1.1	Architecture of the proposed framework . . . . .	4
1.2	Node structure . . . . .	5
2.1	A typical distribution circuit [10] . . . . .	13
2.2	High level architecture of a wireless communication network . . . . .	25
2.3	OSI layers, and the layers included in the IEEE 802.16 standard [64] . . . . .	26
2.4	Protocol layers for LTE radio link . . . . .	29
3.1	Architecture of the proposed distribution system analysis and control framework . . . . .	36
3.2	An $N$ zone distribution system . . . . .	38
3.3	A typical distribution system feeder (a zone) . . . . .	39
3.4	Information sets associated with the proposed node structure . . . . .	40
3.5	Power and communication connectivity layers . . . . .	42
3.6	Implementation of the proposed analysis and control framework . . . . .	45
3.7	NS-3 implementation of the framework. . . . .	47
3.8	<b><i>DspfaApp</i></b> & <b><i>ZcuApp</i></b> nodes . . . . .	49
3.9	18-bus radial balanced distribution system [74] . . . . .	53
3.10	Voltage profile of the 18-bus system . . . . .	54
3.11	Voltage profile of the 18-bus system with automatic voltage regulator . . . . .	56
3.12	34-bus distribution system . . . . .	57

3.13	Voltage profile profile on the main feeder of the 34-bus system . . . . .	58
3.14	Voltage profile of the 34-bus system with capacitors and voltage regulator .	59
3.15	69-bus radial distribution system . . . . .	61
3.16	Voltage profile on the main feeder of the 69-bus system . . . . .	61
3.17	Voltage profile on a lateral of the 69-bus system . . . . .	62
3.18	Average convergence time . . . . .	64
3.19	Average packet delay. . . . .	65
3.20	Average packet delivery ratio. . . . .	66
4.1	Flow chart describing the interaction between system analysis and system control in the proposed framework . . . . .	71
4.2	A switched capacitor bank with $M_i$ stages . . . . .	73
4.3	A 31-bus distribution system . . . . .	80
4.4	Hourly load and wind power data as a percentage of peak load and nominal DG apparent powers respectively . . . . .	93
4.5	Hourly savings for the 69-bus radial system using the variable load and wind data . . . . .	94
4.6	Hourly power factor values for the four DG units during the first 20 hours	95
4.7	Hourly power factor values for the four DG units during the 744 hours . .	96
5.1	Architecture of the proposed smart VVC technique . . . . .	102
5.2	Load profile for IEEE 13-node test feeder from [92] . . . . .	109
5.3	Load profiles for the 31-node feeder from [86, 87] . . . . .	111
5.4	Load profiles for the 69-node feeder from [91] . . . . .	113
6.1	Raspberry PI unit [95] . . . . .	121
6.2	Raspberry PI PCB layout [95] . . . . .	122
6.3	Two processes using sockets to communicate [99] . . . . .	125
6.4	Data connectivity among parents and children in a typical electrical power distribution system . . . . .	126

6.5	The test bed - A photograph . . . . .	129
6.6	The test bed - A photograph . . . . .	130
6.7	Hardware architecture of the test bed . . . . .	131
6.8	Socket communication software architecture of a node . . . . .	132
6.9	Software architecture of <i>DspfNode</i> . . . . .	133
6.10	Software architecture of <i>ZcuNode</i> . . . . .	134
6.11	A 15-node radial distribution feeder . . . . .	136
6.12	Voltage profile obtained through the collaboration of the 15 Raspberry PI nodes in the test bed for test case 0 . . . . .	138
6.13	Voltage profile obtained through the collaboration of the 15 Raspberry PI nodes in the test bed for test case 1 . . . . .	140
6.14	Voltage profiles and losses during the intermediate iterations for test case 1	141
6.15	Voltage profile obtained through the collaboration of the 15 Raspberry PI nodes in the test bed for test case 2 . . . . .	142
6.16	Voltage profile and losses during the intermediate iterations for test case 2	144
6.17	Voltage profile obtained through the collaboration of the 15 Raspberry PI nodes in the test bed for test case 3 . . . . .	145
6.18	Voltage profile and losses during the intermediate iterations for test case 3	146
6.19	24 Hour load profile . . . . .	148
6.20	Voltage profiles for each hour of the 24-hour period investigated . . . . .	149
6.21	Total system losses for the 24-hour period investigated . . . . .	150
6.22	Voltage profiles for all intermediate iterations for the 24-hour period investigated . . . . .	151
6.23	Total system losses for all intermediate iterations for the 24-hour period investigated . . . . .	152
6.24	Screen shot of the ZCU handling the incoming connections . . . . .	154
6.25	Screen shot of the ZCU showing the connected nodes information . . . . .	155
6.26	Screen shot of the ZCU showing the end of the analysis for the 24 load points	156
6.27	Screen shot of node 2 showing a part of the capacitor bank control log . . .	157
6.28	Screen shot of node 4 showing a part of the DG unit control log . . . . .	158



# Chapter 1

## Introduction

### 1.1 Introduction to The Smart Grid

The “Smart Grid” is a multidisciplinary approach toward a fully automated, efficient, reliable and environment-friendly electrical power system in which information, as well as electricity, flows among all the points in the system [1]. In the smart grid, information is continuously collected and processed in order to control the electrical power system and its various components. In addition to electrical power systems, the smart grid research incorporates different areas such as communication systems, computer science and control systems.

Aging infrastructure, reducing carbon emissions, shortage of fossil energy resources and cost reduction are among the main challenges facing the electrical power grid [1, 2, 3]. The smart grid is expected to be a key part of the solution to such challenges.

The US Energy Independence and Security Act of 2007 (EISA) lists multiple characteristics the smart grid should achieve such as [4, 5, 6]:

1. Enable active participation by customers by using real-time pricing.
2. Accommodate all generation options such as solar units and wind-farms.
3. Provide power quality.
4. Operate efficiently and optimize asset utilization.
5. Anticipate and respond to the system disturbances (self-healing).

In order to realize these characteristics, the smart grid implementation should incorporate three key technological components [1, 7, 8, 9]:

1. Distributed intelligence.
2. Communication networks.
3. Automated control systems.

The combination of distributed intelligence and communication networks allows the smart grid to collect and process real-time information in order to perform system analysis and control leading to an optimal real-time system operation.

The focus of this Ph.D. thesis is on implementing the smart grid vision in the electrical power distribution system through the integration of distributed intelligence and communication networks into the distribution system's monitoring, analysis, control and operation. Distribution system is the portion of the electrical power delivery infrastructure that takes the electricity from the highly meshed, high-voltage transmission circuits and delivers it to the customers [10, 11].

## 1.2 Motivation

The motivation behind the research presented in this Ph.D. thesis is to present a unified flexible decentralized approach to implement the smart grid concepts in distribution systems.

### 1.2.1 Decentralized Approach

The current electrical power distribution system has a combination of centralized and decentralized/distributed control systems. However, for the smart grid, several studies have shown that distributed control and management is a preferable approach to design both power and communications networks [12].

In centralized control systems, all computing and control functions are performed in one central location with communication links from the control center to the system's sensors and controllable devices such as switched capacitor banks, voltage regulating transformers,



Distributed Generation (DG) units, and circuit breakers, therefore allowing remote monitoring and control. The Supervisory Control and Data Acquisition (SCADA) system is an example of such centralized control hierarchy [13].

On the other hand, in decentralized/distributed control systems the computing and control functions are distributed among many different locations [14]. The centralized control systems are easier to build but they might not respond quickly to adverse events in the system, whereas the decentralized control systems can respond more promptly to such events.

The lack of information exchange in decentralized/distributed control systems may lead to unreliable or biased decision making [14], therefore communication links must be used to exchange information among the dispersed processing units in decentralized control systems.

### **1.2.2 Unified and Flexible Approach**

There are numerous methods and techniques proposed in literature to control and operate the electrical power distribution system in a decentralized/distributed manner as discussed in chapter 2. Most of these techniques targets only one aspect of the distribution system control and operation problem, e.g. a decentralized system for voltage control, another one for DG control, a third one for protection, etc. Consequently, combining these techniques together to control a distribution system might result in control conflicts and non-optimal performance.

Additionally, most of these decentralized control techniques can be described as “rigid” or “static” because changes in the system connectivity and addition/removal of components cannot be accommodated easily.

Therefore there is a need for a “unified” and “flexible” control approach that can provide a “common ground” to control and coordinate all the distribution system components and that can accommodate changes in the system topology and components.

In the research presented in this Ph.D. thesis, a decentralized/distributed power flow analysis framework provides the required “common ground” for distribution system control and coordination.

### 1.3 Research Objectives

The purpose of the research conducted in this Ph.D. thesis is to build an online unified and flexible framework that performs decentralized/distributed real-time analysis, control and coordination of electrical power distribution systems as illustrated in Figure 1.1.

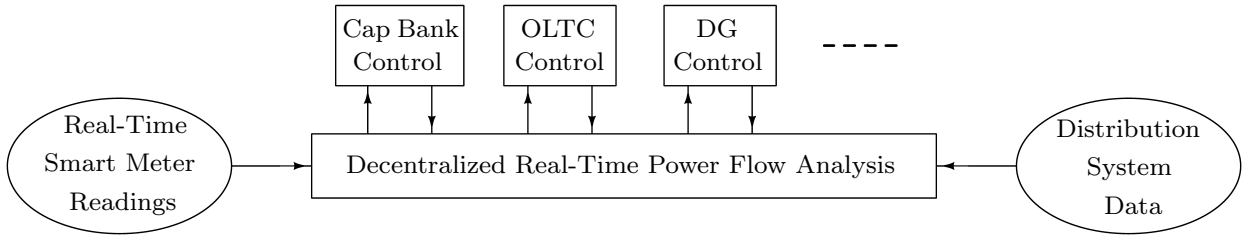


Figure 1.1: Architecture of the proposed framework

The real-time measurements from smart meters and the distribution system data are used to perform decentralized real-time power flow analysis which serves as the “basis” for control and coordination of the different system components such as switched capacitor banks, On-Load Tap Changing (OLTC) transformers and DG units.

The implementation of this analysis and control framework requires the installation of distributed processing units equipped with wireless communication transceivers on distribution system buses. Therefore, creating a “node” structure that includes an electrical power bus, a processing unit with a set of installed applications that handle the power and communication aspects of the node, and a wireless communication transceiver as illustrated in Figure 1.2.

In this framework, the distribution system connectivity is defined and maintained via the local information stored in each node (e.g. IP addresses of neighboring nodes) as well as the global information acquired through the communication links (e.g. neighbors’ calculated voltages and currents), thereby allowing the analysis and control framework to accommodate changes in the system connectivity in a flexible and dynamic manner.

The proposed analysis and control framework represents an integrated design of power and communication systems where information is continuously collected, processed and shared among the system nodes.

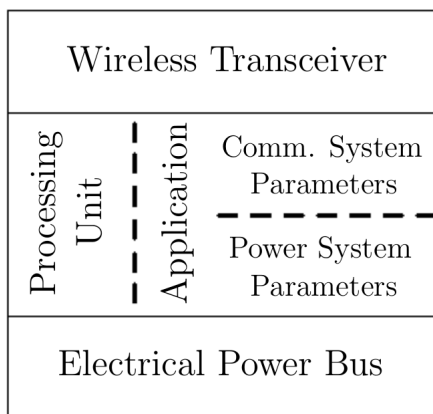


Figure 1.2: Node structure

## 1.4 Thesis Outline

This rest of this thesis is organized as follows, chapter 2 begins with a brief review of the smart grid characteristics and features, followed by a literature review on the smart distribution systems. It also presents a brief review on the WiMAX and LTE communication technologies followed by a brief description of the network simulator NS-3.

The analysis and control framework is presented in details in chapters 3, 4, and 5. Chapter 3 presents a detailed description of the framework and its three main components (i.e. node, connectivity matrix, and the zone control unit). It also discusses a proposed distributed/decentralized implementation of power flow analysis for distribution systems, along with its NS-3 implementation details. GNU-Octave<sup>1</sup>[15] and NS-3<sup>2</sup> [16] simulation results are presented at the end of the chapter.

In chapter 4, control and coordination techniques for multiple switched capacitor banks, and multiple DG units are presented along with their GNU-Octave and NS-3 simulation results.

The proposed analysis and control framework is utilized in chapter 5 to perform smart Volt/Var Control (VVC) for distribution systems. A new approach to control the voltage

---

<sup>1</sup>GNU-Octave is a high-level interpreted language, primarily intended for numerical computations. The Octave language is quite similar to Matlab so that most programs are easily portable.

<sup>2</sup>The network simulator NS-3 is an open-source discrete-event network simulator for internet systems, targeted primary for research and educational use.

regulating transformers and to coordinate them with the existing switched capacitor banks and DG units is presented along with a mechanism to reduce the total number of switching operations. GNU-Octave and NS-3 simulation results are presented at the end of the chapter.

An experimental setup is described in details in chapter 6, this experimental setup is used as a test bed for the proposed analysis and control framework. The hardware and software aspects of this test bed are discussed, and the results of five test cases are presented. Chapter 7 concludes the thesis with a brief summary, some concluding remarks, and a discussion of the possible directions for the future work.

# Chapter 2

## Literature Review

This chapter provides a literature review of the different aspects of the smart grid implementation in electrical power distribution systems. The main challenges facing the electrical power grid are outlined in section 2.1, along with the definition and characteristics of the smart grid.

Section 2.2 starts with a brief description of a typical distribution system and its components followed by a discussion of the backward/forward power flow analysis. The section ends with an overview of the main features of smart distribution systems. The state of the art in smart distribution systems' research is presented in section 2.3.

Communication system is an integral part of the smart distribution system, therefore section 2.4 is dedicated to review two candidate wireless communication technologies that can support the smart distribution system implementation, namely WiMAX and LTE.

Simulation of both the power and communication systems is becoming a necessity for performance evaluation in the smart grid era, section 2.5 outlines the basic features of the network simulator NS-3 which is used to simulate the distribution system analysis and control framework presented in this thesis. A brief summary of the chapter is presented in section 2.6.

### 2.1 The Smart Grid

The smart grid can be defined as a “fully automated, efficient, reliable and environment-friendly power delivery network that can ensure a two-way flow of electricity and information between the power plants, appliances, and all points in between” [1].

In its report “The Smart Grid: An Introduction” [17], the US Department of Energy (DOE) describes the smart grid as “the internet brought to the electric power system”.

The Smart Grid has recently dominated the political landscape in North America and in Europe because it is recognized as a key component of the solution to the challenges in the current electrical power grid such as [1, 2, 3]:

1. Environmental challenges:

The traditional electrical power generation is the largest man-caused carbon dioxide emission source as it accounts for approximately 25% of the world’s carbon dioxide emissions, which means that the traditional electric power production must be changed to reduce the solid and gas emissions and hence mitigate the climate change. Additionally a shortage of fossil energy resources has been foreseen in the next few decades.

2. Infrastructure challenges:

The electrical network congestion is increasing due to the increased load demands and the aging components of the existing infrastructure, thus there is a crucial need to improve the network efficiency and reliability by utilizing fast online analysis tools [2].

3. Economical challenges:

A more efficient grid will reflect positively on the economy and will help to reduce the costs. For instance, the Electrical Power Research Institute (EPRI) estimates 1.8 trillion USD in annual additive revenue in the US by 2020 with a substantially more efficient and reliable grid [3].

4. Shift in generation sources:

The shift toward renewable distributed energy generation sources such as wind and solar presents new challenges in the control and coordination of the power grid. Co-generation from non-traditional sources will be mandated in some places requiring two-way control and monitoring at non-utility owned facilities [1].

5. Transmission congestion:

Investments in the transmission system infrastructure have not kept pace with the growth in demand, which resulted in a heavier utilization, more frequent congestion, increased transmission losses and increased risk of catastrophic failures.

6. Distribution system:

Increased use of information technologies such as computers and consumer electronics resulted in lowered tolerances to outages and power quality disturbances. The growing interest in distributed generation, electric storage devices and emerging trends such as plug-in hybrid electric vehicles (PHEVs) are adding new requirements and stresses on the whole system.

7. Regulatory policy:

Federal governments and many states are passing energy efficiency mandates.

The smart grid is expected to overcome all these challenges and even open new horizons in the electrical power industry.

The three key technological components of the smart grid are [1, 7, 8, 9]:

1. Distributed intelligence:

Distributed intelligence is based on advanced sensors with processing and communications capabilities built into every element of the grid such as switches, transformers, substations, distribution lines, etc. The distributed intelligence will enable real-time monitoring, coordination and control. Advanced sensors can be used to monitor the health of the grid in real-time and respond (perhaps autonomously, without central coordination) to avert system-wide failures and outages.

2. Communication infrastructure:

Communication infrastructure is an essential component in the smart grid implementation because it enables system-wide monitoring and coordination and supports diverse applications such as distribution automation, demand response, outage management and power quality monitoring.

Candidate wireless communication technologies for smart grid implementation include the Worldwide Interoperability for Microwave Access (WiMAX) and Long Term Evolution (LTE) which are the two primary broadband technologies that are used in 4G wireless networks. Both standards provide low latency, high data rates and long-distance coverage, therefore they can be used as the communication backbone for the smart grid and its diverse applications [18].

3. Automated control systems:

The third major element in the smart grid implementation consists of software tools and algorithms for self-healing, self-reconfiguration, executing protocols for demand response, automatic load-shedding, and promoting better coordination within and between utilities.

The US Energy Independence and Security Act of 2007 (EISA) lists multiple characteristics the smart grid should achieve, such as [4, 5, 6]:

1. Enable active participation by consumers through demand response and real-time pricing. The consumer will be able to monitor the price signal and make decisions to curtail the electricity usage.
2. Accommodate all generation and storage options including distributed generation (DG) units and energy storage on the distribution system.
3. Enable new products, services and markets where new opportunities will arise from distributed generation and energy storage assets enabling consumers to interact in real-time with the electricity market [19].
4. Provide varying grades of power quality and support variable prices accordingly, this way the customer can choose whatever power grade that meets his requirements. The advanced control methods will enable the smart grid to mitigate the power quality events that originate in the transmission and distribution elements of the power grid [20].
5. Optimize asset utilization and operate efficiently on the short and long terms based on the collected real-time information. Optimized asset management will deliver the desired functionality more efficiently and at a minimum cost as well as reducing the carbon footprint [6, 21].
6. Anticipate and respond to system disturbances (self-heal) by identifying, isolating and restoring problematic elements of the system with little or no manual intervention, so as to minimize interruptions of service. Self-healing can also mitigate power quality issues, taking such corrective steps as instantly transferring a customer from a disturbed source to a “clean” one [22].
7. Operate resiliently against physical attacks, cyber attacks and natural disasters [6, 23]



## 2.2 Electrical Power Distribution Systems

The electrical power grid consists of generating stations that produce electrical power, high-voltage transmission lines that carry power from distant generating stations to demand centers, and distribution lines that deliver electricity to individual customers.

The research presented in this thesis focuses on implementing the smart grid concepts in the electrical power distribution system through an integrated design of power, communication and control systems.

The basic components of the electrical power distribution system are identified in subsection 2.2.1, the backward/forward sweep power flow analysis method for distribution systems is described in subsection 2.2.2, while subsection 2.2.3 discusses the basic characteristics of smart distribution systems.

### 2.2.1 Distribution Systems [10, 11]

Electric power distribution system is the portion of the power delivery infrastructure that takes the electricity from the highly meshed, high-voltage transmission circuits and delivers it to customers.

The distribution system typically starts with the distribution substation that is fed by one or more transmission/subtransmission lines. Each distribution substation serves one or more primary feeders.

At a distribution substation, a substation transformer takes the incoming transmission-level voltage and steps it down to several distribution primary circuits (feeders), which fan out from the substation. Usually the primary distribution lines are considered medium-voltage lines (between 4 kV and 35 kV).

Close to each consumer, a distribution transformer takes the primary-distribution voltage and steps it down to a low-voltage secondary circuit (commonly 120/240 V). From the distribution transformer, the secondary distribution circuits connect to the consumer.

Figure 2.1 shows a typical distribution circuit and its different components, namely [11]:

1. Three-phase primary main feeder.
2. Three-phase, two-phase and single-phase laterals.

3. Step-type voltage regulators.
4. In-line transformers.
5. Shunt capacitor banks.
6. Distribution transformers.
7. Secondary distribution circuits.
8. Three-phase, two-phase, and single-phase loads.

Most distribution circuits are radial, which means that there is only one path for power to flow from distribution substation to the user. In radial circuits, the relation between nodes can be described in terms of parent/children relationships as discussed in chapter 3. Radial circuits have many advantages over networked circuits including:

1. Easier fault current protection.
2. Easier voltage control.
3. Easier prediction and control of power flow.
4. Lower cost.

## 2.2.2 Power Flow Analysis for Distribution Systems

Power flow analysis is an important tool which analyzes the power system in normal steady-state operation in order to obtain the magnitude and phase angle of the voltage at each bus, and the real and reactive power flowing in each line. Power flow analysis is used for planning future expansions of the power system as well as in determining the best operation of existing systems.

Conventional load flow methods, such as Newton-Raphson and Fast-Decoupled, are well established and efficient for transmission networks. However, such methods exhibit poor convergence characteristics when applied to distribution systems [11].

The special features of distribution systems such as radial or weakly meshed topologies, high R/X ratio of the distribution lines, unbalanced operation and loading conditions, non-linear load models, and dispersed generation [24, 25, 26] make it difficult to use the generic Newton-Raphson method.

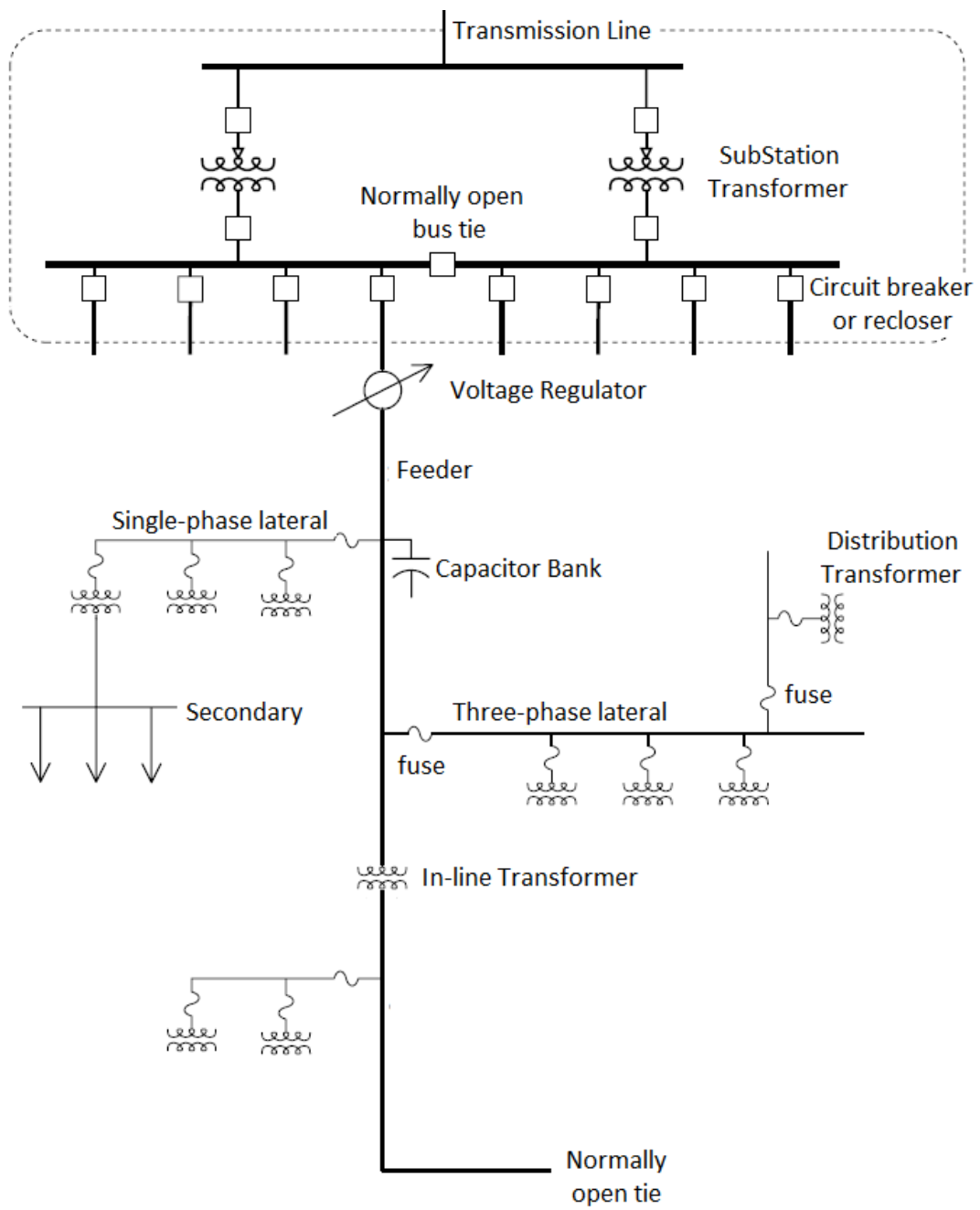


Figure 2.1: A typical distribution circuit [10]

Ladder network method and iterative backward/forward sweep method are suitable for power flow analysis of radial distribution systems because they are known for their computational efficiency and solution accuracy [27, 28].

In the research presented in this thesis, a decentralized/distributed implementation of the iterative backward/forward sweep method is modified to perform on-line power flow analysis of distribution systems.

The backward/forward sweep method can be described as follows:

1. Initial assumptions:

- (a) The initial voltage value for all the system buses is assumed to be 1 p.u. (i.e. flat start).
- (b) Substation voltage is assumed to be fixed at 1 p.u.
- (c) Line impedance of all the branches in the system are known.
- (d) The complex load power and the load model are known for every node in the system. The load model at node  $i$  can be modeled as:
  - i. Constant active and reactive power load model: i.e.  $S_{load,i}$  is constant.
  - ii. Constant impedance load model: the constant impedance is calculated according to equation 2.1 which uses the specified complex load power,  $S_{load,i}$ , and the assumed initial voltage [11].

$$Z_{load,i} = \frac{|V_i|^2}{(S_{load,i})^*} \quad (2.1)$$

- iii. Constant current load model: the magnitude of the current is computed according to equation 2.2, and then held constant while the angle of the voltage  $\delta_i$  changes, resulting in a changing angle of the current so that the power factor of the load  $\theta_i$  remains constant [11].

$$|I_{load,i}| = \left| \frac{S_{load,i}}{V_i} \right| \quad (2.2)$$

where:

$$\begin{aligned} V_i &= |V_i| \angle \delta_i : \text{ Voltage at node } i. \\ S_{load,i} &= |S_{load,i}| \angle \theta_i : \text{ Complex power of the load at node } i. \end{aligned}$$

2. Backward sweep:

- (a) The load currents are calculated for each bus in the system as follows [11]:
- i. Constant real and reactive power loads:

$$I_{load,i} = \left( \frac{S_{load,i}}{V_i} \right)^* \quad (2.3)$$

- ii. Constant impedance loads:

$$I_{load,i} = \frac{V_i}{Z_{load,i}} \quad (2.4)$$

- iii. Constant current loads:

$$I_{load,i} = |I_{load,i}| \angle \delta_i - \theta_i \quad (2.5)$$

- (b) Moving backwards toward the substation, Kirchhoff's Current Law (KCL) is used to calculate the current flowing in each branch of the distribution network.

3. Forward sweep:

Starting from the substation and moving forward, Kirchhoff's Voltage Law (KVL) is used to update the voltage values for all the system buses by utilizing the calculated current values from the backward sweep and the known line impedance of each branch in the network.

4. Convergence check:

The difference between the calculated voltage values for two consecutive iterations is compared with a predetermined voltage tolerance  $\epsilon$ . The analysis is terminated if the voltage difference is less than  $\epsilon$  for "all" the nodes, otherwise the analysis is resumed and additional backward/forward sweeps are performed.

It is important to emphasize that the iterative backward/forward sweep method is a fundamental component in the implementation of the analysis and control framework proposed in this thesis due to its suitability for power flow calculations of distribution systems, its efficiency and accuracy, and more importantly because it can be implemented in a “distributed/decentralized” manner.

The backward/forward sweep method can be easily implemented in a distributed/decentralized manner such that the power flow analysis of whole system is achieved through the collaboration of multiple processing units which use communication links to exchange information with other nodes depending on the power system connectivity as described in chapter 3.

### **2.2.3 Smart Distribution Systems**

The electrical power distribution system, which was originally designed as a passive network with unidirectional power flow, is now begin revolutionized under the smart grid umbrella.

The main characteristics of the smart distribution system include [7, 29]:

1. **Distributed Energy Resources:**

The distribution system, which was not originally designed to accommodate local production of energy on large scale, is now facing new challenges due to the increased number of Distributed Energy Resources (DER) installations such as distributed and renewal generation, and energy storage. Consequently, it is essential to develop novel control and automation techniques that can intelligently and efficiently manage the distribution system.

2. **Advanced Metering Infrastructure:**

The deployment of the Advanced Metering Infrastructure (AMI) and its communication network provides utilities with a system-wide visibility that can be leveraged to efficiently control and manage the distribution system. Each smart meter is actually a smart grid sensor that can deliver interval load profile data and support on-demand readings via the communication system [30]. AMI also supports the time-of-use real-time electricity rates which is anticipated to reduce the system’s peak demand.

3. **Distribution Automation:**

The implementation of Distribution Automation (AD) systems requires installing monitoring and communication devices on the distribution feeder in order to automatically reconfigure the system to restore customers and achieve other operational objectives.

4. Demand response:

Demand response can be defined as the reduction of customer energy usages at times of peak usage in order to improve system reliability, reflect market conditions and pricing, and support infrastructures optimization of deferral [7]. AMI, load control, smart appliances, and dynamic pricing are among the tools that enable the active participation of customers in demand response.

5. Islanding:

Islanding is a situation in which a certain section of the grid comprising loads and DER changes from being grid-connected to operating independent of the grid. Islanding is an expected function of the smart grid and it is intended to improve reliability and security of supply. The islanding situation will require functions such as island identification, control of islanding ability, power flow monitoring within an island, and control of smart interconnection using communication links.

6. Automatic fault location and restoration.

7. Improved operational efficiency, and asset utilization.

The implementation of the aforementioned smart distribution characteristics require an integrated design of power, communication and control systems and new control and automation techniques.

## **2.3 State of the Art in Smart Distribution Systems Research**

This section reviews the state of the art in smart distribution systems research. There are various ideas and approaches in literature to implement the smart grid concepts in distribution systems in order to allow the integration of DER devices into the distribution system and to leverage the AMI generated information.

### **2.3.1 Centralized vs. Decentralized Control**

The smart distribution systems research can be categorized into two groups, centralized techniques, and decentralized/distributed techniques.

In the centralized approach all the computing and control functions are performed in one central location with communication links from the control center to the system's sensors and controllable devices such as switched capacitor banks, voltage regulating transformers, Distributed Generation (DG) units, circuit breakers, etc. therefore allowing remote monitoring and control.

Whereas in decentralized/distributed control systems, the computing and control functions are distributed among many different locations. Exchange of information is a crucial part of decentralized/distributed control systems in order to achieve reliable and unbiased control decisions [14].

The centralized control systems are easier to build but they might not respond quickly to adverse events in the system, whereas the decentralized control systems can respond more promptly to such events.

For instance, in [31] the authors propose a centralized approach to combine the Geographic Information System (GIS) data with the real-time measurements from sensors installed in the distribution system in order to operate existing systems efficiently as well as planning new systems. A Network Operation Center (NOC) uses this real-time location specific data along with historical data to evaluate the status of the network and perform load flow analysis. This centralized approach raises concerns regarding the ability of the NOC to receive, process, and store such huge amount of sensor information. Furthermore, the performance of the communication network need to be evaluated in terms of delays and network congestion.

The challenges associated with the huge amount of information collected in the smart grid is discussed in [32], the authors also suggest moving from centralized decision making to distributed decision making.

For the smart grid, several studies have shown that distributed control and management is a preferable approach to design both power systems and their supporting communication networks [12].

In literature, decentralized/distributed control schemes that utilize communication links have been used in electrical power systems to perform numerous tasks such as protection [33], reactive power control [34], voltage regulation [35, 36], protection and reconfiguration [14], and to perform power control management [12].

For instance, the authors in [34] address the problem of decentralized reactive power control, remote terminal units (RTUs) are installed at each DG unit and each capacitor bank, and communication links are used to coordinate these RTUs. Using this scheme the voltage profile, and changes in the voltage profile can be estimated. These estimated values are used to control DGs and capacitor banks to minimize the estimated losses.



The authors of [35] propose a decentralized voltage regulation architecture by using fuzzy controllers, in which sensors are used to measure the local bus variables and use these measured values to estimate the current grid status, which is then used to identify the proper control actions.

A decentralized architecture for voltage regulation in smart grid is presented in [36], a controller with fuzzy inference system is installed at each node with a DG unit, this controller use sensors to measure the voltage and active/reactive power. The controllers use radio communications to exchange the measured quantities to reach a weighted average of the variables sensed by all controllers in the smart grid.

Neural networks are used in [37] to achieve decentralized voltage control in distribution systems, the authors use genetic algorithm to generate predicted load values of the next day, and use this data to train the neural network via communications infrastructure.

Multi-agent based distribution system automation techniques are proposed in [38, 39, 40] for fault detection, isolation and restoration.

In [41], the authors use a multi-agent system to implement decentralized control of the power system, the agents are assumed to be “situation-aware”. The authors of [41] raise two important questions: 1.) what kind of information needs to be transmitted to make the agent “situation-aware”?, and 2.) how are communications integrated into this process? Similar questions are raised in [7].

### **2.3.2 Real-Time Analysis**

Real-time analysis is discussed in [42] as a necessary tool to achieve acceptable operational efficiency and quality of service of distribution systems. The authors define the real-time analysis as the combination of computerized circuit modeling and analysis with measured real-time customer consumption and power source data to determine the voltages and power flows in all elements on the grid. Analysis is done nearly continuously to determine the real-time characteristics of the grid. The real-time data and computation results are utilized to facilitate generation dispatch, line switching, control of equipment and devices, and customers load control to achieve operational goals [42].

Combining computer analysis with real-time measurements is an effective way of calculating the voltage and current values for the grid elements that are not measured and monitored in real-time [42], therefore reducing the number of installed sensors.

This definition of real-time analysis is adopted in this thesis where the real-time measurements are combined with computerized analysis in order to perform power flow analysis

and hence take control decisions.

In [43], the measured quantities in a SCADA system is being used to perform real-time analysis and control of the system, while in [44] a similar approach is presented, based on measurements, the load profile is estimated and a neural-network is used to achieve real-time control of capacitor banks. A real-time power quality monitoring system is also presented in [45].

### **2.3.3 Distributed Power Flow Analysis**

Distributed power flow analysis is presented in [46, 47, 48] where physically distributed processors are used to perform distributed power flow analysis for distribution systems. The distribution system is divided into partitions, and the power flow analysis is performed for each partition individually; the calculations from each partition are communicated to the other partitions, such that the power flow analysis of the whole system is achieved using the iterative backward/forward sweep method. The authors of [46, 47, 48] suggest that distributed power flow analysis can provide the information necessary for effective distributed control decisions.

A study of distributed capacitor control for electrical power distribution systems is presented in [49]. In this study, the distributed analysis method presented in [46, 47, 48] is used to perform power flow analysis for the whole system at peak load and maximum capacitor bank settings, based on this power flow analysis the distribution system is divided into partitions based on the reactive power domains of shunt capacitors. After partitioning the system, distributed power flow analysis is performed to help control and coordinate the capacitor banks.

Changes in the distribution system connectivity, adding or removing any system component (e.g. DG unit) will affect the distribution system partitioning used in [46, 47, 48, 49] thereby resulting in a different number of partitions with different sizes, and requiring a different number of distributed processing units and a different communication network connectivity.

### **2.3.4 Distributed Generation**

One of the defining aspects of the smart grid is the increased penetration of Distributed Generation (DG) units, which can be defined as an electric power source connected directly to the distribution network or on the customer side of the network [50].

The usage of DG units can provide numerous benefits for consumers and electric utilities, for instance DG owners get a cheaper power source, and they can make profit by selling their energy to the power market especially during the peak demand hours. Utilities can install DG units in order to improve power quality and reliability, and to defer investments in power delivery facilities such as distribution lines and transformers. [51].

The close proximity of the DG units to the consumer premises greatly reduces the transmission and distribution system losses therefore reducing the carbon emissions. Moreover, the renewable DG units such as solar panels and wind turbines are clean and environment-friendly.

Distribution systems and their protection, voltage control, and reactive power control devices are all designed for a unidirectional power flow from the substation to consumers where the voltage level decreases toward the end of the feeder, however this picture has dramatically changed with the introduction of DGs, therefore posing new challenges to the distribution system. For example, the connection of DG units can significantly affect the voltage levels in the system, and can also leads to changes in the fault-current [50], additionally the increased penetration of DGs can result in increased system losses as discussed in [52].

The current DG interconnection standards do not allow DGs to generate or consume reactive power, but changes to these standards appear eminent because the fast reacting VAR-capable DG inverters can provide the necessary reactive power injection or consumption to maintain voltage regulation [53].

The challenges posed by DG installations in distribution systems are addressed in various research efforts, in [54] a coordination technique between on-load tap changer (OLTC), switched capacitor banks and DG units is presented, in this technique the OLTC and the switched capacitor banks are dispatched based on predetermined set points in order to minimize the daily losses and hence it does not use any communication links. The authors of [54] pointed out that the load profile variability will affect the performance of their proposed technique which requires readjustments to the control set points, and that new DG installation also requires readjustments in the OLTC and switched capacitor banks control set points.

A two-stage short term scheduling procedure for OLTC and Distributed Energy Resources (DER) is proposed in [55], 24-hour forecast is used in the day-ahead scheduler and 15-minutes forecast is then used in the intra-day scheduler to adjust the OLTC and DER set points in accordance with operation requirements and constraints. The intra-day scheduler iteratively solves a Mixed-Integer Linear Programming (MILP) algorithm. The authors of [55] did not comment on the computational burden associated with the intra-day

MILP scheduler and whether it can converge within the time frame of 15-minutes, they also did not discuss whether communication links are needed for their proposed approach and how would these communication links affect the performance.

A Multiagent System (MAS)-based scheme is presented in [56] to dispatch DG units to supply reactive power in order to provide voltage support, communication links between DG units and LTC are used. The authors of [56] pointed out that their proposed MAS system can only be developed by knowing the optimal solution obtained by solving the original optimization problem.

In [52] the authors demonstrate that DG units with reactive power control provide a better network voltage profile and lower losses, and they suggest that using a variable power factor for DG units along with a real-time control strategy can reduce the system losses compared to operating at a constant unity power factor. It is reported in [52, 57] that Spain uses an incentive-based time-of-the-day power factor settings for the DG units to encourage DG owners to voluntarily help network operation.

It can be concluded from this discussion that allowing DG units to operate using variable power factors can be beneficial but it also requires new techniques to control and coordinate DG units and other system components.

### **2.3.5 The Role of Communication Systems**

It is evident from the previous discussion that the communication networks play an essential role in the smart grid implementation. The authors of [9] discuss some of the smart grid applications and their communication requirements, and report that the WiMAX technology exhibit very good latency characteristics and substantial network capacity. While the utilities don't currently allow islanding, one of the suggested applications is to use two-way data communication links to monitor and control the DGs in order to allow them to supply power to loads while the grid is down.[9].

Most of the research reviewed in this section uses communication links without including the communication system into the simulation. The simulation of both power and communication systems is becoming a necessary tool in developing new techniques and approaches for the smart grid.

### 2.3.6 The Proposed Decentralized/Distributed Analysis and Control Framework

Most of the approaches and techniques reviewed in this section targets only one aspect of the distribution system control and operation problem, e.g. a decentralized system for voltage control, another one for DG control, a third one for protection, etc. Combining these techniques together to control a distribution system might result in a non-optimal performance.

Additionally, most of these decentralized control techniques can be described as “rigid” or “static” because changes in the system connectivity and addition/removal of components cannot be accommodated easily.

The analysis and control framework presented in this thesis is based on the concept of using multiple processing units to perform distributed power flow analysis and hence control and coordinate the different system components. In our implementation of the distributed power flow analysis, each bus in the system contributes to the analysis by calculating its own voltage, current, and power flow, and hence sharing the calculation results with its neighboring nodes. Therefore eliminating the need for system partitioning as in [46, 47, 48, 49], and hence creating a flexible framework that can accommodate system changes in an adaptive and dynamic manner.

In this thesis we propose an analysis and control framework for smart distribution system with the following characteristics:

1. Decentralized/distributed power flow analysis.
2. Uses real-time measurements from smart meters in the analysis.
3. Various control and coordination techniques for the different system components can be integrated into the analysis framework.
4. Communication network is used to support the exchange of information among the distributed processing units during the system analysis and control stages.
5. This framework can accommodate system changes in a flexible and dynamic manner due to the integration of the distribution and communication systems.

Chapters 3 and 4 provide a detailed description of the analysis and control framework and its main features and characteristics.

## 2.4 Wireless Communication Technology

Communication infrastructure is one of the main technological components involved in the smart grid and its components such as advanced metering infrastructure and distribution automation. It is clear from the literature review in section 2.3 that the communication infrastructure is an integral part of the smart distribution systems research. New smart grid applications are made possible only through the existence of a reliable and fast data communication network.

Worldwide Interoperability for Microwave Access (WiMAX) and Long Term Evolution (LTE) are the two primary broadband technologies used in 4G wireless networks. Both standards use several common technologies with subtle differences, for instance they both use Orthogonal Frequency Division Multiple Access (OFDMA) digital modulation scheme [58].

Both WiMAX and LTE technologies are suitable to support the smart grid implementation because of the large coverage distance they can provide and also because the latency requirement in both of them is small enough to support real-time applications [59].

WiMAX is a commercialization of the IEEE 802.16 standard which has been developed to support wireless communication over long distance ranges up to 31 miles (50 km) and with an expected maximum transmission rates up to 100 Mbps [60]. WiMAX technology has been adopted by multiple utilities in their smart grid implementation.

On the other hand, LTE is a high speed wireless communication standard developed by the 3GPP (3rd Generation Partnership Project) [61]. LTE can support transmission rates up to 300 Mbps with a cell size of up to and beyond 100 km [62].

The high level architecture of wireless communication networks such as WiMAX and LTE consists of three parts as shown in Figure 2.2:

1. The user equipment (UE) which is also known as the Subscriber Station (SS).
2. The radio access network which connects the UE to the network through a Base Station (BS) in a point-to-multipoint infrastructure.
3. The core network which routes user's voice and data to relevant destinations such as Public Switched Telephone Networks (PSTN) and Packet Data Networks (PDN).

This section provides a brief review of some of the basic characteristics of both the WiMAX and LTE technologies.

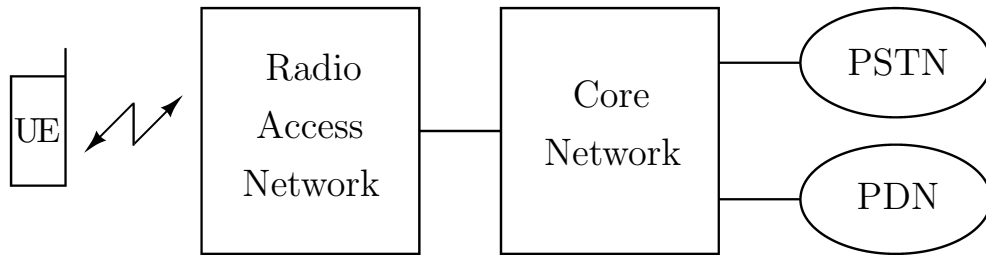


Figure 2.2: High level architecture of a wireless communication network

### 2.4.1 WiMAX [63, 64]

The Institute of Electrical and Electronics Engineers (IEEE) has developed a family of Wireless Metropolitan Area Network (W-MAN) standards collectively known as the IEEE 802.16 to deliver high data rates at large coverage ranges.

The IEEE 802.16 standard specifies the air interface, including the Media Access Control layer (MAC) and Physical Layer (PHY), of combined fixed and mobile point-to-multipoint broadband wireless access system providing multiple services.

Out of the seven layers of the Open System Interconnection (OSI) reference model, only two layers are described in 802.16 standard: the Data Link Layer and the Physical Layer as shown in Figure 2.3.

The physical layer is responsible for Forward Error Correction (FEC), interleaving, symbol mapping, and constructing the Orthogonal Frequency Division Multiplexing (OFDM) symbol in the frequency domain. Pilot symbols/subcarriers are transmitted to allow the receiver to estimate and track the channel state information. The final stage is to convert the OFDM symbol from the frequency domain to the time domain for transmission over the wireless channel.

The data link layer is divided into the Logical Link Control (LLC) layer which is defined in the IEEE 802.2 standard, and the Media Access Control (MAC) layer which is defined in the IEEE 802.16 for WiMAX networks. The MAC layer is further divided into three sub-layers:

1. The Convergence Sub-layer (CS) which is a service-specific layer that performs tasks such as header compression and address mapping.

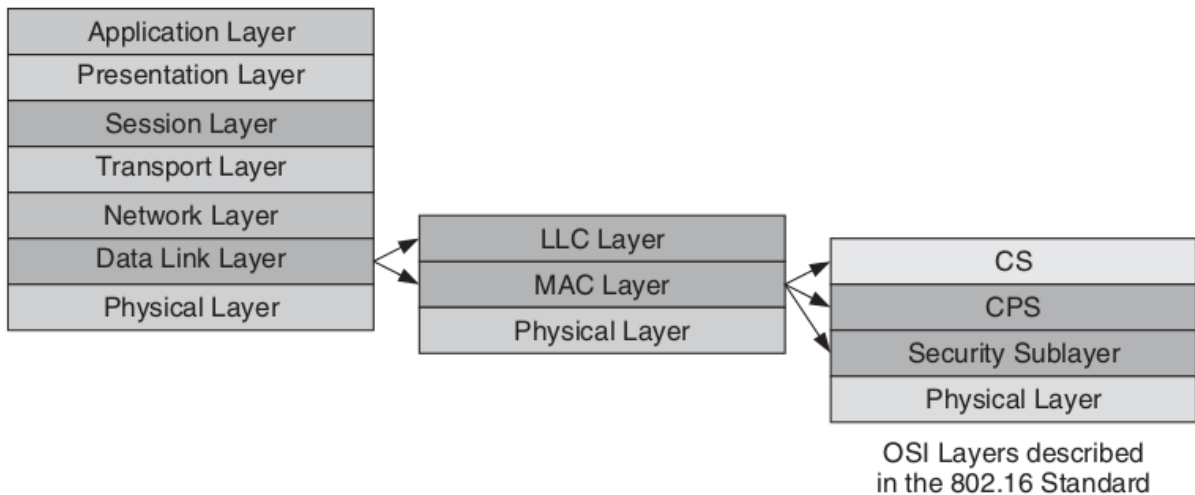


Figure 2.3: OSI layers, and the layers included in the IEEE 802.16 standard [64]

2. The Common-Part Sub-layer (CPS) which performs tasks that are independent of the higher layer such as fragmentation, concatenation, creating MAC Protocol Data Units (PDU), and Quality of Service (QoS) control.
3. The security sub-layer which is responsible for encryption, authorization, and proper exchange of keys between the BS and the SS.

The IEEE 802.16 standard support a multitude of configuration options and features that could lead to non-compatible networks if vendors choose different implementation options. For a complete end-to-end system, several additional service management aspects need to be specified. This task is being performed by the WiMAX Forum [63].

The WiMAX Forum [65] creates guidelines for an end-to-end WiMAX network architecture and the minimum features that should be supported by all vendors in order to make the WiMAX equipment interoperable. The WiMAX Forum enjoys broad participation from the industry including semiconductor companies, equipment manufacturers, and service providers.

### Features of WiMAX

1. The OFDM-based physical layer offers good resistance to multipath and allows non-line-of-sight operation.



2. High peak data rates up to 74 Mbps. The use of multiple antennas and spatial multiplexing can result in even higher data rates.
3. WiMAX systems can use a variety of different bandwidths up to a maximum of 20 MHz.
4. WiMAX supports adaptive modulation and coding (AMC) which selects the highest modulation and coding schemes that can be supported by the signal-to-noise and interference ratio at the receiver.
5. A scheduler is used to allocate both the uplink and downlink resources resulting in a flexible and dynamic per user resource allocation.
6. Advanced antenna techniques such as beamforming and space-time coding are supported by the WiMAX technology.
7. WiMAX can support variety of applications with different Quality-of-Service (QoS) requirements for real-time and non-real-time traffic flow.
8. The MAC layer is designed to support large number of users with multiple connections each with its own QoS requirement.
9. WiMAX provides robust security features for encryption and authentication.
10. The reference network architecture defined by the WiMAX Forum is IP-based, thereby facilitating easy convergence with other networks.

## **Quality of Service (QoS)**

The WiMAX standard offers multiple quality of service (QoS) categories which are defined as a set of requirements on the latency, data rate, packet error rate, and system availability.

A scheduling service is used to determine the mechanism the network uses to allocate uplink and downlink resources to meet the QoS requirements. Five QoS categories are defined:

1. The Unsolicited Grant Service (UGS) category is designed to support real-time services that generate fixed-size data packets on a periodic basis. Fixed-size resources are granted to the Subscriber Station (SS) on a real-time periodic basis therefore the SS does not need to explicitly request bandwidth thus eliminating the overhead and latency associated with bandwidth request.

2. The Real-Time Polling Service (rtPS) category is designed for real-time services that generate variable-size data packets in a periodic basis. The Base Station (BS) provides polling opportunities for the SS to request bandwidth therefor it requires more overhead than UGS does. The polling opportunities are frequent enough to ensure that the latency requirements of real-time services are met.
3. The Non-Real-Time Polling Service (nrtPS) category is very similar to rtPS except that the polling opportunities are less frequent (every few seconds), therefore the SS is allowed to use contention-based polling in the uplink to request bandwidth which can result in collisions and additional attempts.
4. The Best Effort service (BE) category provides very little QoS support where the data is sent whenever resources are available and not required by any other service classes. Only contention-based polling is allowed for SS to request bandwidth.
5. The Extended Real-Time Polling Service (ertPS) category is built on top of rtPS and UGS where the SS can request additional bandwidth during the uplink unlike therefore it can accommodate data services whose bandwidth requirements change with time. Unlike ertPS, UGS allows SS to request additional bandwidth during the uplink for only non-UGS-related connections.

## Security Functions

WiMAX systems are designed to ensure robust security, user data privacy, and preventing unauthorized access. The key aspects of WiMAX security are:

1. User data is encrypted to provide privacy using cryptographic schemes such as Advanced Encryption Standard (AES) and Triple Data Encryption Standard (3DES). The encryption key is generated during the authentication phase and is periodically refreshed for additional protection.
2. WiMAX uses the Extensible Authentication Protocol (EAP) for device/user authentication to prevent unauthorized access. EAP supports a variety of credentials such as username/password, digital certificates, and smart cards.
3. The Privacy and Key Management Protocol (PKM) is employed in WiMAX systems to securely exchange encryption keys between the BS and SS.
4. Message authentication codes are used to protect the integrity of over-the-air control messages.

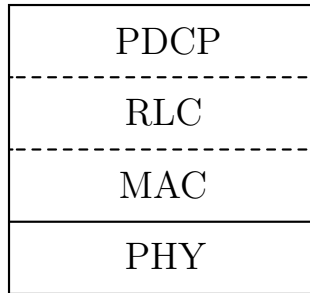


Figure 2.4: Protocol layers for LTE radio link

### 2.4.2 LTE: [64, 66]

The Long Term Evolution (LTE) wireless communication technology is designed by a collaboration of telecommunications standards bodies known as the Third Generation Partnership (3GPP) [61]. LTE evolved from an earlier 3GPP system known as the Universal Mobile Telecommunication System (UMTS), which in turn evolved from the Global System For Mobile Communications (GSM).

The LTE protocol layers are shown in Figure 2.4. The physical layer (PHY) applies error management procedures and creates OFDMA symbols for transmission. The data link layer is divided into three sub-layers [67]:

1. The Packet Data Convergence Protocol sub-player (PDCP), which is responsible for ciphering and IP header compression.
2. The Radio Link Control sub-layer (RLC), which performs data concatenation and segmentation, and ensures an ordered delivery of IP packets.
3. The Media Access Control layer (MAC), which is responsible for low level retransmission for lost data as well as scheduling both the uplink and downlink radio resources.

### LTE Features and Specifications

The requirements specification for the LTE air interface are:

1. High peak data rates of 300 Mbps for downlink and 75 Mbps for uplink. It is worth mentioning that these rates can only be reached in idealized conditions.

2. The time latency for a data packet to travel between the User Equipment (UE) and the fixed network should be less than 5 milliseconds in uncongested air interface.
3. LTE supports cell sizes up to 100 km.
4. LTE can work with a variety of bandwidths ranging from 1.4 MHz up to a maximum of 20 MHz.

The requirements specification for the LTE fixed network are:

1. The core network is all IP-based and provide users with an always-on connectivity.
2. There is no explicit requirement on the latency in the fixed network, but it is suggested that there is a latency of 10 milliseconds for a non roaming user. Considering the air interface and fixed network delays, a typical delay of around 20 milliseconds is estimated for non-roaming users.

### **Quality of Service (QoS)**

LTE specifies a variety of QoS classes identified by an 8-bit number which acts as a pointer into a look-up table that defines four QoS parameters as follows:

1. The resource type which indicates whether or not this class has a Guaranteed Bit Rate (GBR).
2. An upper bound on the packet error/loss rate.
3. An upper bound on the packet delay.
4. A priority level which is used in the scheduling process.

A detailed description of LTE standardized QoS classes can be found in [64, 66].

## Security Features

In LTE systems, the user's communications with the network across the air interface is protected using four main techniques:

1. The network and UE confirms each other identities through authentication.
2. Protecting the user's International Mobile Subscriber Identity (IMSI) by using temporary identities.
3. Encrypting the user's data and the signaling messages.
4. Integrity protection which detects any attempts by intruders to intercept the signaling messages and modify them in order to take control of the UE.

### 2.4.3 WiMAX vs. LTE

The discussion in subsections 2.4.1 and 2.4.2 shows that both the WiMAX and LTE communication networks share multiple features and use common technologies in modulation, encryption, authentication. Both technologies offer multiple QoS classes suitable for a variety of applications with different QoS requirements.

WiMAX and LTE infrastructure is all IP-based which facilitates their integration with packet data networks (PDNs). LTE networks can provide peak data rates up to 300 Mbps and cell sizes up to 100 km, whereas WiMAX networks provide peak data rates up to 74 Mbps and cell sizes up to 50 km. Our simulation results <sup>1</sup> indicates that LTE network exhibit smaller packet delays compared to WiMAX networks.

Both wireless technologies provide fast and reliable communication infrastructure that can support the smart grid implementation in general, and the distribution system analysis and control framework presented in this thesis in particular.

---

<sup>1</sup>NS-3 simulations of the distribution system analysis and control framework in which WiMAX and LTE were used as the communication infrastructure supporting the framework. The NS-3 simulation results of the power flow analysis can be found in chapter 3, while NS-3 simulation results of the distribution system control and coordination can be found in chapters 4, 5.

## 2.5 The Network Simulator NS-3

The distribution system analysis and control framework presented in this thesis represents an interdependent configuration of power and communication systems where the performance of the communication network (e.g. delays and packet delivery ratio) impacts the electrical power distribution system operation.

Therefore, simulation of both the electrical power distribution system and the supporting communication network is an important tool to assess the performance of the proposed analysis and control framework.

The network simulator NS-3 is an open-source discrete-event network simulator for internet systems, targeted primarily for research and educational use [16]. NS-3 provides simulation models for packet data networks that can be used to evaluate their performance.

The simulation core and models of NS-3 are implemented as a group of C++ software libraries that work together where user programs can also be linked with these libraries. User programs are written in either the C++ or Python programming languages. NS-3 is built as a library which can be linked to a C++ main program that defines the simulation topology and starts the simulator [68].

NS-3 includes models for a variety of data communication networks including Ethernet, WiFi, WiMAX, LTE, Underwater Acoustic Networks (UAN), and Wireless Access in Vehicular Environment (WAVE). Simulation models of point-to-point, mesh, ad-hoc, and point-to-multipoint networks are also available. Multiple routing protocols, mobility models, channel models, data collection and flow monitoring modules are also implemented in NS-3.

The distribution system analysis and control framework presented in this thesis is implemented as a set of C++ applications that are integrated into NS-3, therefore allowing the simulation of the distribution system analysis and control framework along with its supporting communication network.

The implementation details of the analysis and control framework as a set of C++ applications for NS-3 are presented in chapter 3, section 3.4.

NS-3 simulations generate two sets of results:

1. Power system results including voltage profiles, total system losses, status of switched capacitor banks, OLTC transformers, and DG units.
2. Communication system performance in terms of the average packets delay, average packet delivery ratio, and the analysis and control convergence times.

The simulation results for the power and communication systems obtained from GNU-Octave and NS-3 are presented in chapters 3, 4, and 5.

## 2.6 Summary

This chapter discussed the main features and characteristics of the smart grid and of smart distribution systems outlining the important role played by communication systems in the smart grid implementation.

Being an essential part of the proposed analysis and control framework, the backward/-forward power flow analysis method was reviewed in this chapter.

WiMAX and LTE wireless communication technologies were briefly discussed in this chapter as well. The two technologies can provide the data connectivity required for the analysis and control framework implementation.

A short review of the network simulator NS-3 was also presented. NS-3 is used throughout this thesis to simulate both the power and communication systems together.





# Chapter 3

## Decentralized/Distributed Power Flow Analysis for Distribution Systems

The distribution system analysis and control framework presented in this thesis is composed of two main parts, the online decentralized/distributed power flow analysis engine, and multiple online control techniques for the different system components.

This chapter presents a detailed description of the online decentralized/distributed power flow analysis technique used and its implementation using multiple processing units equipped with wireless communication transceivers. The next chapter presents the details of the online control and coordination techniques for the different distribution system components.

NS-3 implementation of the decentralized/distributed power flow analysis is also presented in this chapter. The decentralized/distributed power flow analysis technique is implemented as a set of C++ applications which are integrated into the network simulator NS-3, therefore allowing the simulation of both the distributed power flow analysis technique and the supporting communication network.

### 3.1 Introduction

The literature review presented in chapter 2 clearly identifies three technological components as the main pillars of smart grid implementation, distributed intelligence, communi-

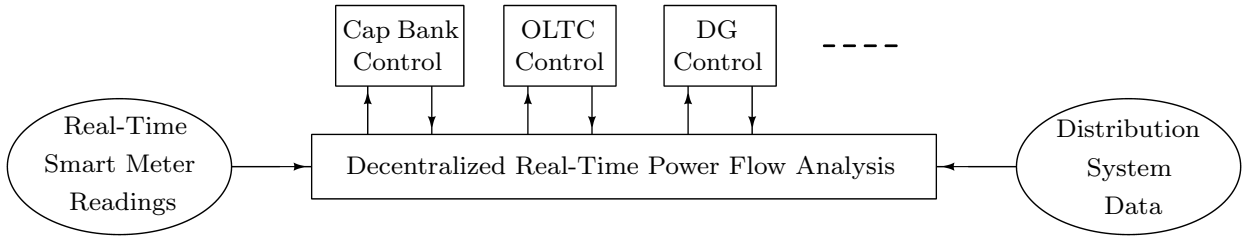


Figure 3.1: Architecture of the proposed distribution system analysis and control framework

cation networks, and automated control techniques.

In this thesis, we propose a unified and flexible framework that integrate these three components together in order to implement the smart grid vision in electrical power distribution systems. The architecture of the proposed framework is depicted in Figure 3.1.

The proposed analysis and control framework is composed of two main parts as illustrated in in Figure 3.1:

1. The online decentralized/distributed power flow analysis which employs multiple distributed processing units collaborating together and exchanging information in order to calculate the voltages, currents, losses, and power flow at each node and branch in the distribution system. This is achieved by combining the distribution system data with the real-time measurements provided by the smart meters.
2. Multiple online control techniques for the different system components such as capacitor banks, DG units, OLTC, etc. The operation of those control techniques is based on the decentralized/distributed power flow analysis calculations.

Using the decentralized/distributed power flow analysis calculations as the basis for the control system prevents any contradicting control decisions, therefore leading to a “seamless” coordination among the different distribution system components.

A detailed description of the decentralized/distributed power flow analysis for distribution systems, its implementation, and simulation are presented in this chapter. The Control techniques for switched capacitor banks and DG units are described in chapter 4.

The rest of this chapter is organized as follows, section 3.2 describes the distribution system model and the implementation details of the “distributed” power flow analysis.

The three main components of the system model are the “node”, “connectivity matrix”, and the “Zone Control Unit” (ZCU).

The execution of the “distributed” power flow analysis is presented in section 3.3. Section 3.4 discusses the C++ implementation of the analysis and control framework for the network simulator NS-3.

GNU-Octave and NS-3 simulations results are presented in section 3.5, while section 3.6 include a brief summary of this chapter and some concluding remarks.

## 3.2 System Model and Assumptions

The distribution system starts at the distribution substation from which multiple feeders fan out toward the customers, typically in a radial structure.

In a pure radial distribution system, only one path exists between any two nodes in the system, which simplifies the neighborhood relationships between nodes because each node has a unique parent, and one or more children, hence a simple parent/child relationship can be used to describe the connectivity between nodes.

Using graph theory terminology, if the distribution system is modeled as a graph, a pure radial system will be a tree. The vertices in this graph represent nodes in the distribution system, and the edges represent the neighborhood relationships.

An edge between two nodes represent electrical power connectivity and communication connectivity as well. In other words, neighborhood means electrical power and data packets can flow between neighbors.

In the proposed analysis and control framework, the distribution system is divided into *zones*, each feeder with its branches, capacitors, DG units, transformers, etc. is considered to be one zone. Figure 3.2 shows a typical distribution substation with  $N$  feeders, each feeder constitutes a separate zone in the system. Figure 3.3 shows a typical distribution system feeder (zone) and its components.

Each zone in the system is comprised of three basic components: nodes, a connectivity matrix, and a zone control unit (ZCU).

### 3.2.1 Node

Within each zone (feeder), a processing unit (a smart agent) is installed at each bus that has a DG unit, capacitor bank, regulating transformer, customer load, or multiple children.

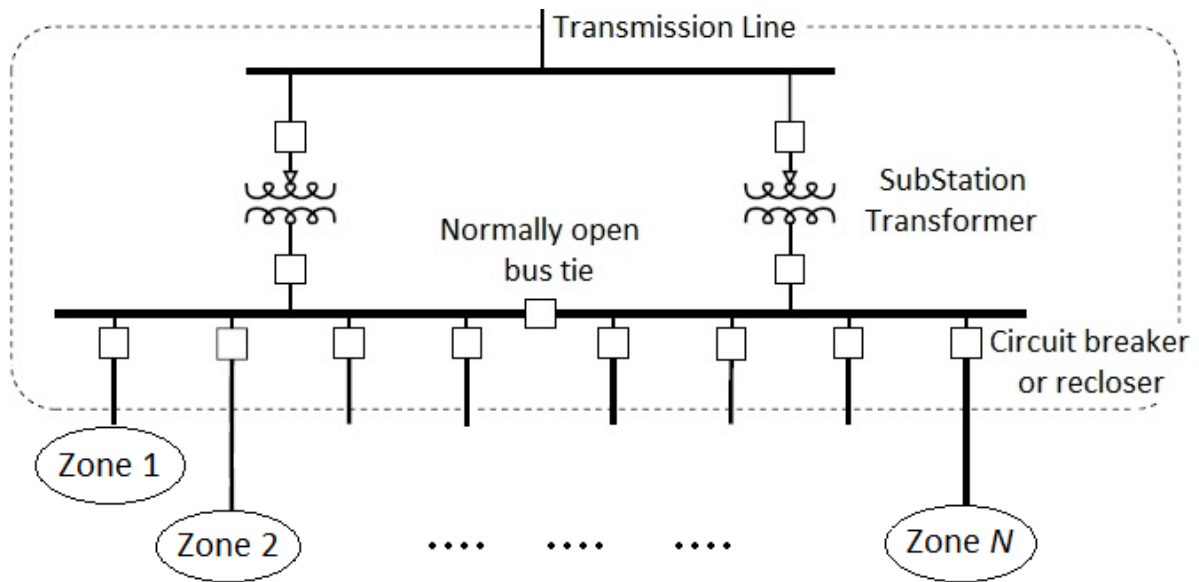


Figure 3.2: An  $N$  zone distribution system

This agent/bus combination is referred to as the *Node*. Few nodes are shown in Figure 3.3 as an illustration; nodes 0 and 1 are installed on the primary and secondary sides of the voltage regulator, node 1 is also responsible for the installed capacitor bank. Nodes 2 and 3 are installed on the primary and secondary sides of the in-line transformer, and they also have multiple children.

Each node is identified by two sets of information as illustrated in Figure 3.4. One set contains the electrical Power Aspects of the Node (PAN), and the other set includes the Communication Link Aspects of the Node (CAN).

The PAN set of information contains:

1. Unique ID of the node
2. Type of the node, e.g., slack bus, load bus, or generator bus
3. Specific information about each bus type, e.g., the generated power for a generator bus, or the demand in the case of a load bus (obtained from smart meters)
4. The devices connected to the node: capacitors, regulators, DG units, etc.

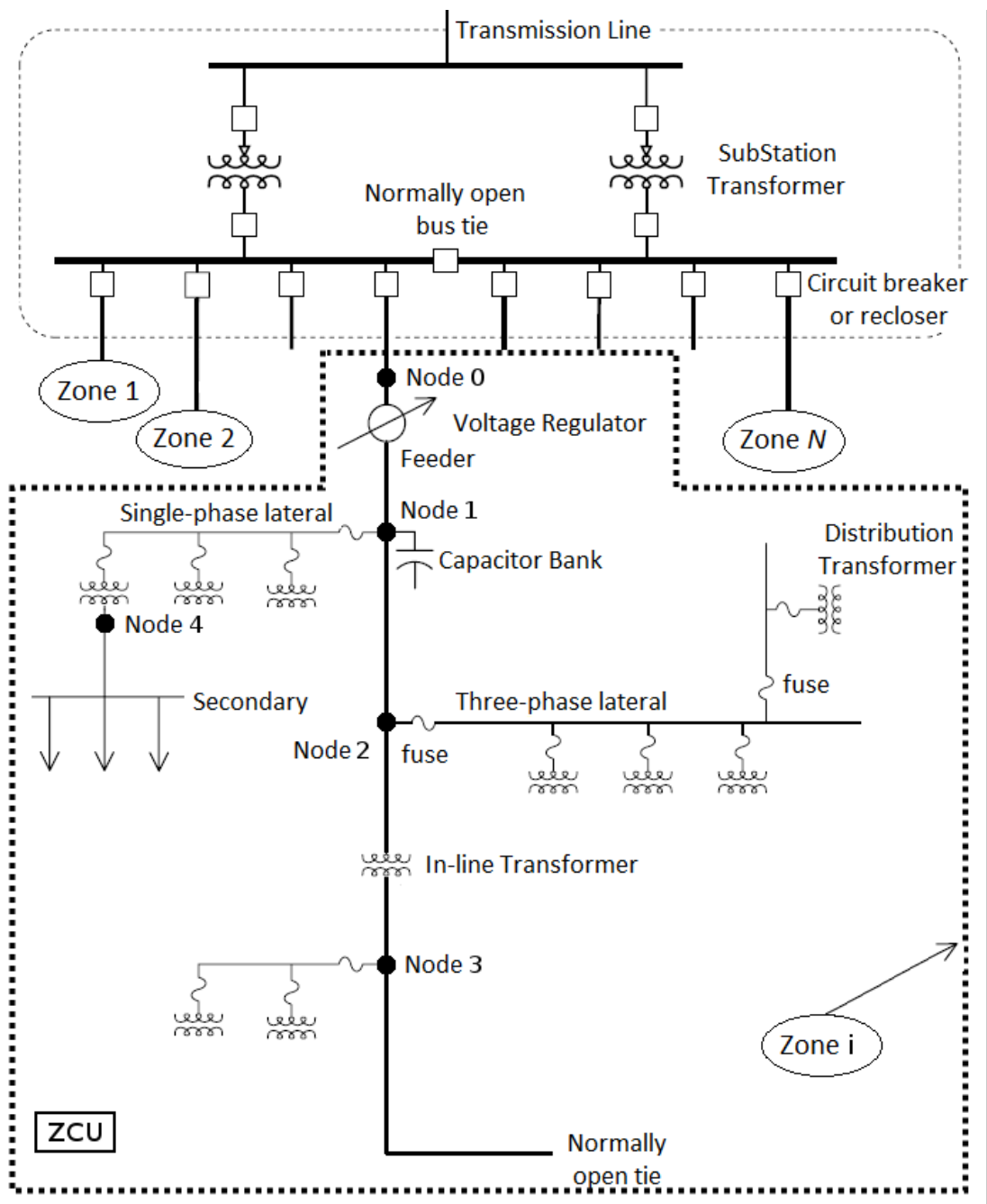


Figure 3.3: A typical distribution system feeder (a zone)

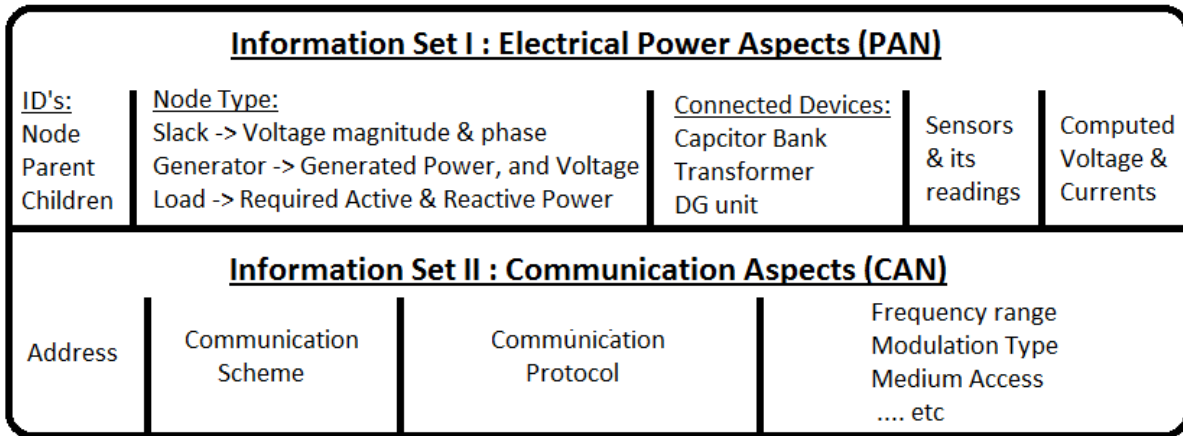


Figure 3.4: Information sets associated with the proposed node structure

5. The status of these devices, e.g., the injected reactive power from the connected capacitor or the tap setting of the transformer
6. The sensing devices connected to this node and their readings
7. The IDs of the node's parent and children, and the line impedance connecting the node to its parent and children
8. The computed voltage, current, power, and losses for the node

Most of this information is updated in real-time, allowing the analysis to include any changes in the demand, power generated, capacitor reactive power, transformer tap settings, etc.

The CAN set contains the following communication link information:

1. A unique address for the node, e.g., the MAC address and the IP address
2. The communication scheme used, e.g., a wireless mesh network or the a BS/SS scheme
3. The communication protocol in use, e.g., WiMAX or LTE
4. The communication frequency range, modulation type, medium-access techniques, etc.

### 3.2.2 Connectivity Matrix

In each zone, two layers of connectivity are defined: electrical power connectivity and communication connectivity. These two layers are threaded together to enable real-time distributed system analysis and control.

1. Electrical power connectivity layer:

The different nodes in a distribution system are usually connected radially, each node is connected to a parent node plus one or more children. Therefore the electrical power connectivity can be described in terms of this parent/children relationship.

The distribution feeder starts at the distribution substation, which is designated as the root node (i.e. it has no parent), and ends with multiple leaf nodes (i.e. they have no children).

In this layer, the exact network topology along with the parameters of the cables or the overhead lines must be identified for each zone, and the real-time load power at each customer node is obtained from the smart meters.

2. Communication connectivity layer:

The communication in this layer can be further divided into three different types:

- (a) Intra-node communication:

This type of communication includes the communication that occurs between the smart agent attached to this node and the other devices connected to the same node, such as smart meters, capacitor banks, voltage regulators, and DG units. This kind of communication guarantees that the smart agent has the most updated information about the status of these devices which is used in the real-time analysis.

- (b) Intra-zone communication:

Within any zone, the nodes must communicate with their parents and child nodes in order to exchange information about the distribution system and the calculated parameters.

- (c) Inter-zone communication:

To allow the exchange of information among different zones.

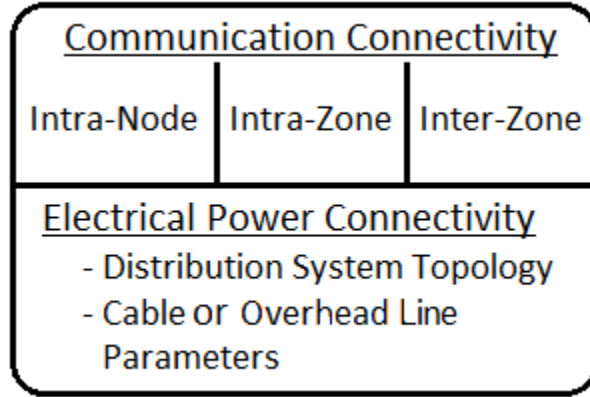


Figure 3.5: Power and communication connectivity layers

Figure 3.5 shows the power and communication connectivity layers as defined with the proposed analysis and control framework. It is worth mentioning that for all NS-3 simulations presented throughout this thesis, the intra-node and the inter-zone communication have *not* been implemented, only the intra-zone communication among the nodes within the same zone has been implemented and simulated using NS-3.

As described in subsection 3.2.1, each node stores the IP addresses of its parent and children, and uses these addresses to exchange the power flow analysis calculations. Therefore the electrical power connectivity is defined and maintained through the communication system connectivity.

This interdependent power and communication systems connectivity results in a flexible analysis and control framework that can dynamically accommodate any changes in the power system connectivity by simply updating the IP addresses of the parents and children, which is immediately reflected on the power flow analysis calculations and hence on the control decisions.

The capability to dynamically adapt to changes in the electrical power system is one of the important characteristics of the proposed analysis and control framework.

### 3.2.3 Zone Control Unit (ZCU)

Each zone in the system has a Zone Control Unit (ZCU) as illustrated in Figure 3.3. The ZCU is responsible for initiating and terminating the analysis, keeping track of the



backward and forward iterations, as well as collecting relevant information from all the nodes within that zone.

The ZCU acts as an “information hub” in which the collected information is aggregated to create some sort of “common knowledge” which is shared with all the nodes in the zone and used for control and coordination purposes.

For instance, the ZCU receives the following information from each node within its zone:

1. Calculated losses in the line-segments between the node and its parent and children.
2. Whether the voltage difference in the past two consecutive iterations is less than the allowed voltage tolerance  $\epsilon$ .
3. Whether the calculated voltage violates the maximum and minimum allowed voltage limit.

This information is aggregated by the ZCU to calculate the total system losses, decide on the analysis convergence, and perform voltage control.

### **3.3 Execution of the Decentralized/Distributed Power Flow Analysis**

As illustrated in Figure 3.1, the power flow analysis is the basis for the control and coordination among the different system components. This section describes the “distributed” execution of the backward/forward sweep method described in chapter 2, section 2.2.

According to the system model described in section 3.2, each node has processing and communication capabilities such that it can exchange information with its neighbors, and process the received and local information. Therefore, all the nodes within a particular zone can collaborate together to perform power flow analysis for the whole feeder using the “distributed” implementation of the backward/forward sweep method.

The ZCU initiates the analysis by triggering the leaf nodes to start the backward sweep, in which each node uses its local and received information to calculate the total load current (its own load current plus its children load currents), and reports that total load current to its parent over the communication network.

The process continues until the root node is reached, this ends the backward sweep and starts the forward sweep. Knowing the calculated load current and the line impedance to each one of its children, the root node calculates the updated values of the children voltages, communication links are used to transmit these calculated voltages to the respective nodes. The process continues until all the leaf nodes are reached, this ends one iteration.

At the end of an iteration, each node reports to the ZCU whether the voltage difference between the last two consecutive iterations is less than the specified voltage tolerance  $\epsilon$ , this allows the ZCU to decide whether the system analysis has converged.

Each node reports additional information to the ZCU such as the calculated losses in the line-segment connecting the node to its parent, and whether the calculated voltage violates the maximum or minimum allowed voltage levels. This information is used by the control techniques described in chapters 4 and 5 in order to reduce the system losses and perform Voltage/VAR Control (VVC).

It is clear from this discussion that the proposed analysis and control framework utilizes the communication network differently. The communication links in this framework are not just used to send/receive the control signal, it is rather deeply involved in the system analysis, and in the decision making process.

This threading of communication and electrical power distribution systems allows the framework to use the real-time measurements obtained from AMI systems, include the continuously changing parameters of renewable DG units into the calculations, and dynamically and easily adapt to the power system connectivity changes.

The implementation and execution of the proposed analysis and control framework with its three components (i.e. the node, the connectivity matrix, and the ZCU) are illustrated in Figure 3.6.

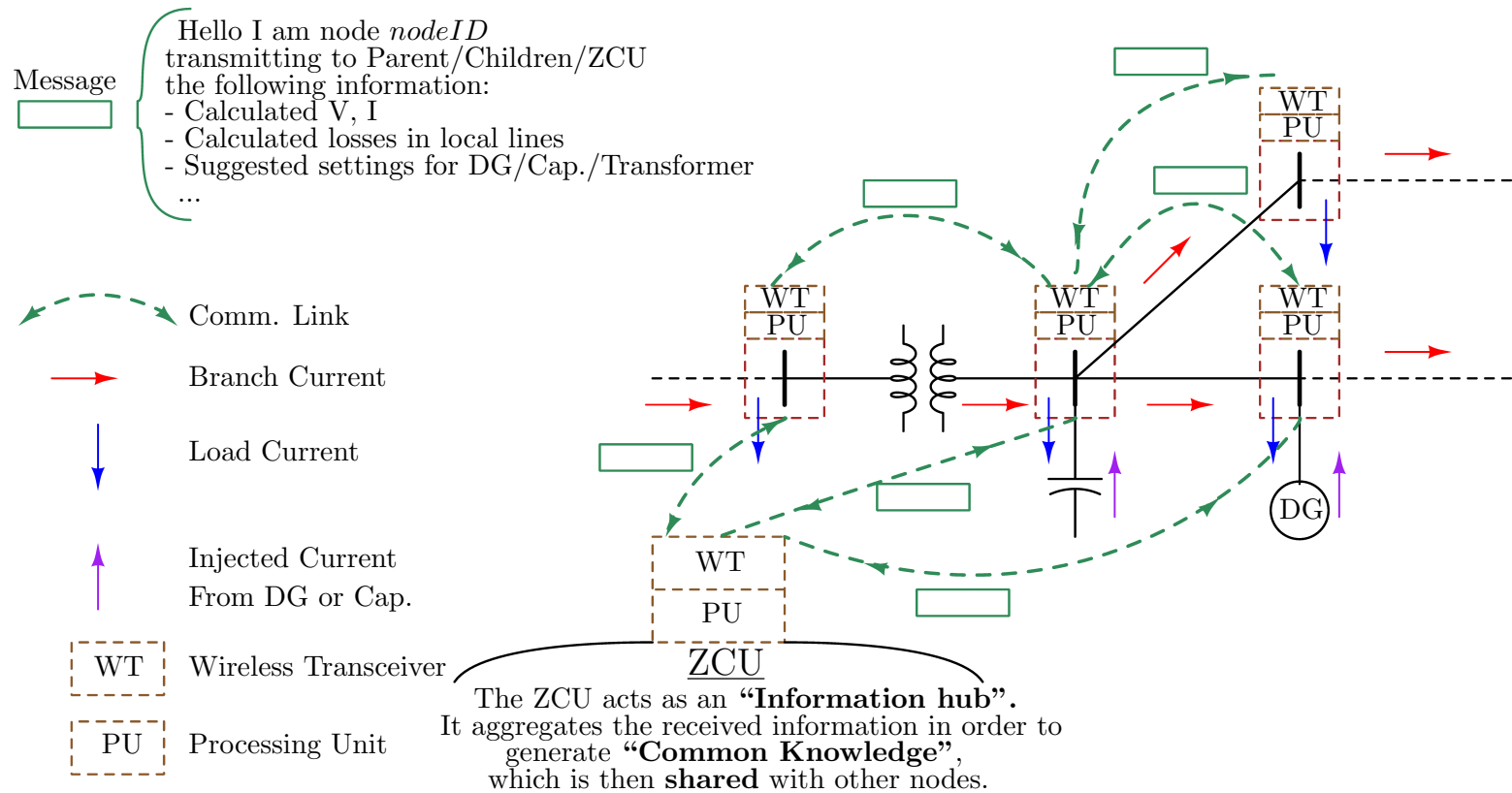


Figure 3.6: Implementation of the proposed analysis and control framework

## 3.4 NS-3 Implementation of the Decentralized / Distributed Power Flow Analysis

NS-3 is a discrete-time network simulator for internet systems built using C++ programming language. NS-3 is designed as a set of libraries that can be combined together and also with other external software libraries [69].

The decentralized/distributed power flow analysis presented in sections 3.2 and 3.3 is implemented as an external C++ software library that is integrated into the network simulator NS-3 in order to allow the simulation of the proposed decentralized/distributed power flow analysis and the communication network supporting its operation.

Figure 3.7 outlines the structure of the C++ library we built with its three main classes, namely *BuildNetworkTopology*, *DspfApp* and *ZcuApp*.

The class *BuildNetworkTopology* extracts the distribution system data and node connectivity matrix from an input binary file (created by GNU-Octave) which is then used to setup NS-3 simulation. The functionality of the ZCU and of the regular distribution system node is implemented in the *ZcuApp* and *DspfApp* classes respectively.

### 3.4.1 Data Connectivity

In the context of establishing the data connectivity among the system nodes, three basic concepts need to be briefly discussed:

- Client/Server Communication Model:  
In client/server communication model, clients and servers are separate logical objects that communicate over a network to perform tasks together. A client makes a request for a service and receives a reply to that request; a server receives and processes a request, and sends back the required response[70].
- Transmission Control Protocol (TCP):  
TCP is a connection-oriented transport protocol that sends data as stream of bytes. By using sequence numbers and acknowledgment messages, TCP can provide a sending node with delivery information about packets transmitted to a destination node. If data has been lost in transit from source to destination, TCP can retransmit the data until either a timeout condition is reached or until successful delivery has been achieved. TCP can also recognize duplicate messages and will discard them appropriately. If the sending computer is transmitting too fast for the receiving computer,

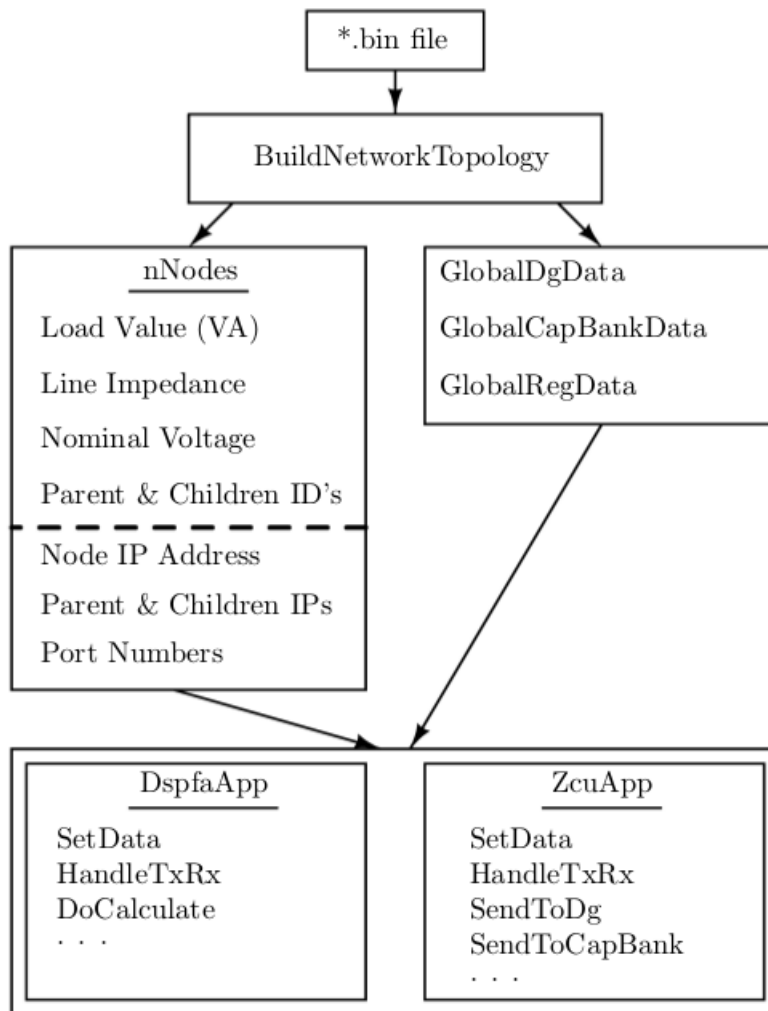


Figure 3.7: NS-3 implementation of the framework.

TCP can employ flow control mechanisms to slow data transfer. All these characteristics makes TCP an end-to-end reliable transport protocol [71]. TCP is specified in RFC 793 [72].

- Sockets:

A network socket is an endpoint of an inter-process communication flow across a computer network. Today, most communication between computers is based on the Internet Protocol; therefore most network sockets are Internet sockets. Sockets provide a standard protocol-independent interface between the application-level programs and the TCP/IP protocol stack [73]. More details on TCP sockets for Linux and on socket programming using C/C++ are provided in chapter 6.

The data communication connectivity among the different distribution system nodes within the zone is established following the client/server communication model using TCP sockets. A server is setup on the ZCU and on each distribution system node with children. Each node in the system must establish a TCP connection with its parent and with the ZCU before the analysis and control framework can start its operation.

### 3.4.2 *BuildNetworkTopology* Class

The class *BuildNetworkTopology* extracts the distribution system data, the node connectivity matrix, and the information related to the attached devices (e.g. DG units, capacitor bank, transformer) from an input binary file generated by GNU Octave. This information is extracted into corresponding data structures as follows:

1. The electrical power connectivity information for each individual node is stored in the data structure *nNodes* which contains:
  - (a) IDs of node, parent and children.
  - (b) Node's active and reactive load power (acquired from smart meter).
  - (c) Line impedance from the node to its parent and children.
  - (d) The node's initial voltage.
2. Information about the electrical power devices attached to each node:
  - (a) Distributed generation (DG) unit information such as the rated power and the allowed range of power factor is stored in the data structure *GlobalDgData*.

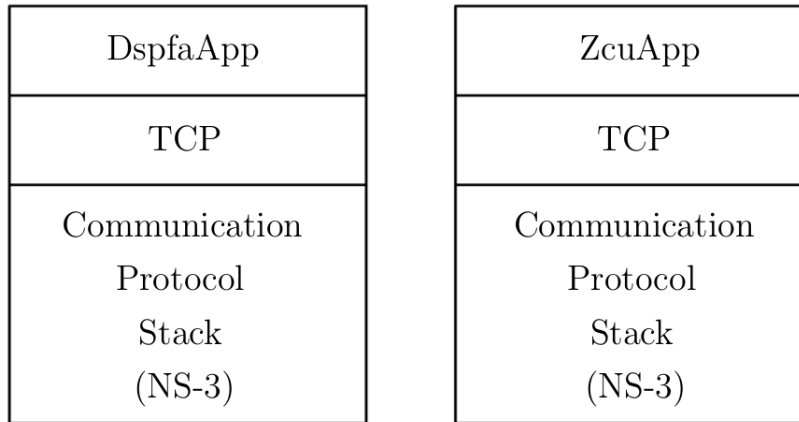


Figure 3.8: *DspfaApp* & *ZcuApp* nodes

- (b) Switched capacitor bank information such as the number of stages and the injected reactive power of each stage is stored in the data structure ***GlobalCapBankData***.
- (c) Voltage regulating transformer information such as the transformer's impedance and the regulation ratio is stored in the data structure ***GlobalRegData***.

The extracted information, which describes a specific distribution system, is employed by another C++ script that automatically setup the corresponding communication network simulation within NS-3. IP addresses and port numbers are assigned to each node and stored in the data structure ***nNodes***.

Once the communication network is setup, the appropriate application (either ***DspfaApp*** or ***ZcuApp***) is installed on each communication node as shown in Figure 3.8. The power and communication systems information stored in the data structure ***nNodes*** is used to set the data for each individual node, this data includes the IP addresses of parent, children, and ZCU, and the complex load power, line impedance, etc.

To provide a reliable, ordered and error-checked data delivery, the Transmission Control Protocol (TCP) is used as the transport layer protocol.

### 3.4.3 *DspfaApp* Class

Within the context of the proposed analysis and control framework, all the nodes in the system collaborate together to perform Distribution System Power Flow Analysis (*Dspfa*) which is used as the basis for the control decisions. This functionality is implemented in the class *DspfaApp* which has multiple member functions used to setup and run NS-3 simulations as illustrated in Figure 3.7.

1. The following member functions of the class *DspfaApp* are used during NS-3 simulation setup for each individual node:
  - (a) *SetParentAddress*: sets the parent IP address and its listening port number.
  - (b) *SetChildrenAddress*: sets the children IP addresses.
  - (c) *SetPeripheralData*: sets the data of attached power devices such as a DG unit, a switched capacitor bank or a voltage regulating transformer.
  - (d) *SetListeningPort*: sets the listening port of the server created in the node.
  - (e) *SetZcuAddress*: sets the IP address and listening port number of the ZCU.
2. The following member functions of the class *DspfaApp* are used while NS-3 simulation is running for each individual node:
  - (a) *StartApplication*: creates a server and waits for incoming connections from the children nodes, and also create a connection with the server installed in the ZCU node.
  - (b) *HandleTxRx*: handles the data transmission and reception over TCP sockets and calls other member functions to process the received data depending on the data source (e.g. parent, children or ZCU).
  - (c) *DoCalculate*: perform the power system calculations based on the received information as well as the locally available information and report the calculation results to the ZCU, parent and children nodes.
  - (d) *DgControl, CapBankControl, RegControl*: take control decisions for the attached devices (if any) based on the results of the power system calculations. The details of the DG control and switched capacitor bank control are described in chapter 4, whereas the details of voltage regulator control are described in chapter 5.



### 3.4.4 *ZcuApp* Class

The ZCU acts as an information hub that collects and aggregates relevant information from each node in the system creating a common-knowledge that is shared with all the system nodes. The collected information include the calculated losses, whether the calculated voltage of each node is within the specified maximum and minimum voltage limits, and whether the difference between the calculated voltage values for the last two consecutive iterations is less than  $\epsilon$  for each node.

Several data tables are maintained in the ZCU to store the communication parameters as well as the power system parameters of each node in the system including nodes with DG units, switched capacitor banks and voltage regulating transformers.

The ZCU functionality is implemented in the *ZcuApp* class which include multiple member functions used during the simulation setup as well as while the simulation is running as illustrated in Figure 3.7.

1. During NS-3 simulation setup, the following member functions are used:
  - (a) ***SetListeningPort***: sets the listening port of the server created on the ZCU.
  - (b) ***SetSystemData***: informs the ZCU with the total number of nodes in the system as well as the number of DG units, switched capacitor banks and voltage regulating transformers.
2. The following member functions are used while NS-3 simulation is running:
  - (a) ***StartApplication***: creates a server and waits for incoming connections. The power flow analysis is initiated once a connection is established with all the nodes in the zone.
  - (b) ***HandleTxRx***: handle the data transmission and reception over TCP sockets.
  - (c) ***PopulateDataTables***: uses the received data to populate and update the data tables of DG units, switched capacitor banks, and transformers, etc.
  - (d) ***DoCheck***: examines the received and stored data to calculate some parameters (e.g. total system losses) and decide whether to continue or terminate the analysis.

This C++ implementation is used in all NS-3 simulations throughout this thesis, and is combined with C/C++ Linux socket programming (a.k.a. network programming) to create the software component of the test bed implementation described in chapter 6.

## 3.5 Simulation Results

In this section, the performance of the online decentralized/distributed implementation of the backward/forward power flow analysis described in sections 3.2 and 3.3 is evaluated through GNU-Octave and NS-3 simulations. Three balanced radial distribution systems are used in these simulations.

Two sets of results are presented in this section:

1. Results related to the distribution system power flow analysis such as the voltage profile and system losses. Three sets of voltage profiles are compared in order to demonstrate the validity and accuracy of the proposed approach:
  - (a) The voltage profile obtained from GNU Octave simulation.
  - (b) The voltage profile obtained from NS-3 simulation.
  - (c) The voltage profile obtained from commercial power flow tools or reported in literature.
2. Results related to the performance of the communication network supporting the distributed power flow analysis. The performance of both WiMAX and LTE technologies is evaluated in terms of:
  - (a) Average packet delay.
  - (b) Average packet delivery ratio.
  - (c) Average convergence time.

For all the simulations in this section, the maximum allowed voltage tolerance for the backward/forward sweep method is  $\epsilon = 10^{-5}$  p.u., and the data packets are transmitted every 100 milliseconds for both WiMAX and LTE simulations.

### 3.5.1 18-Bus Distribution System

GNU-Octave and NS-3 implementations of the proposed distributed backward/forward sweep method are used to perform power flow analysis for the 18-bus radial balanced distribution system shown in Figure 3.9. The Distribution system parameters are given in [74].

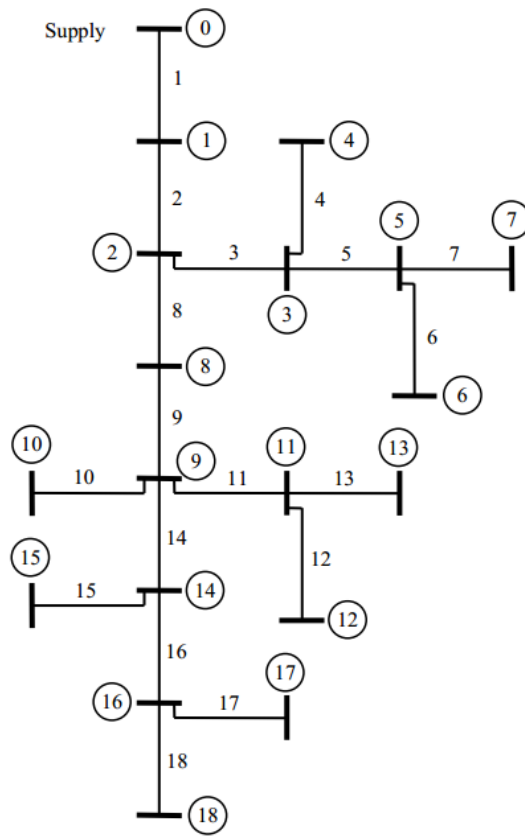


Figure 3.9: 18-bus radial balanced distribution system [74]

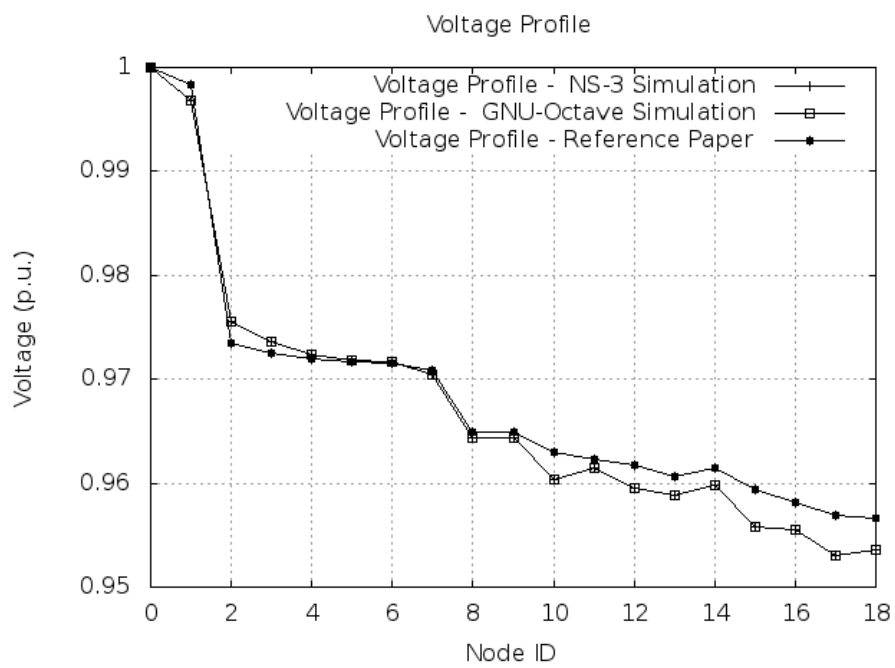


Figure 3.10: Voltage profile of the 18-bus system

Table 3.1: WiMAX and LTE performance comparison - NS-3 simulation of the 18-bus system

	WiMAX	LTE
Average packet delay (ms)	71.2	15.1
Average packet delivery ratio (%)	93.2	99.8
Convergence time (s)	16.2	10.8

Table 3.2: WiMAX and LTE performance comparison - NS-3 simulation of the 18-bus system with automatic voltage regulator

	WiMAX	LTE
Average packet delay (ms)	64.7	15.0
Average packet delivery ratio (%)	94.3	99.8
Convergence time (s)	19.3	13.1

Three voltage profiles are compared in Figure 3.10, the voltage profiles obtained from GNU-Octave and from NS-3 are identical to each other and they are both very close to the voltage profile reported in [74] with a maximum deviation of 0.38%.

The performance of both WiMAX and LTE communication networks is summarized in Table 3.1. LTE provides smaller average packet delays, better packet delivery ratio, and faster convergence time for the distributed power flow analysis.

An automatic voltage regulator is added between nodes 8 and 9 with a set voltage of 1.03 p.u. at the secondary side. The voltage profiles are shown in Figure 3.11, while the communication network performance is summarized in Table 3.2. GNU-Octave and NS-3 voltage profiles are identical and they are both very close to the voltage profile reported in [74], the maximum difference is 0.42%.

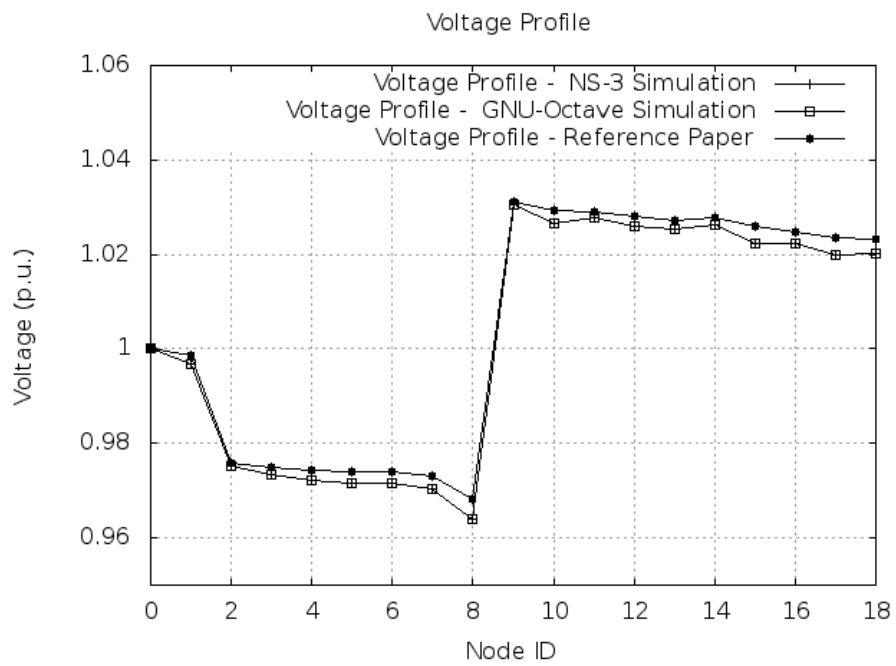


Figure 3.11: Voltage profile of the 18-bus system with automatic voltage regulator

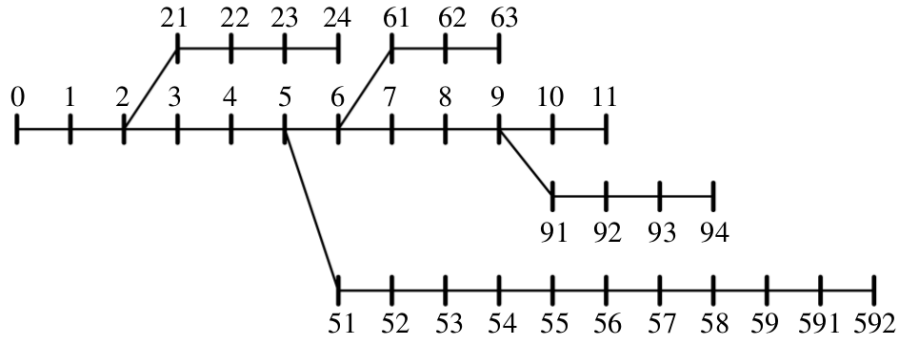


Figure 3.12: 34-bus distribution system

### 3.5.2 34-Bus Distribution System

The 34-bus radial balanced distribution system shown in Figure 3.12 is used to assess the performance of the proposed “distributed” power flow analysis and its supporting wireless communication network. The peak load values and the line impedance of this distribution system is given in [75]. This system has long laterals and is equipped with capacitors and voltage regulators at some nodes.

Figure 3.13 compares the voltage profiles on the main feeder obtained from GNU Octave simulations and those reported in [75] for three cases:

- a) The distribution system with 1050 kVAR and 600 kVAR capacitors at nodes 4 and 55 respectively, and a voltage regulator setting of 1.025: in this case the maximum voltage difference is 0.33%.
- b) The distribution system with 1050 kVAR and 600 kVAR capacitors at nodes 4 and 55 respectively, and no voltage regulator: in this case the maximum voltage difference is 0.43%.
- c) The distribution system with no capacitors and no voltage regulator: in this case, the maximum voltage difference is 0.14%.

Figure 3.14 compares the voltage profile obtained from GNU-Octave, NS-3, and from [75] for the case with two capacitors and voltage regulator. NS-3 and GNU-Octave voltage profiles are identical and they are both very close to the voltage profile in [75] with a maximum voltage difference of 0.33%.

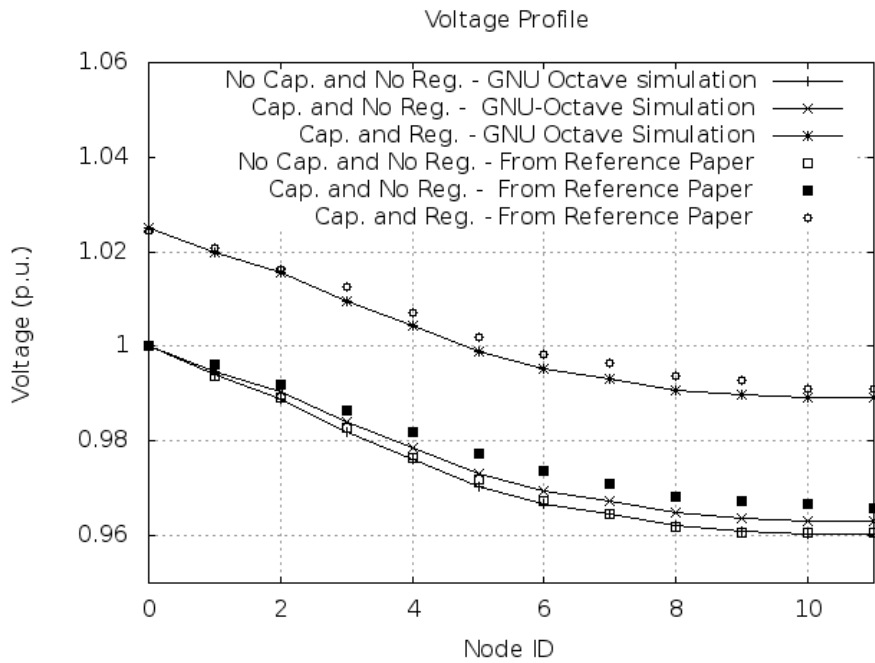


Figure 3.13: Voltage profile profile on the main feeder: comparison of the data obtained using the proposed algorithm with the data reported in [75] (a) with capacitors and voltage regulator tap setting at 1.025; (b) with capacitors and no voltage regulator action; (c) with no capacitors and no voltage regulator action



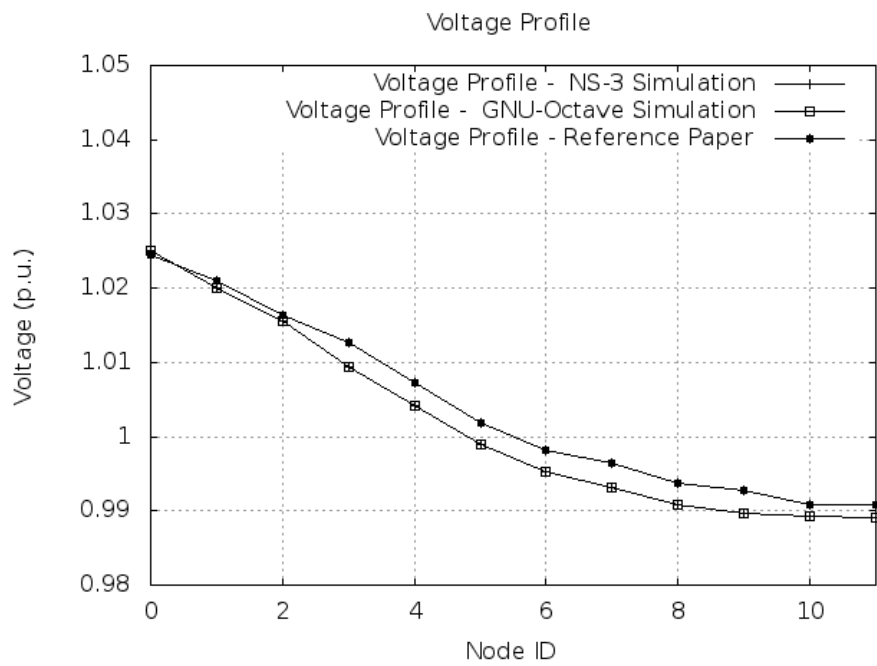


Figure 3.14: Voltage profile of the 34-bus system with capacitors and voltage regulator

Table 3.3: WiMAX and LTE performance comparison - NS-3 simulation of the 34-bus system

	WiMAX	LTE
Average packet delay (ms)	56.0	15.2
Average packet delivery ratio (%)	92.8	99.9
Convergence time (s)	30.9	24.0

Table 3.3 summarizes the performance of both WiMAX and LTE communication networks. LTE provides relatively better performance in terms of the packet delays, packet delivery ratio, and convergence time.

### 3.5.3 69-Bus Distribution System

To further assess the wireless communication network performance for larger distribution systems, the proposed “distributed” power flow analysis is applied to the 69-bus distribution feeder shown in Figure 3.15. The system parameters are given in [76].

The voltage profile reported in [77] is compared with those obtained from GNU Octave and NS-3 simulations of the proposed distributed power flow analysis. Figures 3.16 and 3.17 show the voltage profile on the main feeder (nodes 0 to 26) and on one of the laterals (nodes 42 to 54).

The voltage profiles obtained from GNU Octave and NS-3 are identical, and are very close to the profile reported in [77] with a maximum voltage deviation of 0.08%.

Table 3.4 indicates that LTE technology provides better performance than the WiMAX technology which is similar to the results reported in subsections 3.5.1 and 3.5.2.

Table 3.5 compares the maximum differences between the on-line calculated voltages using the proposed “distributed” power flow analysis and those reported in corresponding reference papers for the three distribution systems used in subsections 3.5.1, 3.5.2, and 3.5.3.

The results summarized in Table 3.5 indicate that the proposed “distributed” power flow analysis can accurately calculate the voltage profile of the feeder with a maximum error of 0.42%.

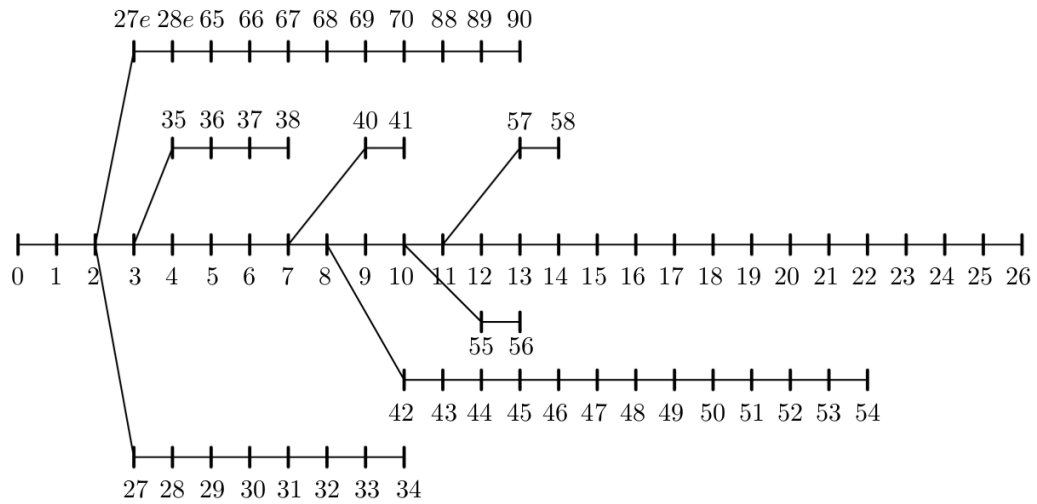


Figure 3.15: 69-bus radial distribution system

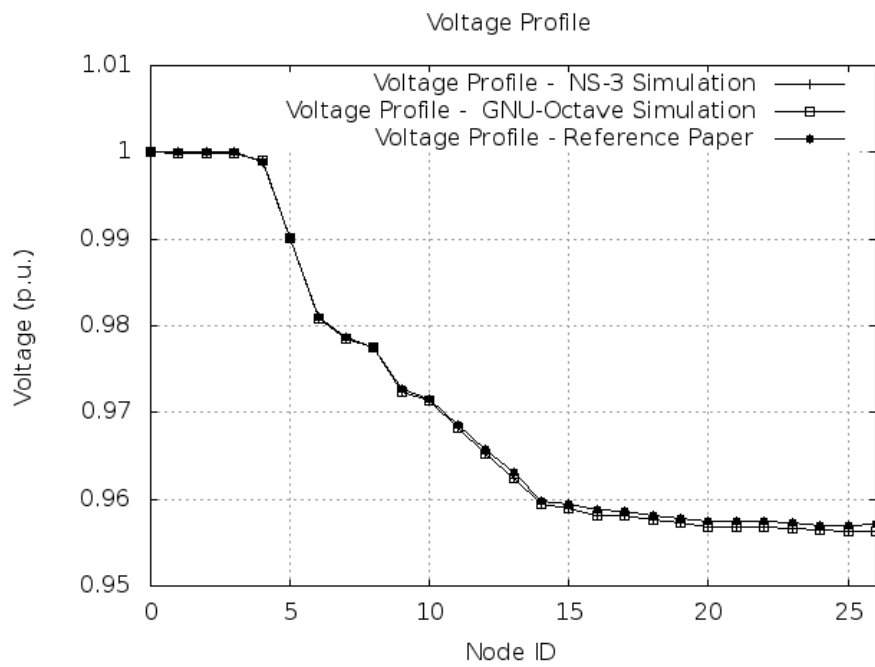


Figure 3.16: Voltage profile on the main feeder of the 69-bus system

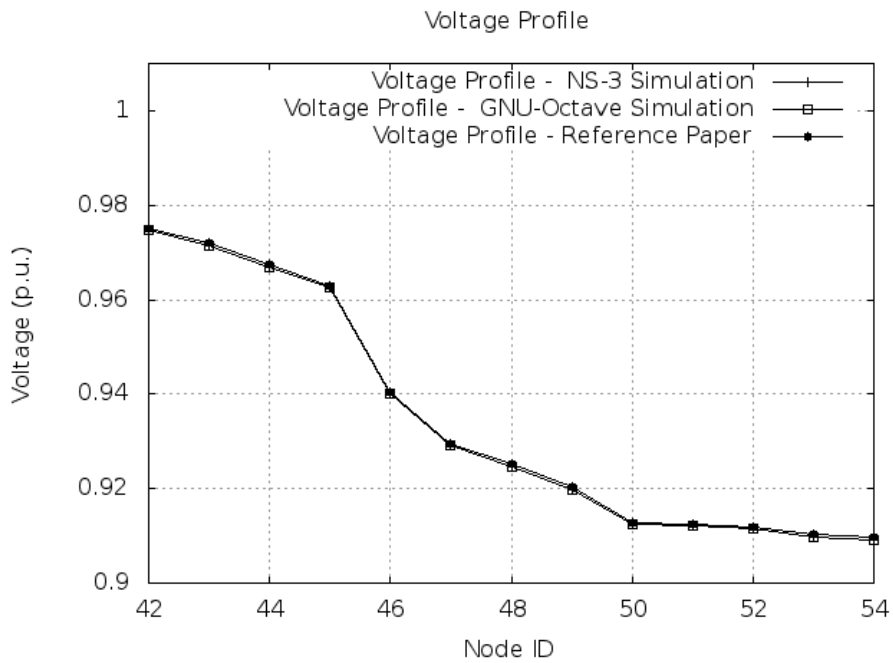


Figure 3.17: Voltage profile on a lateral of the 69-bus system

Table 3.4: WiMAX and LTE performance comparison - NS-3 simulation of the 69-bus system

	WiMAX	LTE
Average packet delay (ms)	51.2	15.6
Average packet delivery ratio (%)	93.6	99.9
Convergence time (s)	57.4	46.2

Table 3.5: Maximum voltage differences for the 18-bus, 34-bus, and the 69-bus systems

	Max. $\Delta V$
18-bus system	0.42%
34-bus system	0.33%
69-bus system	0.08%

### 3.5.4 Communication Network Performance Evaluation

The performance of the communication network supporting the analysis and control framework is evaluated in this section for both WiMAX and LTE technologies in terms of:

1. Average packet delay.
2. Average packet delivery ratio.
3. Average convergence time of the decentralized load flow analysis.

Five radial distribution systems are used for this purpose, a 34 bus system from [75], a 33 bus system from [78], a 19 bus system from [74], a 30 bus system from [44], and a 69 bus system from [76].

Theses distribution systems are repeatedly altered to change the number of nodes in each system to be 30, 25, 20, 15, 10, and 5 nodes. This is achieved by absorbing or adding leaf nodes while maintaining the same total load power. For each network size, each one of the five distribution systems is simulated and the relevant parameters (such as packet delay, number of lost packets, and convergence time) are recorded and averaged.

Figures 3.18, 3.19, and 3.20 compare the average convergence time, the average packet delay, and the average packet delivery ratio for both WiMAX and LTE technologies, for different number of nodes.

The average convergence time for a 30 bus distribution system is around 30 seconds for both WiMAX and LTE networks, which indicates the ability of the proposed framework to quickly perform the load flow analysis and hence perform real-time control for non-emergency normal operation.

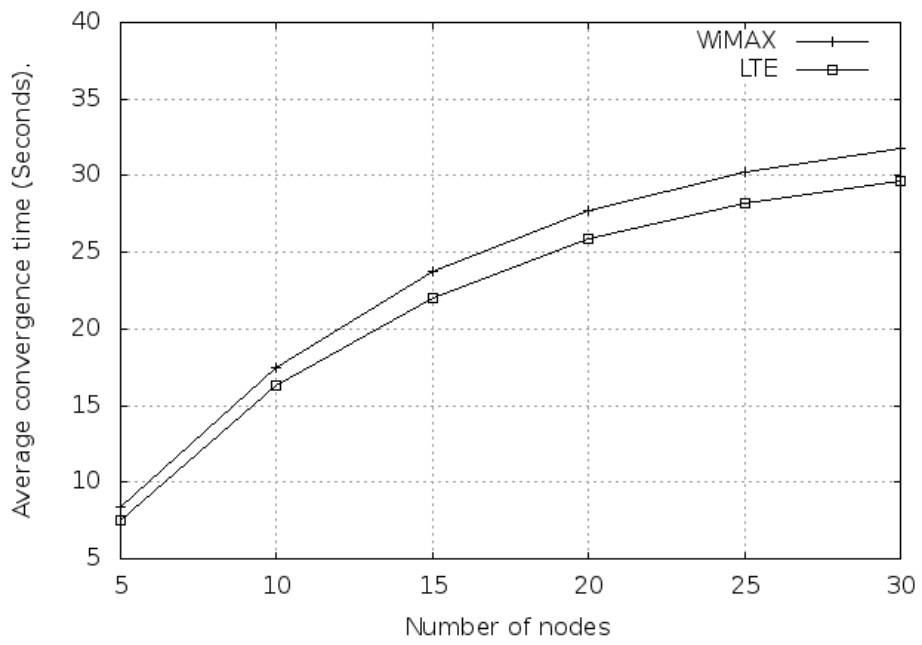


Figure 3.18: Average convergence time

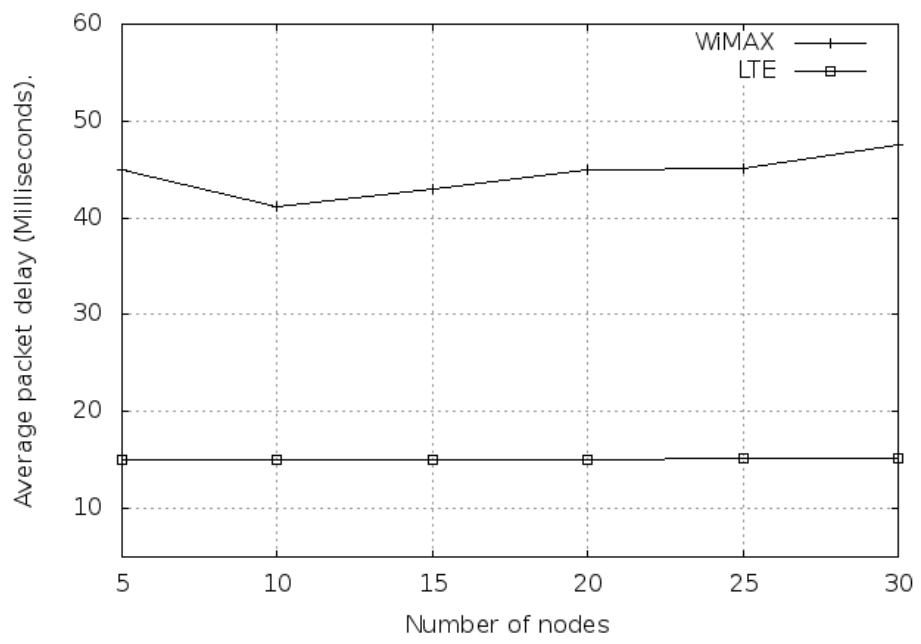


Figure 3.19: Average packet delay.

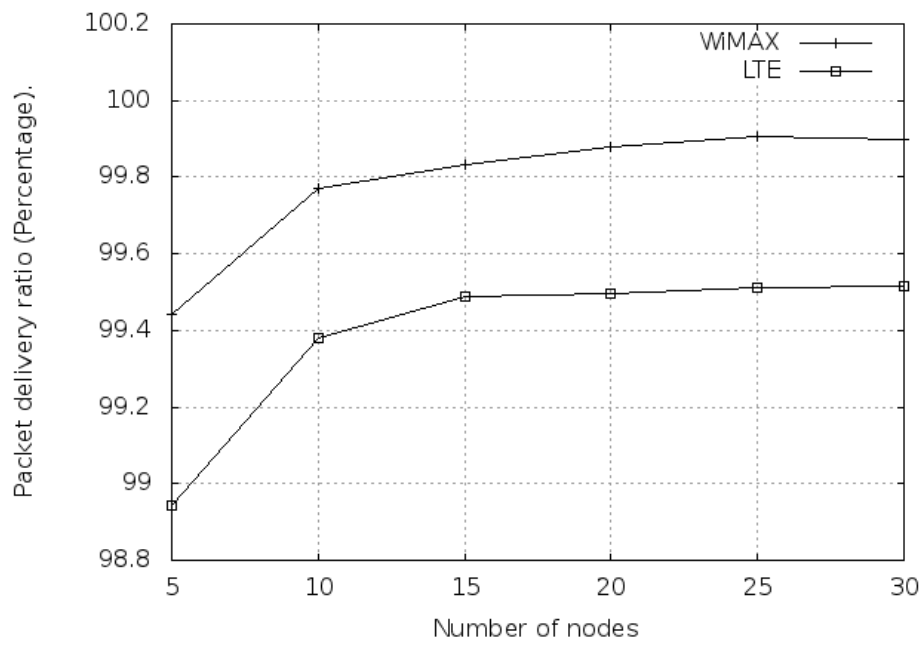


Figure 3.20: Average packet delivery ratio.



The average packet delay fluctuates between 40 and 50 milliseconds for the WiMAX network, while it is around 15 milliseconds for LTE, which suggests that LTE has a better latency characteristics. As for the quality of service, the packet delivery ratio for both technologies is very close to 100%.

## 3.6 Summary

A “distributed” implementation of the backward/forward sweep method is presented in this chapter in order to perform power flow analysis for electrical power distribution systems. Multiple processing units equipped with wireless communication transceivers collaborate together in order to perform the power flow analysis in a “distributed” manner.

In this implementation, the structure of each node in the distribution system resembles an integrated configuration of power and communication systems. The locally calculated parameters at each node (e.g. voltage, current, power, losses) are affected by the information received over the communication network (e.g. parent/children voltage/current, smart meter measurements, status of neighboring switched capacitor bank), therefore resulting in a real-time power flow analysis in which the system changes are shared with all the nodes in the system over the communication network as soon as they occur.

The system connectivity is defined and maintained through the local information stored in each node, thereby any changes in the system connectivity can be accommodated in a dynamic and flexible manner.

The proposed distributed implementation of the power flow analysis is built in GNU-Octave and the network simulator NS-3, and applied to multiple electrical power distribution systems. The obtained voltage profiles from GNU Octave and NS-3 simulations are in close agreement with those reported in literature for the corresponding distribution system.

The performance of the communication network supporting the distributed power flow analysis is also evaluated using NS-3 simulations in terms of the average packet delay, packet delivery ratio, and the power flow analysis convergence time for both WiMAX and LTE technologies.

This distributed power flow analysis implementation acts as the basis for control techniques for multiple system components such as DG units, switched capacitor banks, and OLTC transformers, therefore preventing any contradicting control decisions, and hence leading to a “seamless” coordination. The details of these proposed control techniques are presented in chapters 4 and 5.



# Chapter 4

## Decentralized/Distributed Control Techniques for Distribution Systems

The online decentralized/distributed implementation of the backward/forward power flow analysis presented in chapter 3 can serve as the basis for online control and coordination techniques for the different distribution system components.

Decentralized/distributed online control techniques for switched capacitor banks, and DG units are presented in this chapter, while an online control technique for OLTC transformers is presented in chapter 5. These techniques can be used to achieve different operational goals, for instance: in this chapter the objective is to reduce the total system losses while in chapter 5 the objective is to perform Volt/VAR control.

These control techniques are integrated into the power flow analysis implemented in chapter 3 resulting in a “seamless” coordination among the different system components.

The performance of the wireless communication network supporting the combined analysis and control framework is obtained through NS-3 simulations of both the power and communication systems.

### 4.1 Introduction

The distribution system analysis and control framework presented in this thesis has two main components as illustrated in Figure 3.1. The first component is the distributed implementation of power flow analysis in which multiple processing units with wireless com-

munication capabilities collaborate together, share information, and calculate the voltages, currents, power flows, and losses in the distribution system.

This power flow analysis “engine” can be utilized by different control algorithms (which constitute the second component of the proposed framework) to operate the distribution system in an optimal and efficient manner. The control algorithms proposed in this thesis are integrated into the application *DspfApp* (subsection 3.4.3) which is installed on the processing unit in each node in the system (except the ZCU) as illustrated in Figure 3.8.

The interaction between the power flow analysis engine and the control algorithms is illustrated in the flow chart in Figure 4.1. The execution of the analysis and control framework begins by performing power flow analysis using the current smart meters readings and the current system state.

The results from this initial power flow analysis are utilized in the next iteration by the control algorithms in order to “suggest” a new state for the different system components (e.g. DG units, switched capacitor banks, and OLTC transformers). Power flow analysis is then performed for this suggested “hypothetical” state, and the ZCU shares the aggregated information (e.g. system losses, voltage violations, number of switching operations) with all the nodes in the system.

The processing unit attached to each node with a switched capacitor bank keeps a data structure that stores the iteration number and the aggregated information received from the ZCU. A similar data structure is kept at each node with a DG unit or an OLTC transformer.

The control algorithms then suggest another hypothetical state, and the power flow analysis is performed for this new suggested state. This procedure is repeated for a certain number of iterations  $N_{iter}$ . Afterwards, each node with an attached DG unit, switched capacitor bank, OLTC transformer selects the state that achieves the required operational goal (e.g. reduce system losses, perform voltage control, etc.), and sends a control signal to apply the selected state.

In this chapter, random search heuristic techniques are proposed to control switched capacitor banks and DG units in order to minimize the total system losses, while a random search heuristic control technique for OLTC transformers is proposed in chapter 5. Appendix A presents a brief review of the random search algorithms used in this chapter and in chapter 5.

The rest of this chapter is organized as follows, the implementation details of the proposed control and coordination techniques for switched capacitor banks and DG units are presented in sections 4.2 and 4.3 respectively. Section 4.4 describes the simulation

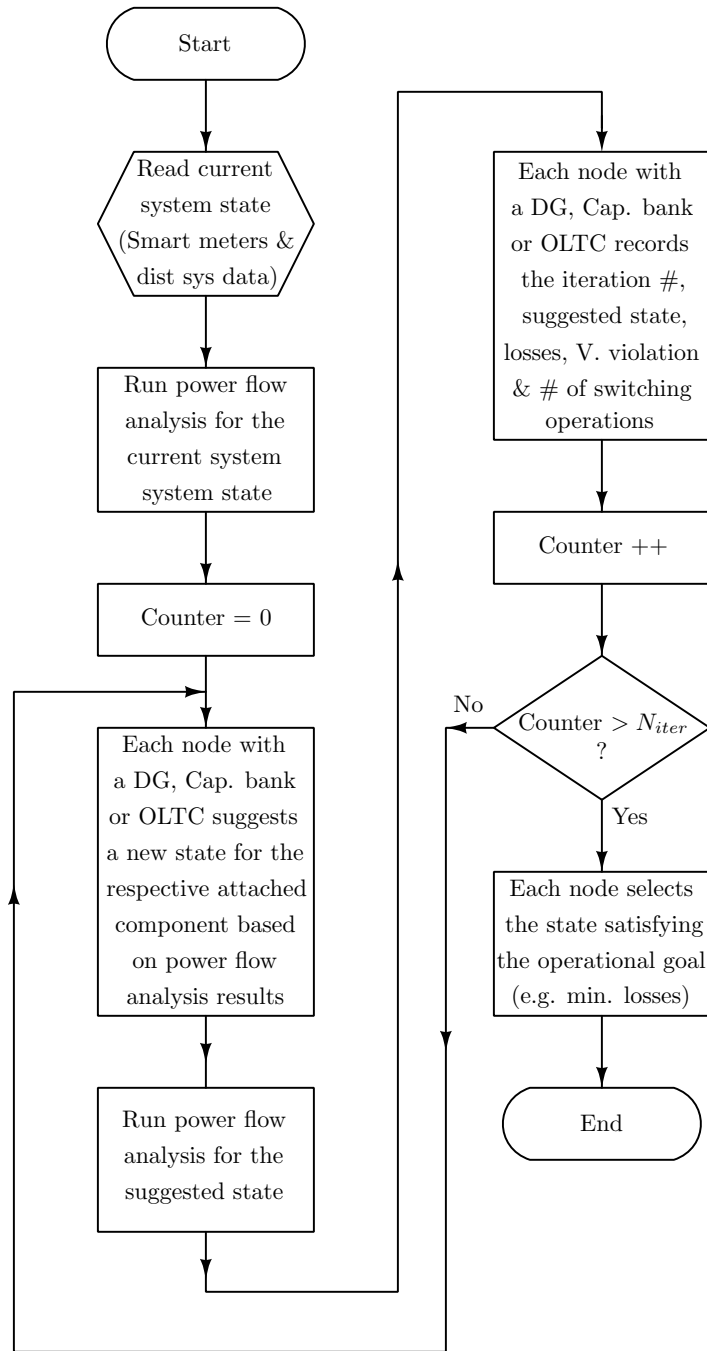


Figure 4.1: Flow chart describing the interaction between system analysis and system control in the proposed framework

methodology, while sections 4.5, and 4.6 present the simulation results for both control techniques.

The information exchange among the different nodes in the system, combined with the fact that all the control decisions are based on the common ground of power flow analysis, lead to a “seamless” coordination among the different system components such as capacitor banks and DG units. This concept is discussed in section 4.7 along with some simulation results of distribution system with multiple switched capacitor banks and multiple DG units. Section 4.8 illustrates the ability of the proposed framework to utilize the hourly values of the load and of the DG-generated power in order to control the distribution system and reduce the total system losses on hourly basis. The chapter is summarized in section 4.9.

## 4.2 Multiple Switched Capacitor Banks Control and Coordination

In this section, a heuristic technique based on random search is proposed to control and coordinate multiple switched capacitor banks installed in a distribution system. This technique can quickly obtain a combined “state” for all the switched capacitor banks such that the total system losses are brought to a close-to-minimum value.

### 4.2.1 Introduction

Switched capacitor banks are installed in a distribution system to provide voltage support, control the reactive power, and hence reduce the system losses. Switched capacitor banks control is an important task that aims to reduce the operating costs in terms of the monetary value of the saved energy, and the released system capacity which can delay costly expansions [79].

There are multiple options to control capacitor banks, for instance, the capacitor can be switched ON and OFF based on the time of the day, voltage, current or VAR measurements [10].

The number of capacitor switching operations per day is usually limited, one energization and one deenergization per day is reported in [10]. This suggests that the capacitor control action would take place every few hours, which allows enough time for the proposed control algorithm to obtain a state that brings the overall system losses to a close-to-minimum value.

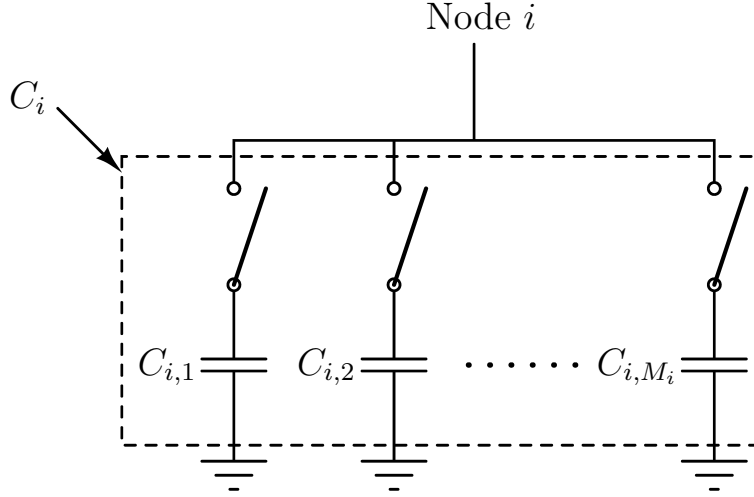


Figure 4.2: A switched capacitor bank with  $M_i$  stages

### 4.2.2 The Proposed Control Algorithm

Figure 4.2 shows a typical switched capacitor bank with  $M_i$  stages installed at node  $i$  in a distribution system. Each stage can be switched ON or OFF in order to change the total injected reactive power  $Q_i$  at node  $i$ .

In a distribution system with  $N_C$  switched capacitor banks each with  $M_i$  stages, the state of all the capacitor banks in the distribution system,  $\alpha$ , is defined as the vector of the injected reactive power from all capacitors as indicated in equation 4.1.

$$\alpha = [Q_1, Q_2, \dots, Q_{N_C}] \quad (4.1)$$

where  $Q_i$  is the injected reactive power from the capacitor bank installed at node  $i$ , and  $1 \leq i \leq N_C$ .

If each stage of the switched capacitor bank at node  $i$  has a distinct value, i.e.

$$C_{i,1} \neq C_{i,2} \neq \dots \neq C_{i,M_i} \quad (4.2)$$

then the total number of possible values of injected reactive power the capacitor at node  $i$  will be  $(2^{M_i})$ . This number is reduced to  $(M_i + 1)$  in case all the stages have the same value, i.e.

$$C_{i,1} = C_{i,2} = \dots = C_{i,M_i} \quad (4.3)$$

Therefore, in a typical distribution system with  $N_C$  switched capacitor banks, the total number of possible states (i.e. the size of the search space) of switched capacitor banks is  $\left[ \prod_{i=1}^{N_C} 2^{M_i} \right]$  for distinct-value stages, and is reduced to  $\left[ \prod_{i=1}^{N_C} (M_i + 1) \right]$  in case all stages have the same value.

The proposed technique employs a heuristic search technique to select a state  $\alpha_o$  that brings the total system losses to a close-to-minimum value. Appendix A provides a brief overview of heuristic search algorithms. The proposed technique is comprised of three consecutive steps:

1. Step 1:

The processing unit installed at each node in the distribution system calculates its local voltage, current, power flow, and losses according to the distributed power flow analysis described in chapter 3, sections 3.2 and 3.3. Such information is used to control the capacitor bank attached to this node.

In this step, the reactive power supplied by the capacitor bank installed at node  $i$  is set to match the downstream reactive power flow at this node, i.e.

$$Q_i = Im [V_i \times I_i^*] \quad (4.4)$$

where,  $V_i$  and  $I_i$  are the calculated voltage and current at node  $i$ .

Each node with a switched capacitor bank stores the injected reactive power  $Q_i$  and the corresponding total system losses calculated by, and received from the ZCU.

The resulting capacitor banks state  $\alpha_{step_1}$  is used as an initial state for the second step of the algorithm.

2. Step 2:

In this step, the reactive power supplied from each capacitor bank is incremented by one step by switching ON an additional capacitor bank stage. Then, the distributed power flow analysis is executed, and the total system losses are calculated by the ZCU and shared with all the nodes in the system.

Each node with a switched capacitor bank compares the calculated total system losses of the current state and the previous state. If the losses are reduced, the change is accepted and the process is repeated, otherwise, the change is rejected and the algorithm goes to the third step. The resulting capacitor banks' state  $\alpha_{step_2}$  is used as an initial state for the third step.



### 3. Step 3:

Starting from state  $\alpha_{step2}$ , a random search is used to obtain a capacitor banks state  $\alpha_o$  that brings the overall system losses to a close-to-minimum value. The random search stops after a certain number of iterations ( $N_{iter}$ ).

- (a) Each node with a capacitor bank uses a data structure to record the injected reactive power from the capacitor and the corresponding total losses value calculated by, and received from the ZCU.
- (b) The processing unit at each node with a capacitor bank uses the state that corresponds to the least losses recorded in the data structure as the initial state. The injected reactive power is changed “independently” and “randomly” by one step. The distributed power flow analysis is performed, and the overall system losses is calculated (by ZCU) and recorded in the data structure.
- (c) The process is repeated for a given number of iterations ( $N_{iter}$ ), the state with the least losses  $\alpha_o$  is selected.
- (d) A control action is executed in accordance with the obtained capacitor banks state  $\alpha_o$ .

It is important to note that:

1. This three-step technique is executed at the processing unit installed at each node with an attached switched capacitor bank.
2. The ZCU acts as an information hub that creates a “common knowledge” which is shared with all the nodes in the system, therefore allowing each node to make an informed decision.
3. The communication network plays an essential role in reaching a control decision in a dynamic decentralized / distributed manner such that any change in the load values, component status, system connectivity etc. is accounted for immediately.
4. All the intermediate changes of the capacitor banks’ injected reactive power described in this three-step technique are used only for calculation purposes and they are *NOT* applied to the actual distribution system. A control signal is applied to set the injected reactive power of each capacitor bank, in accordance with the selected state  $\alpha_o$ , *ONLY* when the three steps of the algorithm have been executed and a final state  $\alpha_o$  has been selected.

## 4.3 Multiple DG Units Control and Coordination

This section provides a detailed description of a random search based heuristic technique proposed to control and coordinate multiple DG units installed in a distribution system. The objective of this technique is to control the “power factor” of each DG unit in the system in order to bring the system losses to a close-to-minimum value.

### 4.3.1 Introduction

Distributed Generation (DG) units are being installed on the distribution network as an alternative power generation at a smaller but distributed scale.

The presence of DG units is beneficial for consumers and utilities. It is a new tool for utilities to optimize the performance of the distribution system but it also poses new challenges in the system operation and control.

DG units are usually operated with a unity power factor,  $pf = 1$ , in order to maximize the DG owner revenue. But, as discussed in chapter 2 subsection 2.3.4, operating DG units using variable power factor can positively affect the distribution network performance in terms of voltage regulation and loss reduction, however this requires new control and coordination techniques to be devised as presented in this section.

Additionally, operating the DG units using variable power factor will reduce the DG owner revenue, therefore the electric utilities need to provide an incentive in order to encourage the DG owners to voluntarily help the network operation.

### 4.3.2 The Proposed Control Algorithm

For a distribution system with  $N_{DG}$  distributed generation (DG) units, each with a rated power  $S_i$  and a power factor  $pf_i$ , where  $1 \leq i \leq N_{DG}$ , the proposed algorithm controls the power factor  $pf$  of each DG unit in the system in order to reduce the total system losses.

The vector of power factors of all the DG units in the system,  $\beta = [pf_1, pf_2, \dots, pf_{N_{DG}}]$ , is referred to as the state of the DG units. The proposed control and coordination algorithm uses a random search technique (as explained in appendix A) to obtain a state  $\beta_o$  that brings the the total system losses to a close-to-minimum value, the algorithm can be explained as follows:

1. The processing unit at each node with an attached DG maintains a data structure that records the history of the DG power factor and the corresponding overall system losses value calculated by and received from the ZCU.
2. The power factor of any DG unit  $pf_i$  is limited between a maximum and a minimum value,  $pf_{min} \leq pf_i \leq pf_{max}$ , with a step  $\Delta pf$ .
3. Starting with the state corresponding to the least system losses recorded in the data structure, the power factor of each DG unit is changed randomly and independently. The corresponding system losses (received from the ZCU) is recorded in the data structure.
4. The process is repeated for a specific number of iterations  $N_{iter}$  and the state corresponding to the least losses,  $\beta_o$ , is selected.

For a distribution system with  $N_{DG}$  DG units installed, the total number of possible states (i.e. the size of the search space) is  $\left[ \prod_{i=1}^{N_{DG}} \left( \left( \frac{pf_{max} - pf_{min}}{\Delta pf} \right) + 1 \right) \right]$ .

It is important to note that:

1. This technique is executed at the processing unit installed at each node with an attached DG unit.
2. The communication network is used to share the common knowledge created by the ZCU in order to help each node in the system to make an informed decision to control the attached DG unit.
3. All the intermediate changes of the DG power factors described in the technique are used only for calculation purposes and they are *NOT* applied to the actual distribution system. A control signal is applied to set the power factor of each DG unit, in accordance with the selected state  $\beta_o$ , *ONLY* when the algorithm has been executed and a final state  $\beta_o$  has been selected.

## 4.4 Simulation Methodology

This section outlines the simulation methodology used to assess the performance of the proposed capacitor bank and DG control and coordination technique presented in sections 4.2 and 4.3 respectively. Two simulation tools are used, GNU-Octave and the network simulator NS-3.

### 4.4.1 Exhaustive Search

For a distribution system with  $N_C$  switched capacitor banks, GNU-Octave is used to perform power flow analysis for all possible capacitor banks' states  $\alpha = [Q_1, Q_2, \dots, Q_{N_C}]$ . The resulting system losses for each state are calculated, recorded, and used to:

1. Obtain the global optimum state,  $\alpha_{opt}$ , that minimizes the total system losses.
2. Compare the state obtained from the proposed control scheme,  $\alpha_o$ , with the global optimum state  $\alpha_{opt}$ . The percentile rank is used to perform this comparison.

A similar approach is used to perform the exhaustive search for a distribution system with  $N_{DG}$  DG units in order to get  $\beta_{opt}$ , and calculate the percentile rank of state  $\beta_o$  obtained from the proposed control technique.

### 4.4.2 Percentile Rank

The list of all possible states and their corresponding system losses, which is obtained from exhaustive search, can be used to rank any given state.

The “percentile rank” of a state  $\alpha_o$  is the percentage of all states that result in a performance that is similar to or worse than that of state  $\alpha_o$ . For example, a 75% percentile rank indicates that 75% of all the possible states result in the same or more system losses than the losses corresponding to state  $\alpha_o$ .

### 4.4.3 Performance Evaluation

The proposed control and coordination techniques for switched capacitor banks and DG units presented in sections 4.2 and 4.3 are based on random search, hence the obtained results will be different each time the algorithms are run.

To capture the randomness of the results, GNU Octave is used to execute the control and coordination algorithms for a 1000 times, and the percentile rank of the minimum, maximum and mean losses are used to evaluate the performance.

#### 4.4.4 Wireless Communication System Simulation

Both the distributed power flow analysis and the proposed control and coordination techniques are implemented as a set of C++ applications which are integrated into the network simulator NS-3. NS-3 is used to simulate the proposed control schemes along with the supporting wireless communication network. WiMAX and LTE wireless communication technologies are used in the simulation.

For a distribution system with  $N_C$  switched capacitor banks, the NS-3 simulation of the proposed control and coordination scheme obtains a state  $\alpha_o = [Q_1, Q_2, \dots, Q_{N_C}]$  for all the capacitor banks that results in a close-to-minimum losses. Similarly for distribution systems with  $N_{DG}$  DG units, a state  $\beta_o = [pf_1, pf_2, \dots, pf_{N_{DG}}]$  is obtained.

The performance of both WiMAX and LTE communication networks is evaluated in terms of the average packet delay, average packet delivery ratio, and the convergence time of the power system analysis and control algorithm.

#### 4.4.5 Simulation Parameters

The accuracy of the proposed control schemes depends on multiple factors, e.g. voltage tolerance  $\epsilon$ , number of iterations used in the random search  $N_{iter}$ , the power factor step  $\Delta pf$ , and the inter-packet interval in the wireless network.

For all the simulation results presented in this chapter, the allowed voltage tolerance in the backward/forward analysis method,  $\epsilon$ , is set to be  $10^{-5}$ , the number of random search iterations,  $N_{iter}$ , is set to be 20,  $\Delta pf$  is 0.01, the maximum and the minimum power factors are  $pf_{max} = 1$  and  $pf_{min} = 0.85$  capacitive (i.e. supplying reactive power), and data packets are sent every 100 milliseconds for both WiMAX and LTE networks.

### 4.5 Multiple Switched Capacitor Banks Control and Coordination - Simulation Results

Two balanced radial distribution systems are used to investigate the performance of the proposed capacitor bank control and coordination technique presented in section 4.2, a 31-bus radial distribution system from [44] and a 69-bus radial distribution system from [76], shown in Figures 4.3 and 3.15 respectively.

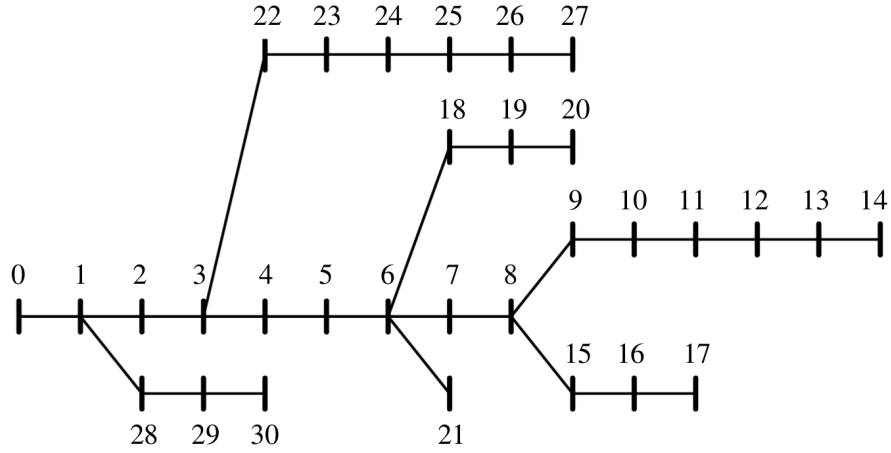


Figure 4.3: A 31-bus distribution system

### 4.5.1 31-Bus Distribution System

Five capacitor banks are installed in the 31-bus distribution system shown in Figure 4.3 at nodes 13, 15, 19, 23 and 25, each capacitor bank has ten stages of 175 kVAR each. The proposed analysis and control framework is applied to this distribution system to select a state  $\alpha_o = [Q_{13}, Q_{15}, Q_{19}, Q_{23}, Q_{25}]$  for the capacitor banks that reduces the overall system losses.

Table 4.1 summarizes the GNU-Octave simulation results obtained by applying the proposed framework and those by the exhaustive search method. GNU-Octave simulation was run a 1000 times, the best losses obtained is 0.905 MW with a percentile rank of 100%, i.e. it is the global optimal state. The worst losses obtained by the algorithm is 0.908 MW, and it is the same as or better than 99.80% of all the possible states. Over the 1000 runs, the algorithm achieves an average losses of 0.907 MW with a percentile rank of 99.92%.

Table 4.2 presents the network simulator NS-3 simulation results using WiMAX and LTE. In less than 11 minutes, the algorithm obtained a state for the five capacitor banks that reduces the overall system losses to a value that is the same as of better than 99.8% of all possible states.

A voltage regulator is then added between nodes 5 and 6 in order to maintain a fixed voltage ( $V_{sec}$ ) at its secondary terminal. Table 4.3 presents the GNU Octave simulation results for  $V_{sec} = 1.05$  p.u. The algorithm was run a 1000 times, the best losses obtained is 0.8099 MW with a percentile rank of 100%, on the other hand, the worst losses obtained

Table 4.1: A 31-bus distribution system with five capacitor banks and no voltage regulator - GNU-Octave simulation results

	Proposed Control Scheme - 1000 run			Exhaustive Search
	Min. Losses	Mean Losses	Max. Losses	Optimum State
Losses (MW)	0.905	0.907	0.908	0.905
Percentile Rank	100%	99.92%	99.80%	—
$Q_{13}$ (kVAR)	875	—	875	875
$Q_{15}$ (kVAR)	875	—	875	875
$Q_{19}$ (kVAR)	875	—	875	875
$Q_{23}$ (kVAR)	1750	—	1050	1750
$Q_{25}$ (kVAR)	1050	—	1225	1050

Table 4.2: A 31-bus distribution system with five capacitor banks and no voltage regulator - NS-3 simulation results

	WiMAX	LTE
$Q_{13}$ (kVAR)	875	875
$Q_{15}$ (kVAR)	875	875
$Q_{19}$ (kVAR)	875	875
$Q_{23}$ (kVAR)	1050	1225
$Q_{25}$ (kVAR)	1225	1050
Losses (MW)	0.9075	0.9071
Percentile Rank	99.8%	99.9%
Convergence Time (minutes)	10.6	9.6

Table 4.3: A 31-bus distribution system with five capacitor banks and a voltage regulator ( $V_{sec} = 1.05$  p.u.) - GNU-Octave simulation results

	Proposed Control Scheme - 1000 run			Exhaustive Search
	Min. Losses	Mean Losses	Max. Losses	Optimum State
Losses (MW)	0.8099	0.8111	0.8115	0.8099
Percentile Rank	100%	99.92%	99.85%	—
$Q_{13}$ (kVAR)	875	—	875	875
$Q_{15}$ (kVAR)	875	—	875	875
$Q_{19}$ (kVAR)	875	—	875	875
$Q_{23}$ (kVAR)	1750	—	1050	1750
$Q_{25}$ (kVAR)	875	—	1250	875

is 0.8115 MW with a percentile rank of 99.85%. On average, the algorithm obtains losses of 0.8111 MW with a 99.92% percentile rank.

NS-3 simulation results are summarized in Table 4.4 for both WiMAX and LTE technologies. The proposed control algorithm obtained a state with a percentile rank of 99.85% in less than 11 minutes.

### 4.5.2 69-Bus Distribution System

Four capacitor banks are installed in the 69-bus system shown in Figure 3.15 at nodes 10, 19, 51 and 53, each capacitor bank has 10 stages of 200 kVAR each. The algorithm tries to obtain a state  $\alpha_o = [Q_{10}, Q_{19}, Q_{51}, Q_{53}]$  that brings the total system losses to a close-to-minimum value.

Table 4.5 presents GNU-Octave simulation results. In the 1000 run simulation, the best losses obtained is 145.70 kW with a percentile rank of 100%, while the worst losses found is 154.34 kW with a percentile rank of 97.1%. The mean value of the losses is 147.86 kW with a percentile rank of 99.7%.



Table 4.4: A 31-bus distribution system with five capacitor banks and a voltage regulator ( $V_{sec} = 1.05$ ) - NS-3 simulation results

	WiMAX	LTE
$Q_{13}$ (kVAR)	875	875
$Q_{15}$ (kVAR)	1050	875
$Q_{19}$ (kVAR)	700	875
$Q_{23}$ (kVAR)	1225	1050
$Q_{25}$ (kVAR)	1225	1225
Losses (MW)	0.8111	0.8115
Percentile Rank	99.92%	99.85%
Convergence Time (minutes)	10.9	9.1

Table 4.5: A 69-bus distribution system with four capacitor banks - GNU-Octave simulation results

	Proposed Control Scheme - 1000 run			Exhaustive Search
	Min. Losses	Mean Losses	Max. Losses	Optimum State
Losses (kW)	145.70	147.86	154.34	145.70
Percentile Rank	100%	99.7%	97.1%	—
$Q_{10}$ (kVAR)	400	—	600	400
$Q_{19}$ (kVAR)	200	—	400	200
$Q_{51}$ (kVAR)	1000	—	200	1000
$Q_{53}$ (kVAR)	200	—	600	200

Table 4.6: A 69-bus distribution system with four capacitor banks - NS-3 simulation results

	WiMAX	LTE
$Q_{10}$ (kVAR)	400	600
$Q_{19}$ (kVAR)	200	200
$Q_{51}$ (kVAR)	400	400
$Q_{53}$ (kVAR)	800	600
Losses (kW)	148.21	148.48
Percentile Rank	99.63%	99.53%
Convergence Time (minutes)	$\approx 15.92$	$\approx 14.65$

Table 4.6 summarizes the NS-3 simulation results, the algorithm reached a state with a percentile rank of 99.5% in less than 15 minutes.

The convergence times of WiMAX and LTE are very close to each other, and they indicate that the proposed algorithm can make a control decision within minutes, while the capacitor bank control actions are usually performed every few hours [10].

The percentile rank of the mean losses obtained by the algorithm was more than 99%, i.e. on average, the proposed algorithm is able to obtain a losses that is very close to the optimum losses.

## 4.6 Multiple DG Units Control and Coordination - Simulation Results

The 31-bus and 69-bus radial distribution systems used in section 4.5 are used in this section to assess the performance of the proposed DG control and coordination technique presented in section 4.3.

Table 4.7: A 31-bus distribution system with three DG - GNU-Octave simulation results

	Proposed Control Scheme - 1000 run			Exhaustive Search	Unity Power Factor
	Min. Losses	Mean Losses	Max. Losses	Optimum State	Operation
Losses (kW)	404.87	405.64	409.96	404.87	465.56
Percentile Rank	100%	97.00%	55.20%	—	—
$pf_5$	0.93	—	0.99	0.93	1.00
$pf_{17}$	0.93	—	0.91	0.93	1.00
$pf_{27}$	0.94	—	0.91	0.94	1.00

#### 4.6.1 31-Bus Distribution System

Three DG units are installed at nodes 5, 17 and 27 in the 31-bus distribution system, the DG units' rated powers are 2, 2 and 1.5 MVA respectively. If all the DG units are operated using unity power factor, the total calculated system losses are 465.56 kW.

The proposed control algorithm performs random search to find a state  $\beta_o = [pf_5, pf_{17}, pf_{27}]$  that brings the losses to a close-to-minimum value. The DG power factor is allowed to change in the range  $0.85 \leq pf \leq 1$  capacitive.

Table 4.7 summarizes the GNU-Octave 1000-run simulations, the maximum obtained losses is 409.96 kW with a percentile rank of 55.20%, which far-off the optimal case, but on average, the algorithm achieves losses of 405.64 kW with a percentile rank of 97.00%.

Applying the proposed DG control technique reduces the total system losses by 12.87% compared to the unity power factor operation.

NS-3 simulation results are presented in Table 4.8, the algorithm selects a state with a percentile rank of 92.8% in less than 9 minutes.

A voltage regulator is then added between nodes 5 and 6 in order to maintain a fixed voltage ( $V_{sec} = 1.05$ ) at its secondary terminal. GNU-Octave simulation results presented in Table 4.9 reveal that the worst-case losses is 356.40 kW with a percentile rank of 60.18%, but on average the algorithm obtains a state for the three DG units of 352.83 kW with a percentile rank of 97.29%.

Table 4.8: A 31-bus distribution system with three DG units - NS-3 simulation results

	WiMAX	LTE
$pf_5$	0.92	0.92
$pf_{17}$	0.90	0.95
$pf_{27}$	0.92	0.94
Losses (kW)	406.22	405.55
Percentile Rank	92.8%	97.5%
Convergence Time (minutes)	$\approx 8.5$	$\approx 7.8$

The unity power factor operation of the DG units results in a total system losses of 405.61 kW, whereas the proposed DG control algorithm reduces the losses by 13%.

Table 4.10 summarizes NS-3 simulation results which show that the algorithm selects a state with a percentile rank of 99.8% in less than 8 minutes.

#### 4.6.2 69-Bus Distribution System

For the 69-bus distribution system, four DG units are installed at nodes 26, 45, 47 and 54, with 0.5, 0.4, 0.5 and 0.3 MVA rated power respectively. A state  $\beta_o = [pf_{26}, pf_{45}, pf_{47}, pf_{54}]$  is to be selected by the proposed technique in order to bring the system losses to a close-to-minimum value.

Table 4.11 summarizes the GNU-octave simulation results, the worst case losses in the 1000-run simulation is 81.64 kW with a percentile rank of 58.23%, but on average the algorithm obtains losses of 77.78 kW with a percentile rank of 95.71%.

Operating the DG units at unity power factor results in a total system losses of 110.28 kW, whereas the proposed DG control algorithm reduced the losses by 29.47%.

NS-3 simulations results are presented in Table 4.12, which shows that the algorithm obtains a state with a percentile rank of more than 93% in approximately 12 minutes.

The proposed DG control and coordination algorithm achieves an average losses with a percentile rank of 95% or more, which indicates that most of the time the algorithm obtains a close-to-minimum losses even though the worst-case losses has a percentile rank as low as 55%.

Table 4.9: A 31-bus distribution system with three DG and a voltage regulator ( $V_{sec} = 1.05$  p.u.) - GNU-Octave simulation results

	Proposed Control Scheme - 1000 run			Exhaustive Search	Unity Power Factor Operation
	Min. Losses	Mean Losses	Max. Losses	Optimum State	
Losses (kW)	352.15	352.83	356.40	352.15	405.61
Percentile Rank	100%	97.29%	60.18%	—	—
$pf_5$	0.93	—	0.95	0.93	1.00
$pf_{17}$	0.93	—	0.87	0.93	1.00
$pf_{27}$	0.94	—	0.89	0.94	1.00

Table 4.10: A 31-bus distribution system with three DG units and a voltage regulator ( $V_{sec} = 1.05$  p.u.) - NS-3 simulation results

	WiMAX	LTE
$pf_5$	0.92	0.93
$pf_{17}$	0.93	0.92
$pf_{27}$	0.95	0.94
Losses (kW)	352.270	352.274
Percentile Rank	99.80%	99.83%
Convergence Time (minutes)	$\approx 7.9$	$\approx 7.3$

Table 4.11: A 69-bus distribution system with four DG units - GNU-Octave simulation results

	Proposed Control Scheme - 1000 run			Exhaustive Search	Unity Power Factor Operation
	Min. Losses	Mean Losses	Max. Losses	Optimal State	
Losses (kW)	76.37	77.78	81.64	76.34	110.28
Percentile Rank	99.99%	95.71%	58.23%	—	—
$pf_{26}$	0.85	—	0.97	0.85	1.00
$pf_{45}$	0.86	—	0.85	0.85	1.00
$pf_{47}$	0.85	—	0.95	0.85	1.00
$pf_{54}$	0.85	—	0.89	0.85	1.00

Table 4.12: A 69-bus distribution system with four DG units - NS-3 simulation results

	WiMAX	LTE
$pf_{26}$	0.91	0.85
$pf_{45}$	0.93	0.89
$pf_{47}$	0.89	0.85
$pf_{54}$	0.86	0.85
Losses (kW)	78.09	76.51
Percentile Rank	93.65%	99.96%
Convergence Time (minutes)	$\approx 12.1$	$\approx 10.9$

## 4.7 Multiple Capacitor Banks and DG Units Control and Coordination

This section illustrates the “seamless” coordination of the capacitor banks and DG units control techniques presented in sections 4.2 and 4.3.

As illustrated in Figure 3.1, power flow analysis calculations act as the common ground on which all control actions are based, therefore eliminating the possibility of contradicting control actions.

### 4.7.1 Seamless Coordination

In the analysis and control framework presented in this thesis, each node in the system exchanges information with its neighbors which, in turn, process the received information and exchange the results with their neighbors, therefore, the information “propagates” to the entire system and affect the analysis and control decisions system-wide.

This exchange of information results in a “seamless coordination” among the multiple components in the system. For instance, if the injected reactive power from one capacitor bank is changed, this information - embedded in the calculated current and voltage - travels to all the nodes in the system including other nodes with capacitor banks, DG units and voltage regulating transformers. Now, if the power factor of a DG unit or the tap setting of a voltage regulating transformer is to be changed, the change that already happened in that capacitor bank will be taken into account.

Therefore different control and coordination techniques can be easily coordinated since they all exchange information over the communication network, and rely on the same common ground of power flow analysis calculations.

This coordination takes place in real-time, and any change in the system is immediately reflected in the voltages, currents, active/reactive power values calculated locally at each node.

### 4.7.2 31-Bus Distribution System

Multiple capacitor banks, DG units and a voltage regulating transformer are installed in the 31-bus radial distribution system used in sections 4.5 and 4.6 in order to assess the

Table 4.13: A 31-bus distribution system with three capacitor banks, two DG units and a voltage regulator ( $V_{sec} = 1.05$  p.u.) - GNU-Octave simulation results

	Proposed Control Scheme - 1000 run			Exhaustive Search
	Min. Losses	Mean Losses	Max. Losses	Optimum State
Losses (kW)	583	588.1	595.2	583
Percentile Rank	100%	99.50%	94.84%	—
$Q_{13}$ (kVAR)	1050	—	700	1050
$Q_{19}$ (kVAR)	1225	—	700	1225
$Q_{23}$ (kVAR)	1750	—	1750	1750
$pf_{17}$	0.99	—	0.99	0.99
$pf_{27}$	0.99	—	1	0.99

performance of combining the capacitor banks and DG units control techniques described in sections 4.2 and 4.3 respectively.

Three capacitor banks are installed at nodes 13, 19, and 23, each with ten stages of 175 kVAR, two DG units are installed at nodes 17 and 27 with rated power of 1 and 0.75 MVAR respectively, and a voltage regulating transformer is added between nodes 5 and 6 in order to maintain a fixed voltage ( $V_{sec} = 1.05$ ) at its secondary terminal.

Tables 4.13, and 4.14 summarize the simulations results. On average, the proposed control and coordination technique achieves a state with a percentile rank of 99.50%, and converges in less than 10 minutes for both WiMAX and LTE.

The simulation results reported in sections 4.5, 4.6, and 4.7 indicate that the analysis and control framework can achieve a state with a high percentile rank, i.e. close to the global optimum state.



Table 4.14: A 31-bus distribution system with three capacitor banks, two DG units and a voltage regulator ( $V_{sec} = 1.05$  p.u.) - NS-3 simulation results

	WiMAX	LTE
$Q_{13}$ (kVAR)	875	1050
$Q_{19}$ (kVAR)	875	1050
$Q_{23}$ (kVAR)	1575	1575
$pf_{17}$	0.97	0.98
$pf_{27}$	0.92	0.99
Losses (kW)	590.5	585.3
Percentile Rank	98.61%	99.94%
Convergence Time (minutes)	$\approx 9.98$	$\approx 9.78$

## 4.8 Real-Time Operation

As discussed in section 2.3, real-time analysis is defined, in the context of this thesis, as the combination of computerized circuit modeling and analysis with measured real-time customer consumption and power source data to determine the voltages and power flows in all elements on the grid [42]. Analysis is done nearly continuously to determine the real-time characteristics of the grid, and to control the system accordingly [42].

This definition of real-time analysis and control is suitable to be used during non-emergency normal operating conditions where the operational goal is to reduce the system losses or to keep the voltage profile within limits.

The electrical power distribution system analysis and control framework presented in this thesis is designed for non-emergency normal operational conditions where the data acquired from smart meters are utilized to perform system analysis, and hence to control and coordinate the different system components in real-time.

The convergence times, obtained from NS-3 simulations, reported in sections 4.5, 4.6, and 4.7 are in the range of few minutes (e.g. 16 minutes for 69-bus system with 4 capacitor banks - Table 4.5), which falls within the time frame of non-emergency operation of the distribution system where switched capacitor banks and OLTC transformers are switched few times per day.

To further illustrate the ability of the proposed analysis and control framework to handle the variable load, and DG generated powers in real-time, this section presents the simulation results of the 69-bus radial distribution system used in sections 4.5 and 4.6 with variable load, and variable DG-generated power.

### 4.8.1 69-Bus Distribution System

The 69-bus radial distribution system shown in Figure 3.15 is used in the simulation with the exact same configuration as in subsection 4.6.2, where four DG units are installed at nodes 26, 45, 47 and 54 with nominal apparent powers of 0.5, 0.4, 0.5 and 0.3 MVA respectively. The peak load values are given in [76].

The hourly load and wind power data recorded in Denmark during the 31 days of January 2000 [80] is normalized with respect to the peak load power and the peak generated wind power respectively, the normalized data is shown in Figure 4.4 in percentage.

The resulting 744-hour time series representing the normalized load and wind power data is applied to the load and the DG power in the 69-bus system. In our simulations, the hourly load and wind power values are used to replace the hourly readings from smart meters as an input to the analysis and control framework.

The DG control and coordination technique presented in section 4.3 uses the hourly data in real-time in order to obtain a state  $\beta_o = [pf_{26}, pf_{45}, pf_{47}, pf_{54}]$  that minimizes the total system losses for each hour in the 744-hour time series.

Three operational scenarios are simulated and compared, the first scenario is operating the system without any DG units, the second is operating all DG units at a fixed unity power factor, while the third scenario is to operate all DG units using the variable power factors obtained from the DG control technique presented in section 4.3.

Figure 4.5 presents the hourly losses reduction for the second and third operational scenarios as a percentage of the hourly losses in the no-DG case.

The total system losses during the simulated period (31 days of January 2000) is summarized in Table 4.15, the unity power factor operation results in savings of 32.2% of the no-DG case losses, while the proposed technique results in 41.8% savings in losses compared to the no-DG case.

The hourly values of the power factors selected for the four DG units installed at nodes 26, 45, 47 and 54 are shown in Figure 4.6 for the first 20 hours, and in Figure 4.7 for the whole 744 hours.

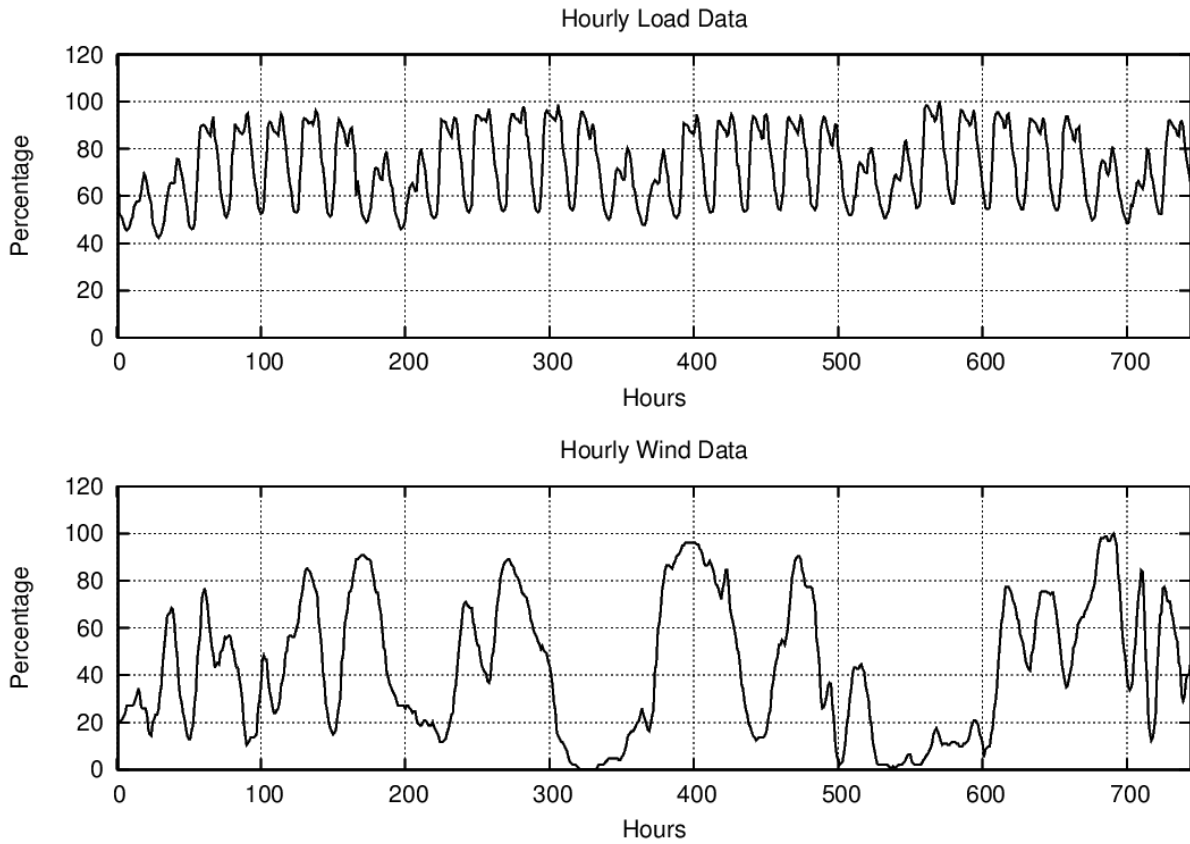


Figure 4.4: Hourly load and wind power data as a percentage of peak load and nominal DG apparent powers respectively

Table 4.15: Total system losses for the simulated time period (31 days of January 2000)

		Losses (MWh)
No DG Units		89.36
DG Units	Unity PF	61.57
	Proposed Technique - Variable PF	53.59

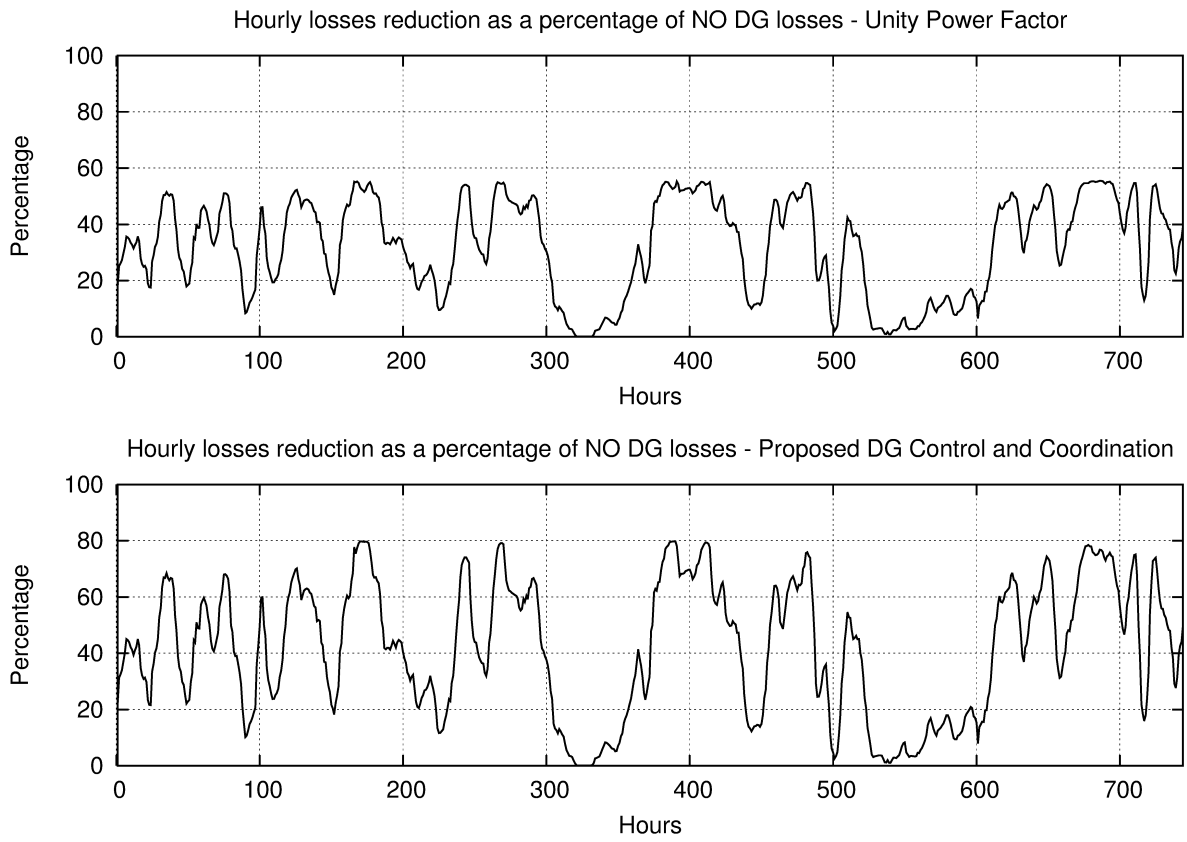


Figure 4.5: Hourly savings for the 69-bus radial system using the variable load and wind data

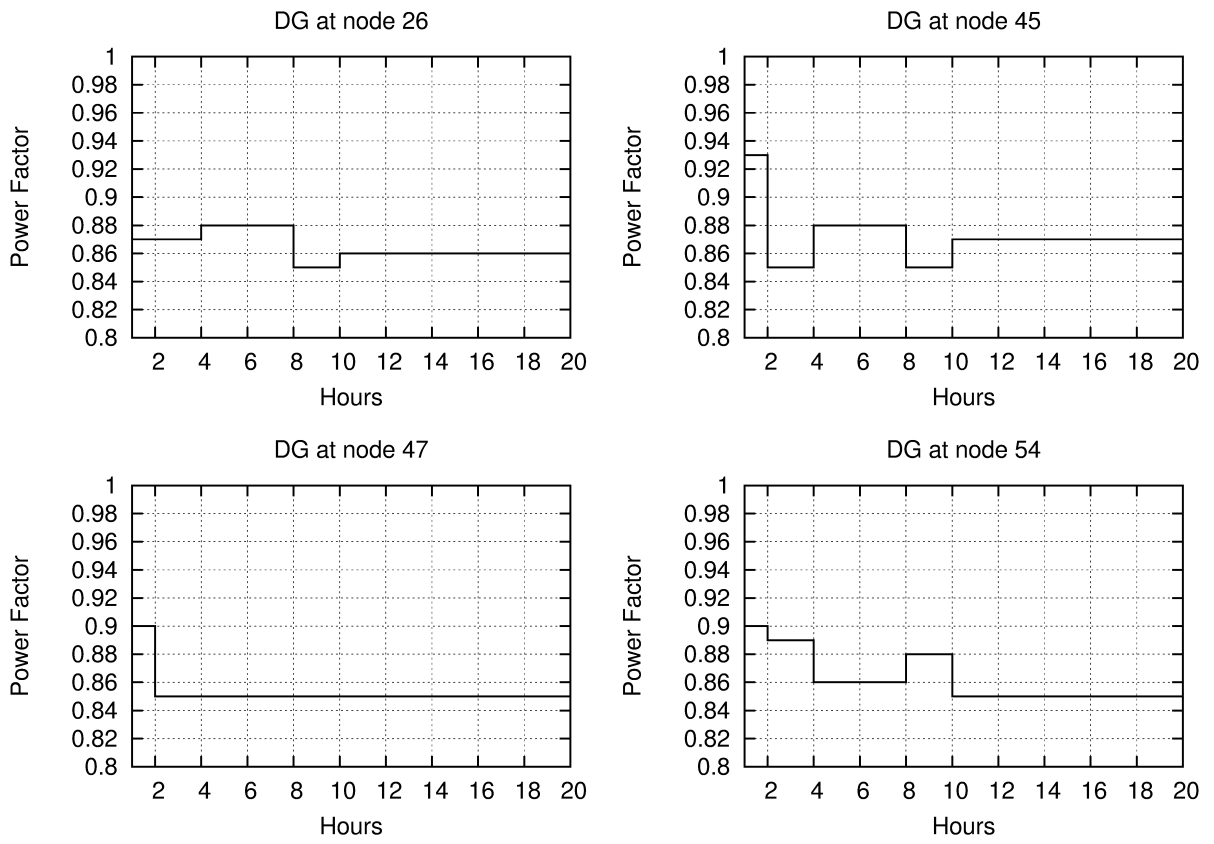


Figure 4.6: Hourly power factor values for the four DG units during the first 20 hours

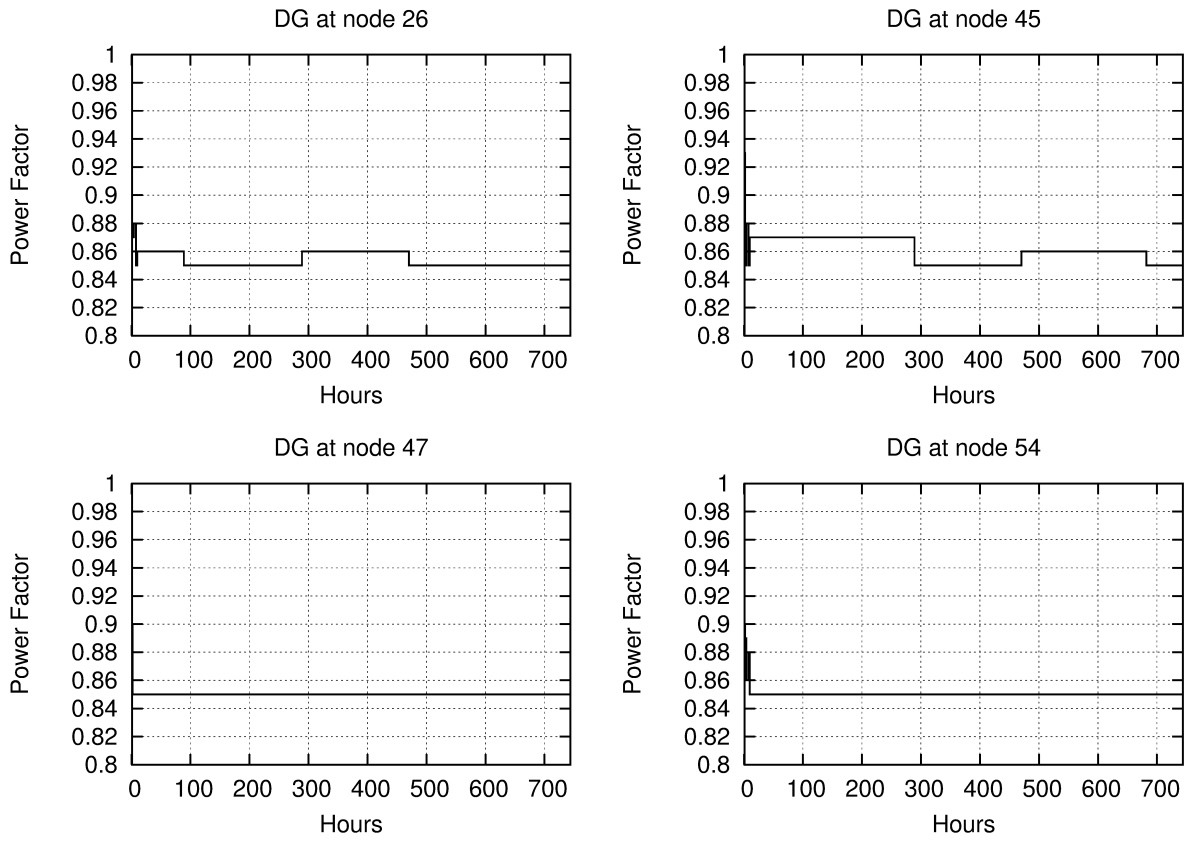


Figure 4.7: Hourly power factor values for the four DG units during the 744 hours

The DG control and coordination technique resulted in a limited number of power factor switching operations, the the value of the power factors  $pf_{26}$ ,  $pf_{45}$ ,  $pf_{47}$  and  $pf_{54}$  have been changed 6, 7, 1 and 4 times respectively during the 744 hours simulated.

Nevertheless, additional mechanisms are required to guarantee a limited total number of switching operations. In chapter 5 a mechanism that controls the total number of switching operations for capacitor banks, DG units, and OLTC transformers is presented.

## 4.9 Summary

Two new control techniques are proposed in this chapter to control and coordinate multiple switched capacitor banks and multiple DG units installed in an electrical power distribution system in order to bring the total system losses to a close-to-minimum value.

The two proposed algorithms are integrated into the real-time distributed power flow analysis described in chapter 3. Both algorithms are based on random search where each node with a capacitor bank or a DG unit randomly changes the state of the attached component (i.e. injected reactive power form a capacitor bank, or power factor of a DG unit).

Each node with a capacitor bank or a DG unit maintains a data structure in which all the previous states are recorded along with the corresponding total system losses (calculated by, and received from the ZCU). In each iteration, the state corresponding to the least total losses is used as the initial state of the random search.

The capacitor bank and DG control and coordination techniques are implemented in the network simulator NS-3 as a set of C++ applications that are combined with the distributed power flow analysis C++ applications developed in chapter 3. Therefore allowing the simulation of the combined analysis and control framework along with the supporting communication network.

The simulation results reported in sections 4.5, 4.6, and 4.7 indicate that the analysis and control framework can achieve a state with a high percentile rank, i.e. close to the global optimum state.

The convergence times obtained from NS-3 simulations are in the range of few minutes which is perfectly within the normal non-emergency operational time frame of distribution systems. The real-time operation of the proposed analysis and control framework is simulated in section 4.8. The hourly load and DG power for a period of 744 hours are used to

represent the hourly measurements from smart meters. The proposed analysis and control framework reduced the total system losses by 13% as illustrated in Table 4.15.

Combining the distributed real-time power flow analysis presented in chapter 3 with the control techniques presented in this chapter creates a framework that can control and coordinate the different components found in electrical power distribution systems in a distributed/decentralized real-time manner.

The combined analysis and control framework provides a seamless coordination among the different system components because all control decisions are based on power flow calculations, and also due to the ongoing exchange of information among the system nodes.

Control techniques for other distribution system components can be developed and easily integrated to the framework. For instance, a control technique for On-Load Tap Changing (OLTC) transformers is developed in chapter 5 and combined with the switched capacitor bank control technique proposed in this chapter to perform Volt/VAR control.

This chapter focused on controlling the injected reactive power (VAR control) from switched capacitor banks and DG units in order to reduce the total system losses, whereas in chapter 5 the switched capacitor banks and the voltage regulators are controlled and coordinated in order to perform Volt/VAR control.



# Chapter 5

## Smart Volt/VAR Control Using the Analysis and Control Framework

A “Smart Volt/VAR Control” technique for smart distribution systems is presented in this chapter. The proposed technique is designed to be integrated into the distributed real-time analysis and control framework discussed in chapters 3 and 4.

In this smart VVC technique, the distributed processing units collaborate together to perform load flow analysis based on smart meters’ measurements and hence control and coordinate the switched capacitor banks and voltage regulating transformers. The objective is to maintain acceptable voltage levels along the distribution feeder, minimize the system losses and limit the number of switching operations.

GNU-Octave simulations are used to evaluate the performance of the proposed smart Volt/VAR Control (VVC) technique in terms of loss reduction, voltage profile and number of switching operations.

The network simulator NS-3 is used to simulate the distributed processing units executing the proposed smart VVC and the supporting communication network. The performance of WiMAX and LTE technologies is evaluated in terms of the smart VVC technique execution time, average packet delays, and average packet delivery ratio.

### 5.1 Introduction

Volt/VAR control is one of the essential tasks in any distribution system, the primary purpose of which is to maintain an acceptable voltage levels at all points along the distri-

bution feeder under all loading conditions. VVC can also be used to improve the efficiency by reducing the system losses, reduce the electrical demand through Conservation Voltage Reduction (CVR) [81, 82], and enable widespread deployment of Distributed Energy Resources DER [81].

On-Load Tap Changing (OLTC) transformers and switched capacitor banks are the two primary tools used by utilities to perform VVC. Additionally, it has been suggested that fast reacting VAR-capable Distributed Generation (DG) inverters can provide the necessary reactive power generation or consumption to maintain voltage regulation [53] and hence serve as an additional tool to perform VVC.

The optimal dispatch of switched capacitor banks in distribution systems has been addressed in several publications using dynamic programming [83], neural networks [44] and fuzzy load models [84].

A two-stage neural network is used in [44] to predict the load profile assuming a pre-determined number of non-conforming load groups, and then select the optimal capacitor banks tap settings, while in [84] fuzzy load models are used to address the uncertainties in system data, especially those in load demands.

The voltage level and the reactive power flow in a feeder are closely related and dependent variables. Control actions to change one of them might results in an opposite action for the other variable, this effect is magnified if there is no coordination between the different VVC tools (e.g. OLTC and switched capacitor banks). The absence of coordination in VVC may cause a hunting and oscillatory behavior of the taps [85]. Therefore the coordinated control of the different VVC tools in a distribution system is inevitable.

Numerous off-line methods and techniques [86, 87, 88, 89, 90, 91, 92, 85] have been proposed in literature to control and coordinate the OLTC, and the switched capacitor banks installed both at the substation and along the feeder, in order to regulate the feeder voltage and the reactive power flow along the feeder. Most of these methods formulate the VVC as an optimization problem with an objective function subject to a set of constrains such as power flow equations, the voltage level, and the number of switching operations of OLTC and switched capacitor banks.

A time-interval based VVC is used in [86, 87] where a genetic algorithm is used in dividing the load profile into partitions, and another genetic algorithm generates the dispatch schedule for the OLTC and switched capacitor banks that minimizes the system losses. A similar approach that includes harmonics into the VVC problem is used in [88]. Particle swarm optimization technique is used in [89] to perform VVC with harmonic consideration, while fuzzy logic and particle swarm optimization are employed in [90] to perform VVC.

An algorithm based on nonlinear interior-point method and discretization penalties is presented in [91] to perform reactive power and voltage control in distribution systems to minimize the daily energy losses with limited switching operations.

All of aforementioned methods employ historical load data and/or load profile forecasts for the next 24 hours, and hence solve the optimization problem and generate a dispatch table for OLTC and switched capacitor banks that minimizes the objective function (e.g. system losses, electric demand, number of switching operations or a combination of these objectives) while satisfying the problem constraints.

Optimal power flow is used in [92] to control the OLTC and switched capacitor banks in order to minimize the energy drawn from the substation while minimizing the number of switching operations of OLTC and capacitors. The authors suggest that the real-time data from the Advanced Metering Infrastructure (AMI) allows the local distribution companies to control their equipment in real-time, but they did not comment on how the communication system delays will affect their proposed algorithm and its execution time. The solution obtained in [92] is locally sub-optimal due to the use of a series of approximations to simplify the optimization problem at hand.

It is evident from the previous discussion that the off-line optimal dispatch solutions of the VVC might not provide the anticipated performance for the smart distribution system, and that greater VVC benefits can be achieved using partially or fully online control systems that leverage the abundance of information made available by the AMI.

Even though the online VVC system inherently depends on communication networks, none of the aforementioned literature presents any details on how exactly the communication networks are used, and none of them provide a performance evaluation of the communication system used and how it interacts with the distribution system analysis and control techniques proposed in the respective literature.

The smart VVC technique presented in this chapter is based on the analysis and control framework described in chapters 3 and 4, as illustrated in Figure 5.1. The DG control and coordination technique presented in chapter 4 can be easily employed in the proposed smart VVC technique but, for the sake of simplicity, the focus in this chapter is on using OLTC and switched capacitor banks to perform VVC.

Switched capacitor banks and OLTC transformers exchange information about the system losses and voltage level violations. This information is aggregated, and hence used to control and coordinate the switched capacitors and OLTCs in order to minimize the system losses while maintaining a good voltage profile. This task is achieved with a limited number of switching operations.

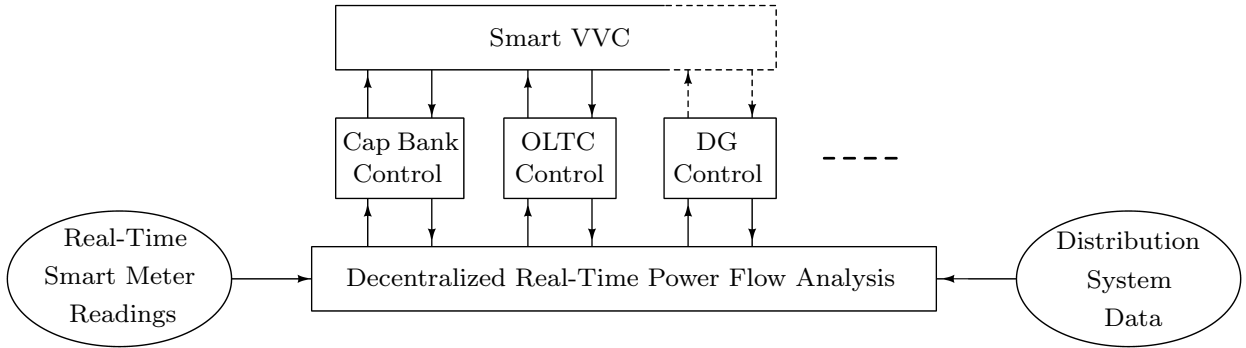


Figure 5.1: Architecture of the proposed smart VVC technique

The performance of the proposed smart VVC technique is evaluated through GNU-Octave and NS-3 simulations.

The rest of this chapter is organized as follows, section 5.2 presents the details of the proposed smart VVC technique, the OLTC control technique, and a mechanism to limit the total number of switching operations.

Sections 5.3 and 5.4 present GNU-Octave and NS-3 simulation results respectively. A brief summary is presented in section 5.5.

## 5.2 Smart Volt/VAR Control

The two primary tools used by utilities to perform VVC are OLTC transformer and switched capacitor banks. In this section, a novel smart VVC technique is presented. An algorithm is proposed to control OLTC transformers, this algorithm is combined with the switched capacitor bank control algorithm presented in chapter 4, section 4.2 in order to perform Volt/VAR control.

The control algorithms for switched capacitor banks and for OLTC transformers are integrated into the analysis and control framework presented in chapter 3, therefore resulting in a seamless coordination among the control techniques for OLTC and switched capacitor banks.

Switched capacitor banks and OLTC transformers exchange and process the information related to the system losses and the voltage profile, and take control actions accordingly. The objective of proposed smart VVC technique is to reduce the total system losses while

keeping the voltage within the acceptable levels  $V_{min} \leq |V| \leq V_{max}$ . A proposed mechanism to limit the number of switching operations for OLTC and switched capacitor banks is also presented in this section.

### 5.2.1 OLTC Control in The Smart Grid Environment

As previously discussed in chapters 3 and 4, the ZCU aggregates the information received from the different system nodes in order to calculate:

1. The total system losses.
2. Number of nodes violating the voltage limits.
3. Magnitude and direction of the node with the maximum deviation from the voltage limits.

This aggregated common information is sent back to all the capacitor banks, OLTCs and DG units within the zone to be used in the control process.

The processing unit installed at the primary and secondary sides of the OLTC transformer maintain data structures that record the history of tap settings and the corresponding total system losses taking voltage level violations into account. Therefore the tap setting corresponding to minimal system losses which meets the voltage violation criteria can be retrieved from these data structures.

OLTC control has three modes of operation:

1. Mode-0:  
The OLTC transformer is controlled using the traditional Line-Drop Compensation (LDC) mechanism implemented as a software installed on the transformer's primary and secondary sides' processing units. The calculated voltages from the distributed load flow analysis framework are used to calculate the tap settings, the detailed description and equations of the LDC mechanism can be found in [93].
2. Mode-1:  
The information received from the ZCU is used to compensate the voltage level violations. This mode is used in case the distribution system does not have any switched capacitor banks, therefore the voltage level violation is compensated only by the OLTC transformer action.

- (a) In case of voltage level violation, the maximum voltage deviation (received from the ZCU) is used by the processing units at the transformer’s primary and secondary sides to control the tap settings as follows:

$$tap_{new} = tap_{old} \pm \frac{max [V_{deviation}]}{V_{step}} \quad (5.1)$$

where  $V_{step} = (5/8) \% = 0.00625 \text{ p.u.}$ .

- (b) In case of no voltage level violation, the tap settings is randomly changed (as discussed in appendix A) and the corresponding total system losses is maintained in a data structure in the local processing unit. A certain number of iterations  $N_{iter}$  is performed and then the tap setting which corresponds to the minimum system losses and meets the voltage level violation criteria is selected.

### 3. Mode-2:

The information received from the ZCU is used to compensate the voltage level violations. This mode is used when the distribution system has switched capacitor banks, in this case the voltage level violation is compensated by the both the OLTC transformers and the switched capacitor banks.

- (a) In case of voltage level violation, the tap settings is changed by one step at a time.

$$tap_{new} = tap_{old} \pm 1 \quad (5.2)$$

- (b) In case of no voltage level violation, the tap settings are randomly changed as described for “Mode-1”. The random changes are only allowed during the third stage of the capacitor bank control technique described in chapter 4.

It is important to emphasize that:

1. This OLTC control technique is executed at the processing units installed at the primary and secondary sides of the OLTC transformer.
2. The ZCU acts collects information from all the nodes in the system in order to create a “common-knowledge” that is shared with all the system nodes.
3. The communication network plays an essential role in reaching a control decision in a dynamic decentralized/distributed manner such that any change in the load values, component status, etc. is accounted for immediately.

4. The tap setting changes mentioned before are only for calculation purposes in the proposed OLTC control algorithm. The control signal that changes the tap settings of the OLTC transformer is *NOT* sent until the algorithm has converged.

### 5.2.2 Limiting The Number of Switching Operations

A common constraint in the VVC problem is to limit the number of switching operations of the OLTC transformers and the switched capacitor banks in order to increase their life expectancy.

Let's assume that the smart meter readings are collected at time instants  $\{t_i ; i = 0, 1, 2, \dots\}$ . The proposed smart VVC technique utilizes the smart meter readings at instant  $t_i$  and calculates a state  $S_i$  for each switched capacitor bank and each OLTC transformer that reduces the system losses while keeping the voltage within the acceptable levels  $V_{min} \leq |V| \leq V_{max}$ .

This process is repeated every time a new set of readings is collected from smart meters, which might result in excessive number of switching operations and hence reduces the life expectancy of OLTCs and switched capacitors.

Therefore an additional mechanism is proposed to limit the number of switching operations, two scenarios are compared at each instant  $t_i$  as follows:

1. Scenario 1:

At instant  $t_i$ , the smart VVC technique suggests a new state  $S_i$  for OLTCs and switched capacitor banks which results in a new (calculated) system losses,  $losses_i^{S_i}$ , as well as a certain number of switching operations for OLTCs  $N_i^{OLTC}$ , and for switched capacitor banks  $N_i^{cap}$ .

2. Scenario 2:

Using the set of measurements at instant  $t_i$  while keeping the OLTCs and switched capacitors in their previous state  $S_{i-1}$ , the total system losses is re-calculated  $losses_i^{S_{i-1}}$ .

3. The two scenarios are compared in terms of:

- (a) Savings at instant  $t_i$  due to losses reduction from  $losses_i^{S_{i-1}}$  to  $losses_i^{S_i}$ .
- (b) Costs associated with switching the OLTCs and the capacitors from state  $S_{i-1}$  to state  $S_i$ , these costs depend on the number of switching operations  $N_i^{OLTC}$  and  $N_i^{cap}$ .

4. Both the savings and costs are converted to monetary values using the following coefficients:
  - (a)  $K_{kWh}$  : monetary cost per kWh.
  - (b)  $K_{OLTC}$  : monetary cost per one OLTC tap change.
  - (c)  $K_{CAP}$  : monetary cost associated with one switching operation of a capacitor bank.
5. The monetary savings and costs at instant  $t_i$  are calculated as follows

$$savings_i = K_{kWh} \times [losses_i^{S_i} - losses_i^{S_{i-1}}] \quad (5.3)$$

$$cost_i = K_{OLTC} \times N_i^{OLTC} + K_{CAP} \times N_i^{cap} \quad (5.4)$$

6. The calculated savings and costs at instant  $t_i$  are compared and a decision is made:
  - (a) If  $savings_i > cost_i$ , then the state  $S_i$  is selected and a control signal is sent out to switch the OLTCs and capacitors accordingly.
  - (b) If  $savings_i \leq cost_i$ , then the state  $S_i$  is rejected, the the previous state  $S_{i-1}$  remains unchanged.

The cost per kWh,  $K_{kwh}$ , can be changed in accordance with the time-of-use electricity rates. It is worth mentioning that  $K_{OLTC}$  and  $K_{CAP}$  are treated in this research as pseudo-costs or pretend-costs which are merely used to limit the number of switching operations. Nevertheless actual average costs  $K_{OLTC}$  and  $K_{CAP}$  could be calculated based on the life expectancy of OLTCs and switched capacitors, maximum number of switching operations, installation and maintenance costs.

### 5.3 GNU-Octave Simulation Results of the Smart VVC Technique

In this section, GNU-Octave simulations are used to evaluate the performance of the proposed smart VVC technique in terms of:

1. Whether the voltage profile is within the acceptable limits,  $V_{max}$  and  $V_{min}$ .



2. Losses reduction.
3. Number of switching operations.

The performance of the communication network which supports the analysis and control framework is assessed in section 5.4 using NS-3 simulations.

In GNU-Octave simulations, the backward/forward load flow analysis for unbalanced three phase distribution systems is implemented using the *abcd* parameters modeling approach described in [93] for distribution system line models, loads, transformers and step-voltage regulators.

Hourly load profile values are used in the simulations to represent the smart meter readings. For all the simulations in this section, the two coefficients  $K_{OLTC}$  and  $K_{CAP}$  are equal to each other,  $K_{OLTC} = K_{CAP} = K$ .

Three distribution feeders are used in this section, the unbalanced three-phase IEEE 13-node feeder, and a 31-node and a 69-node balanced feeders represented as single-phase systems. For balanced single-phase feeders, the single-phase calculated losses is used to obtain the savings and costs according to equations 5.3 and 5.4. Whereas for three-phase systems, the equivalent single-phase losses - (1/3) of the calculated three-phase losses - is used to obtain the savings and costs according to equations 5.3 and 5.4.

### 5.3.1 IEEE 13-Node Test Feeder

Three test cases are used in this subsection for the unbalanced three-phase IEEE 13-node test feeder. The objective is to keep the voltage profile within  $V_{min} = 0.95$  p.u. and  $V_{max} = 1.05$  p.u., reduce the system losses, while limiting the total number of switching operations.

1. Base case:  
The original IEEE 13-node test feeder operating at the peak load values with fixed capacitors, where the OLTC transformer between nodes 650 and 632 operating in “Mode-0”, i.e. controlled using a line-drop compensation mechanism.
2. Test case 1:  
The original IEEE 13-node test feeder operating at the peak load values with fixed capacitors, where the OLTC transformer is operated in “Mode 1”. The tap settings is controlled individually for each phase to reduce the system losses while satisfying the voltage limits constraints.

3. Test case 2:

The IEEE 13-node test feeder where the capacitor data is modified such that five blocks of 100 kVAR capacitors are connected at each phase of node 675, and five blocks of 50 kVAR capacitors are connected in phase-c of node 611 [92]. The OLTC transformer is operated in “Mode-2”, and its taps are group controlled, i.e.  $\{tap_a = tap_b = tap_c\}$ .

GNU-Octave implementation of the proposed smart VVC technique is applied for the “Base case”, the tap settings obtained using “Mode-0” are [11, 8, 11] with a total system losses of 110.51 kW.

For “Test case 1”, the proposed smart VVC algorithm is applied with the OLTC control set to “Mode-1”. The obtained OLTC tap settings are [14, 7, 15] corresponding to a total system losses of 107.31 kW.

In “Test case 2”, the proposed smart VVC technique is applied to the feeder with the OLTC control set to “Mode-2”. The 24-hour load profile shown in Figure 5.2 is used to replace the hourly readings from smart meters which are used as an input to the proposed smart VVC technique.

The daily number of switching operations for the OLTC transformer, and the switched capacitor banks are calculated using equations 5.5 and 5.6 respectively.

$$N^{OLTC} = \sum_{i=2}^{24} |tap_i - tap_{i-1}| \quad (5.5)$$

$$N^{CAP} = \sum_{i=2}^{24} |cap_i - cap_{i-1}| \quad (5.6)$$

The proposed smart VVC technique is based on random search, hence the obtained results are not deterministic. Therefore, the proposed smart VVC technique is executed for 100 times, and the percentile rank of the minimum, maximum, and mean losses are used to capture the randomness in the obtained results.

Table 5.1 summarizes GNU-Octave 100-run simulation results for “Test case 2” of the IEEE 13-node test feeder. Multiple values of  $K$  are used in the simulation and the cost per kWh,  $K_{kWh}$ , is set to be 0.1.

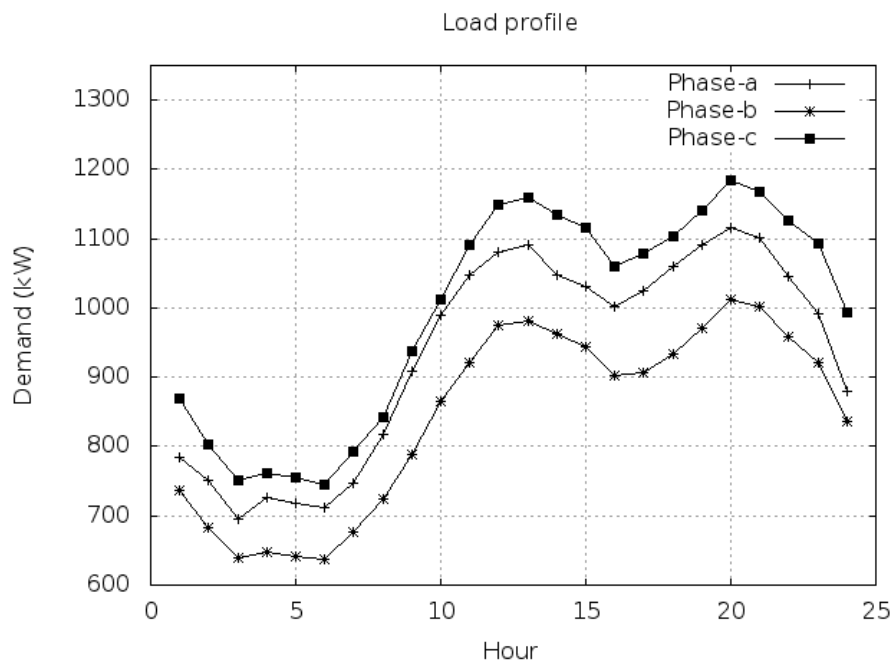


Figure 5.2: Load profile for IEEE 13-node test feeder from [92]

Table 5.1: IEEE 13-node test feeder: test case-2  
The proposed smart VVC - 100-run results  
(Two capacitors & an OLTC)

		$K = 0.00$	$K = 0.05$	$K = 0.10$
Daily 3 – $\Phi$ losses (MWh)	Min.	1.6110	1.6235	1.6134
	Mean	1.6170	1.6511	1.6563
	Max.	1.6245	1.6800	1.6887
Total daily num. of switching operations	Min.	4	0	0
	Mean	12.53	1.67	0.95
	Max	24	4	4
Min. voltage (p.u.)		0.95634	0.95001	0.95001
Max. voltage (p.u.)		1.0500	1.0496	1.0491
Mean computation time (minute)		$\approx 2.3$	$\approx 2.07$	$\approx 2.05$

Table 5.2: Switched capacitor banks information for the 31-node feeder

Bus No.	1	1	13	15	19	23	25
Cap. (KVar)	900	600	600	600	300	900	900

### 5.3.2 31-Node Feeder

The balanced 31-node feeder with six switched capacitors and one OLTC transformer from [86, 87] is used to assess the performance of the proposed smart VVC technique. The objective is to minimize the system losses, limit the number of switching operations while keeping the voltage level at all nodes between 0.95 and 1.05 p.u.

The capacitor bank data is given in Table 5.2. The load at each node in the system is assumed to be 50% constant power and 50% constant impedance. The base power is 52.9 MVA and the daily load profile shown in Figure 5.3 is used. It is also assumed that the initial position of the OLTC tap is 0 and the initial status of all capacitor banks is “OFF”.

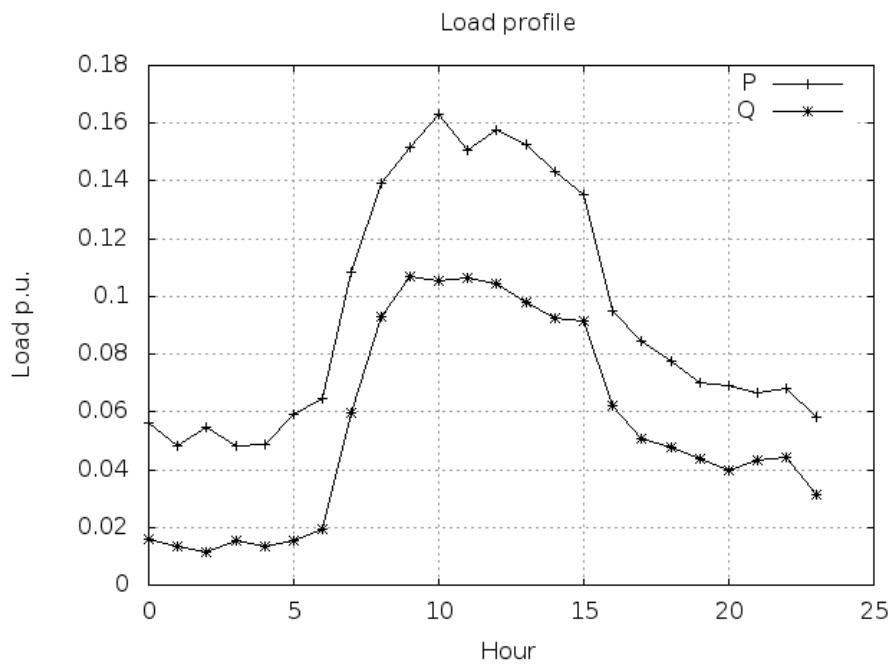


Figure 5.3: Load profiles for the 31-node feeder from [86, 87]

Table 5.3: 31-node test feeder  
The proposed smart VVC - 100-run results  
(Six capacitors & an OLTC)

		$K = 0.00$	$K = 0.05$	$K = 0.10$
Daily $1 - \Phi$ losses (MWh)	Min.	2.2833	2.2881	2.2973
	Mean	2.2883	2.2950	2.3075
	Max.	2.2938	2.3023	2.3218
Total daily num. of switching operations	Min.	22	14	14
	Mean	30.22	19.08	17.83
	Max	53	26	24
Min. voltage (p.u.)		0.95312	0.95275	0.95275
Max. voltage (p.u.)		1.039	1.0256	1.039
Mean computation time (minute)		$\approx 1.93$	$\approx 1.82$	$\approx 1.79$

The smart VVC technique is applied to this feeder for different values of  $K$ . The 100-run results are summarized in Table 5.3.

### 5.3.3 PG&E 69-Node Feeder

The PG&E 69-node feeder from [76] is modified in [91] by adding a regulating transformer installed at the substation with its taps adjusted such that the voltage at the secondary side of the transformer is fixed at 1.05 p.u. The loads in the system are groups into six types of loads, each with a different daily load curve as shown in Figure 5.4. As described in [91], ten switched capacitor banks are installed at nodes 9, 19, 31, 37, 40, 47, 52, 55, 57 and 65, where 3 and 4 sets of 0.3 MVAR capacitors are installed at nodes 37 and 52 respectively and 2 sets of 0.3 MVAR for all other nodes.

The proposed smart VVC technique is applied to the modified 69-node system, the 100-run results for different values of  $K = K_{CAP}$  are presented in Table 5.4.

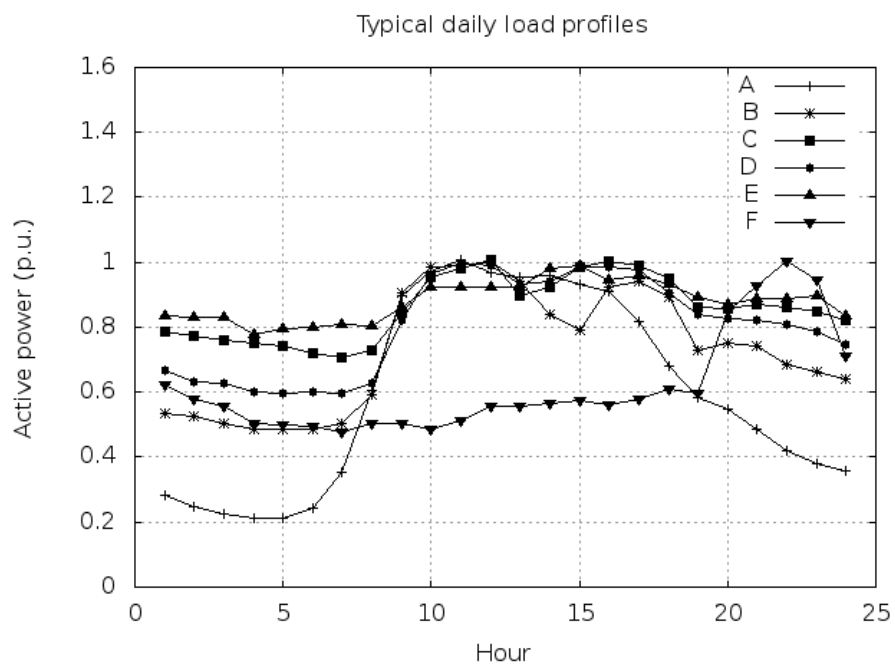


Figure 5.4: Load profiles for the 69-node feeder from [91]

Table 5.4: PG&E 69-node feeder  
The proposed smart VVC - 100-run results  
(Ten capacitors)

		$K = 0.00$	$K = 0.05$	$K = 0.10$
Daily $1 - \Phi$ losses (MWh)	Min.	1.7578	1.7402	1.7695
	Mean	1.8899	1.8946	1.9004
	Max.	2.0193	2.0473	2.0615
Total daily num. of switching operations	Min.	5	0	0
	Mean	31.17	16.86	10.87
	Max	68	49	26
Min. voltage (p.u.)		0.9771	0.97383	0.97489
Max. voltage (p.u.)		1.0552	1.0552	1.0552
Mean computation time (minute)		$\approx 4.61$	$\approx 4.50$	$\approx 4.75$

### 5.3.4 Comments on the Simulation results

The main advantage of the proposed smart VVC technique is its ability to leverage the smart meter readings in real-time to control and coordinate OLTC transformers and switched capacitor banks in order to achieve the required operational goals.

Another important feature of the proposed smart VVC technique is that it relies on performing decentralized/distributed power flow analysis as the first step before any control action can be taken, therefore resulting in a seamless coordination. This feature facilitates the integration of other components into the VVC technique such as VAR-capable DG units.

Instead of using a “hard” limit the number of daily switching operations, the introduction of the coefficients  $K_{OLTC}$  and  $K_{CAP}$  limits the number of switching operations based on a comparison between the anticipated benefits and costs, therefore providing a more flexible approach that can allow more/less switching operation in a particular day based on the load values and the time-of-use electricity rates.

Additionally, the proposed smart VVC approach does not use complex optimization techniques in order to achieve the results, it is a simple approach that can be easily imple-



mented on any processing unit, and yet it can achieve good performance as indicated by the simulation results reported in chapter 4 and in this chapter.

The voltage profile of the three distribution feeders simulated in this section is within the specified limits of 0.95 and 1.05 except for the 69-node feeder where the maximum voltage is 1.055 p.u., this can be attributed to the fact that in this system the voltage regulating transformer is set a fixed voltage of 1.05 p.u., hence there is no coordination between the capacitor banks and the OLTC transformer.

The average number of switching operations is reduced by increasing the cost  $K = K_{OLTC} = K_{CAP}$  which indicates the effectiveness of the proposed method of limiting the number of switching operations by comparing the anticipated benefits and costs. Increasing the cost  $K$  results in increasing the average daily losses of the system.

For instance, in the IEEE 13-node feeder, increasing the cost  $K$  from 0.00 to 0.10 reduces the average number of daily switching operations by 92.4% and increased the average daily losses by 2.43%.

## 5.4 NS-3 Simulation Results of the Smart VVC Technique

The network simulator NS-3 is used in this section to evaluate the performance of the proposed smart VVC technique. The 31-node feeder with six capacitor banks and one OLTC transformer described in subsection 5.3.2 is used in NS-3 simulation. The generated OLTC and switched capacitor banks dispatch tables obtained from NS-3 simulations for  $K = 0.1$  are given in Table 5.5. The daily system losses are 2.312 MWh with a total number of switching operations of 22, which agrees with the results reported in Table 5.3 in section 5.3.

Table 5.6 compares the performance of WiMAX and LTE supporting wireless networks in terms of the average execution time of the smart VVC technique (for one load point), the average packet delay and the average packet delivery ratio. LTE technology provides a relatively smaller packet delay and slightly faster convergence time compared to WiMAX technology.

The smart VVC technique needs approximately 10 minutes to process the load data acquired from the smart meters in order to obtain a state for the OLTC and switched capacitor banks that satisfies specific operational goals. The time between the switching events for capacitors (and also for OLTC) are practically few hours, therefore the 10

Table 5.5: 31-node test feeder - Smart VVC results  
Dispatch table obtained from NS-3 simulation

Hour	OLTC Tap Setting	Injected Reactive Power (kVAR) at Switched Capacitor Bank Node					
		1	13	15	19	23	25
1	0	0	0	0	300	0	0
2	0	0	0	0	300	0	0
3	0	0	0	0	300	0	0
4	0	0	0	0	300	0	0
5	0	0	0	0	300	0	0
6	0	0	0	0	300	0	0
7	0	900	600	600	0	900	0
8	3	900	600	600	300	900	900
9	3	900	600	600	300	900	900
10	4	900	600	600	300	900	900
11	6	900	600	600	300	900	900
12	6	900	600	600	300	900	900
13	6	900	600	600	300	900	900
14	6	900	600	600	300	900	900
15	6	900	600	600	300	900	900
16	6	900	600	600	300	900	900
17	6	900	600	600	300	900	900
18	6	900	600	600	300	900	900
19	6	900	600	600	300	900	900
20	6	900	600	600	300	900	900
21	6	900	600	600	300	900	900
22	6	900	600	600	300	900	900
23	0	0	0	600	300	900	0
24	0	0	0	600	300	900	0

Table 5.6: NS-3 simulation results of the 31-node feeder for WiMAX and LTE

	WiMAX	LTE
Average Execution Time (minutes)	$\approx 9.6$	$\approx 7.6$
Average Packet Delay (milliseconds)	$\approx 41.7$	$\approx 15.1$
Average Packet Delivery Ratio ( % )	$\approx 99.3\%$	$\approx 99.9\%$

minutes required for the VVC technique is well within the operation time frame for these components.

## 5.5 Summary

This chapter presents a smart VVC technique that employs the analysis and control framework presented in chapters 3 and 4. The proposed smart VVC technique leverages the data acquired from smart meters, and use it to perform system analysis and control.

The switched capacitor banks and OLTC transformers exchange information about the system losses and voltage level violations, this information is aggregated by the ZCU and hence used to control and coordinate the capacitors and OLTCs to perform VVC.

A new approach is proposed to limit the total number of switching operations on hourly basis, the switching operations suggested by the smart VVC technique is evaluated by comparing the costs associated with the switching operations and the corresponding reduction in system losses.

GNU-Octave simulations of the proposed smart VVC technique indicate the effectiveness of the smart VVC technique in achieving the operational goals with a limited number of switching operations.

The implementation of the proposed smart VVC and the supporting wireless communication network is simulated using the network simulator NS-3. WiMAX and LTE communication technologies are used to provide the data connectivity for the proposed analysis and control framework and for the smart VVC technique.



# Chapter 6

## A Test Bed to Examine the Analysis and Control Framework

The core idea presented in this thesis is to integrate distributed processing units, and wireless communication networks into the electrical power distribution system analysis, control, and operation.

In this chapter, an experimental setup, composed of multiple single-board computers connected over a data network, is created, and used as a test bed to examine the ideas and concepts presented in this thesis. Each computer in this test bed represents a node in the distribution system.

The functionality of the analysis and control framework is implemented as a set of C++ applications installed on each computer (i.e. node). Network programming (a.k.a. socket programming) is used to establish the data connectivity among the computers (i.e. nodes) such that they can exchange information, and collaborate together in order to perform distribution system analysis and control.

This experimental setup serves as a proof of concept for the distribution system analysis and control framework presented in this thesis.

### 6.1 Introduction

Throughout chapters 3, 4, and 5, the performance of the distribution system analysis and control framework was evaluated using computer simulations. GNU-Octave and NS-3 were

used to assess the performance of the framework in terms of voltage profiles, the reduction in system losses, the obtained state for the different system components (e.g. DG, capacitor bank, and OLTC transformers), as well as the average packet delay, the average packet delivery ratio, and the average execution time.

In this chapter, an experimental setup is used to examine the analysis and control framework. This experimental setup consists of multiple “Raspberry PI” [94, 95] computers equipped with WiFi<sup>1</sup> Network Interface Cards (NIC). Each Raspberry PI unit represents one node in the distribution system.

The WiFi technology is *not* suitable for the actual deployment of the analysis and control framework in an actual distribution systems due to its limited communication range which is typically less than a hundred meters. Therefore, the use of the WiFi technology in this test bed is *not* intended to evaluate the performance of the wireless communication network, but it is intended to be a proof-of-concept that “multiple processing units communicating over a wireless network can achieve the functionality of the analysis and control framework presented throughout this thesis”.

The C/C++ applications developed in chapter 3, section 3.4 are modified and combined with C/C++ network programming (a.k.a. socket programming) in order to provide data connectivity among the different nodes in the distribution system, therefore allowing the nodes to collaborate, exchange information over Transmission Control Protocol (TCP) sockets, process the received data, and hence take control actions.

In this experimental setup, the interface with smart meters, switched capacitor banks, DG units, OLTC transformers is done in software using input/output files.

The rest of this chapter is organized as follows, a description of the Raspberry PI single-board computer and its different aspects is presented in section 6.2. An introduction to socket programming and to the client/server communication model is presented in section 6.3.

Section 6.4 discusses the hardware and software aspects of the test bed and its operation. Five test cases for a 15-node distribution feeder are discussed in details in section 6.5. Section 6.6 presents a brief summary and some concluding remarks.

---

<sup>1</sup>Wireless Local Area Network (WLAN) technology based on the IEEE 802.11 standard.



Figure 6.1: Raspberry PI unit [95]

## 6.2 Raspberry PI Computer

Raspberry PI is a low cost credit-card sized single-board Linux computer developed by the Raspberry PI foundation [94].

The Raspberry Pi has a Broadcom<sup>2</sup> system on a chip (SoC)<sup>3</sup> which includes an ARM<sup>4</sup> 700 MHz processor, a 512 MB of RAM, and a Graphics Processing Unit (GPU). It does not include a built-in hard disk or solid-state drive, but uses an SD card for booting and persistent storage.

Figures 6.1 and 6.2 shows a Raspberry PI unit and its Printed Circuit Board (PCB) layout respectively.

The Raspberry PI modules have a set of low-level peripherals that can be used to interface with sensors and actuators. These low-level peripherals include [96]:

---

<sup>2</sup>Broadcom Corporation is an American fabless semiconductor company in the wireless and broadband communication business.

<sup>3</sup>A System on a Chip (SoC) is an integrated circuit that integrates all components of a computer or other electronic system into a single chip. SoC is typically used for powerful processors, capable of running software such as the desktop versions of Windows and Linux.

<sup>4</sup>ARM is a family of computer processors architectures developed by British company ARM Holdings.

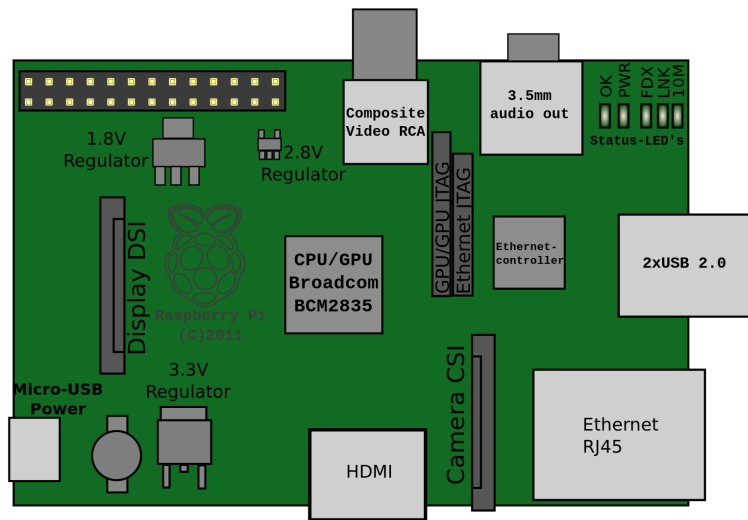


Figure 6.2: Raspberry PI PCB layout [95]



1. General Purpose Input Output (GPIO) pins:  
GPIO is a generic pin on an integrated circuit whose behavior, including whether it is an input or output pin, can be controlled by the user at run time.
2. Universal Asynchronous Receiver/Transmitter (UART) pins:  
A UART is usually an individual (or part of an) integrated circuit used for serial communications over a computer or peripheral device serial port.
3. Inter-Integrated Circuit (I<sup>2</sup>C) bus:  
I<sup>2</sup>C is serial bus invented by the Philips semiconductor division, today NXP Semiconductors, used for attaching low-speed peripherals to a motherboard, embedded system, cellphone, or other digital electronic devices.

In the current implementation of this test bed, the interface with smart meters, switched capacitor banks, DG units, OLTC transformers is done in software using input/output files, whereas in the future work the low-level peripherals can be used to interface the Raspberry PI to actual smart meters or switched capacitor bank actuators.

There are many Linux distributions optimized for Raspberry PI computers including the Debian-based operating system, “Raspbian” [97], and the Fedora-remix operating system, “Pidora” [98]. The test ted described in this chapter uses “Pidora” operating system.

A WiFi adapter is attached to the Raspberry PI unit on a Universal Serial Bus (USB)<sup>5</sup> port. Therefore, allowing the Raspberry PI to connect to WiFi networks and exchange information with other Raspberry PI units.

The Raspberry PI unit can be operated with a full set of peripherals such as a keyboard, a mouse, and a monitor, and it can also be operated in the so-called “headless” mode without any peripherals. When the Raspberry PI is operated in the “headless” mode it can be accessed over the network in several ways such as:

1. Secure Shell (SSH) protocol:  
SSH is a cryptographic network protocol for secure data communication, remote command-line login, remote command execution, and other secure network services between two networked computers.

---

<sup>5</sup>Universal Serial Bus (USB) is an industry standard that defines the cables, connectors and communications protocols used in a bus for connection, communication, and power supply between computers and electronic devices.

2. Virtual Network Computing (VNC) system:

VNC is a graphical desktop sharing system that uses the Remote Frame Buffer protocol (RFB) to remotely control another computer. It transmits the keyboard and mouse events from one computer to another, relaying the graphical screen updates back in the other direction, over a network.

## 6.3 Socket Programming

In computer network programming (a.k.a. socket programming), computer programs are written to allow different processes to communicate over a computer network.

A socket is an endpoint in a communication link between two processes running on the same or different computers. A socket consists of an IP address and a port number. An IP address identifies a host (i.e. computer), and a port number identifies a process running on that host [99]. The process associated with a port is usually a server program waiting for incoming connections.

Figure 6.3 illustrates the socket communication between two processes on two different hosts. When a Process A on Host A sends a message to a socket, the network management software (i.e. the protocol stack) divides the message into several packets and sends these packets through Host A's NIC to the destination (Host B). Each packet contains the destination's IP address and port number. Host B protocol stack receives the packets through the NIC and reassembles them into the original message, which is then made available to process B [99].

Sockets are classified according to communication properties. Each socket has an associated type, which describes the semantics of communications using that socket. The socket type determines the socket communication properties such as reliability, ordering, and prevention of duplication of messages. The two basic internet socket types are:

1. Stream Sockets:

Stream sockets provide a connection-oriented communication link between two hosts. This means that the connection between two hosts remains open throughout the duration of the dialogue between them [100]. Stream sockets relies on the Transmission Control Protocol (TCP) to provide a reliable, ordered, error-checked delivery of data packets.

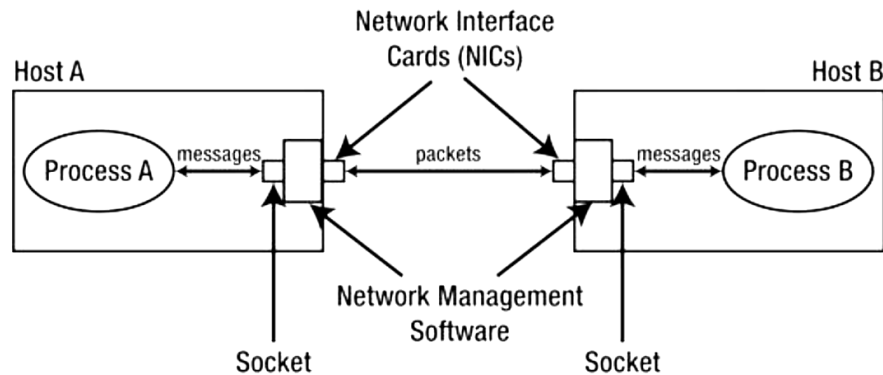


Figure 6.3: Two processes using sockets to communicate [99]

## 2. Datagram Sockets:

Datagram sockets provide a connectionless communication. This means that a connection is not maintained throughout the duration of the dialogue [100]. Data packets are sent as an isolated transmissions, individually addressed and routed. Datagram sockets uses the User Datagram Protocol (UDP). UDP is an unreliable protocol where data packets can be lost, or arrive out of order. UDP is mainly used in real-time applications such as Voice over IP (VoIP) where the latency is the primary concern, and a few lost packets would not affect the performance.

The test bed implementation described in this chapter uses TCP stream sockets to provide reliable, ordered, and error-free data connectivity among the different nodes.

### 6.3.1 Client/Server Communication Model

Clients and servers are the most common categories of network software. A server is a process or application running on a certain host listening for incoming connections on a specific port. Whereas a client is another process or application running on the same or different host, the client initiates the dialogue with the server by trying to connect to the server's host machine on the specified port [100].

The World Wide Web does not allow clients to communicate directly with each other. Instead, a server is used as an intermediary, in order to provide a “simulated” peer-to-peer (P2P) facilities [100].

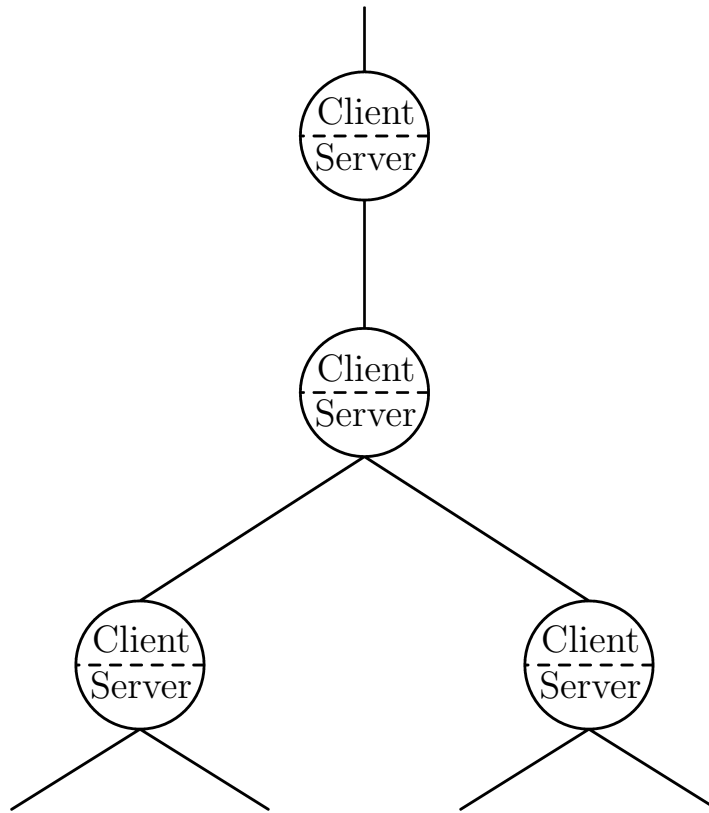


Figure 6.4: Data connectivity among parents and children in a typical electrical power distribution system

It is possible for two connected hosts to act as both client and server, which is another way of establishing a P2P connectivity. This approach is used in the test bed implementation described in this chapter.

As illustrated in Figure 6.4, each node in this test bed acts as a server that waits for incoming connections from its children nodes. The same node also acts as a client that initiates a connection with its parent. The parent/children relationship in radial distribution systems was discussed in chapter 3, section 3.2.

## 6.3.2 C/C++ Socket Programming - Data Structures and Linux System Calls

Linux socket programming involves multiple data structures and system calls, a detailed description of which can be found in multiple books and online tutorials such as [99, 100, 101, 102, 103].

The data structures used in C/C++ socket programming include [101]:

1. ***addrinfo***: contains information about the address family (i.e. IPv4<sup>6</sup> or IPv6<sup>7</sup>), socket type (i.e. stream or datagram socket), and socket address.
2. ***sockaddr***: contains information about the destination address and port number. Similar data structures are ***sockaddr\_in*** and ***sockaddr\_in6*** are used for IPv4 and IPv6 respectively. Alternatively, the data structure ***sockaddr\_storage*** can be used for both IPv4 and IPv6.

The Linux system calls involved in C/C++ socket programming include [101]:

1. ***getaddrinfo()***:  
Prepares for establishing a connection to a remote host. It uses the following information as input and returns a linked-list of all possible IP's corresponding to the remote host.
  - (a) Remote host name or one of its IP addresses.
  - (b) Remote host port number or service identifier (e.g. http).
  - (c) Socket type (as a part of an ***addrinfo*** structure).
2. ***socket()***:  
Uses the results from ***getaddrinfo()*** to create a socket connecting the local host to the remote host.
3. ***bind()***:  
Associates a socket with a port number on the local host. This is commonly done when creating a server that is going to ***listen()*** for incoming connections on a specific port.

---

<sup>6</sup>Internet Protocol version 4 (IPv4) is the fourth version in the development of the Internet Protocol (IP). It uses 32-bit addresses.

<sup>7</sup>Internet Protocol version 6 (IPv6) is the latest version of the Internet Protocol (IP). It uses 128-bit addresses, therefore it will overcome the anticipated IPv4 exhaustion problem.

4. ***connect()***:  
Used by clients to connect to a remote host using a socket created by the ***socket()*** system call.
5. ***listen()***:  
Used by servers to listen for incoming connections on a socket created by the ***socket()*** system call.
6. ***accept()***:  
Used by servers to accept incoming connections the specified socket.
7. ***send()*** and ***recv()***: Sends and receives data to/from the specified socket.
8. ***close()*** and ***shutdown()***: Terminates the communication session on the specified socket.
9. ***select()***: This system call allows monitoring several sockets at the same time, waiting until one of them is ready for some input/output operation [104].

## 6.4 The Test Bed

This section briefly describes the hardware and software components of the test bed, as well as its operation. Photographs of the test bed are shown in Figures 6.5 and 6.6.

### 6.4.1 Hardware

The hardware architecture of the test bed implementation described in this chapter consists of seventeen Raspberry PI computers equipped with WiFi network interface cards. Five Raspberry PI units are operated with a full set of I/O peripherals (i.e. monitor, keyboard, and mouse), while twelve units are operated in the headless mode.

As illustrated in Figure 6.7, the seventeen Raspberry PI computers connect to a WiFi access point (AP) with a Service Set Identifier (SSID): “SmartDistSys”. In order to allow remote access to the test bed over the Internet, an additional laptop with two network interface cards is connected to “SmartDistSys”, and to the Internet.



Figure 6.5: The test bed - A photograph

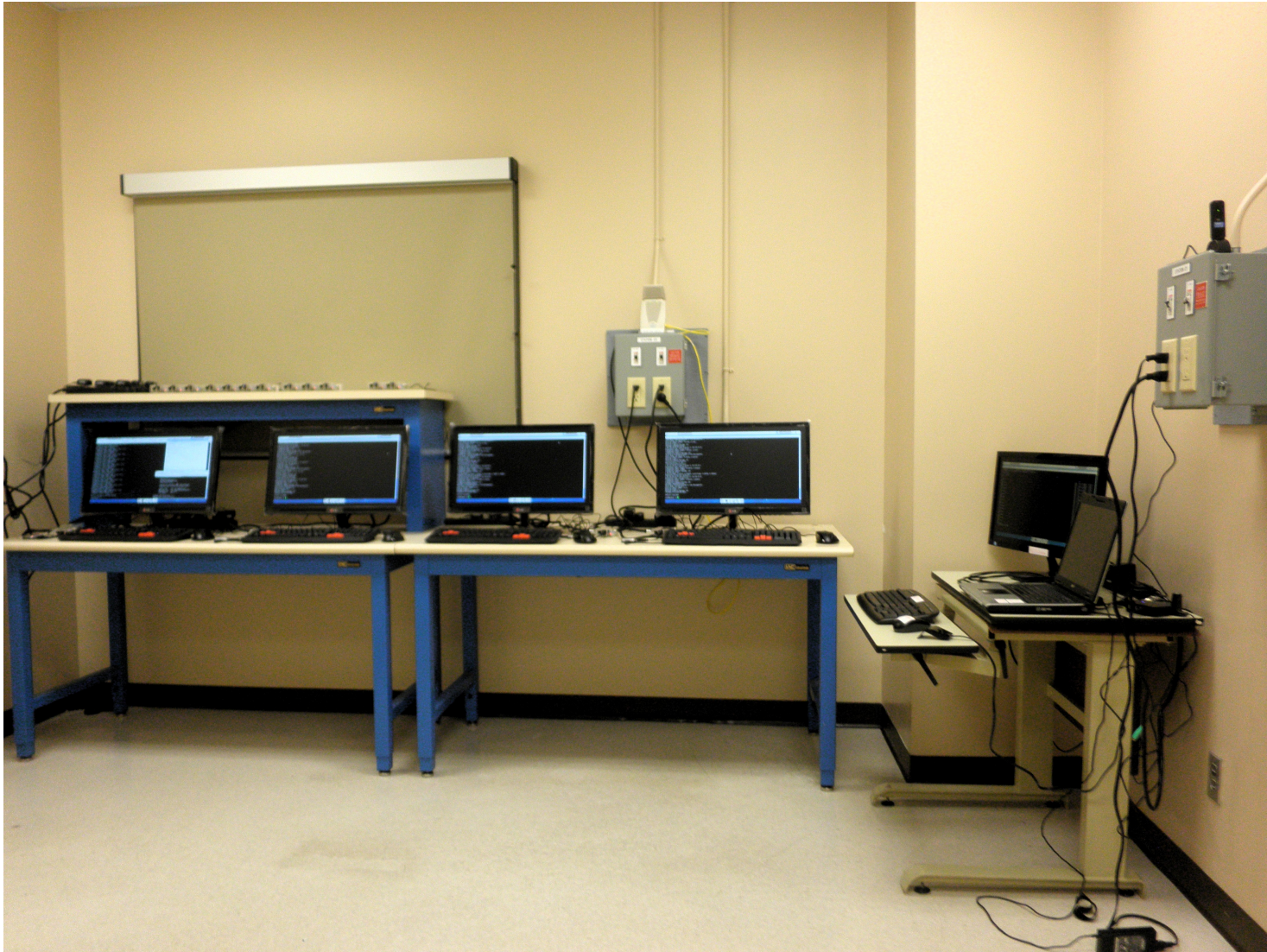


Figure 6.6: The test bed - A photograph



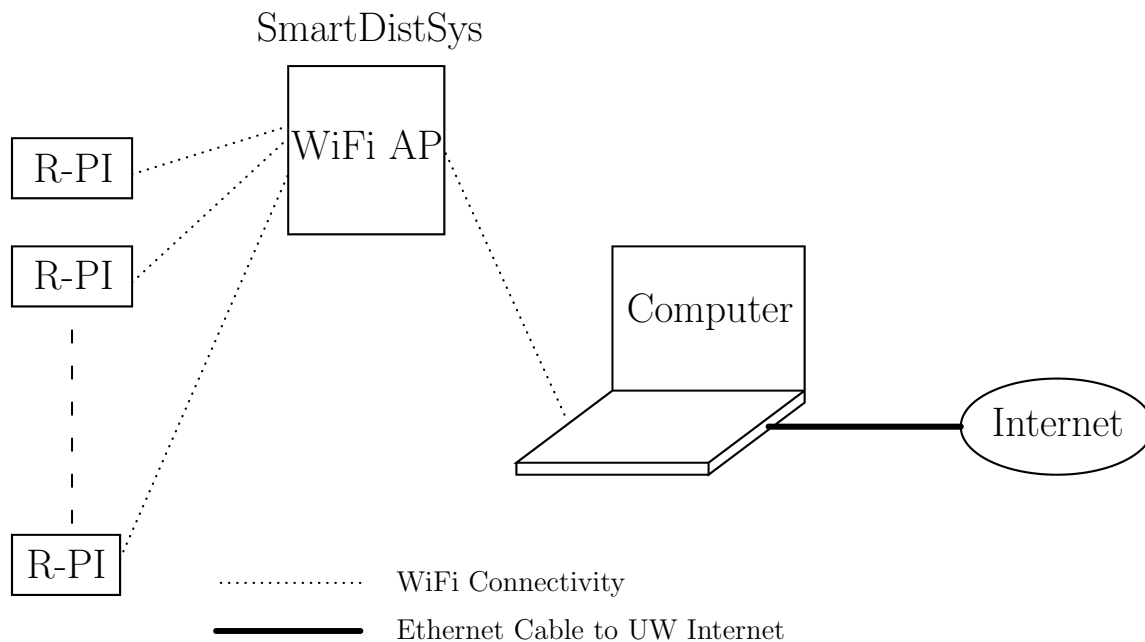


Figure 6.7: Hardware architecture of the test bed

## 6.4.2 Software

In terms of software, three C++ classes are designed based on the socket programming data structures and Linux system calls described in section 6.3. These classes are:

1. ***Node***:

An object of type ***Node*** is created for each node (a node is an electrical power bus, combined with a processing unit and a communication transceiver) in the system. This object can perform the following functions:

- (a) Create server: used to listen for incoming connections from children.
- (b) Create client: used to connect to the server running on the parent node.
- (c) Handle the data received from sockets.
- (d) Allow the user to enter commands using keyboard. There are few command implemented to display the system status (e.g. number of connected sockets, their IP addresses), and to send text messages to other nodes manually.

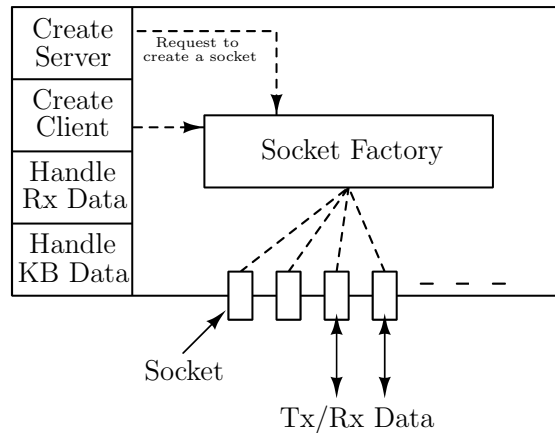


Figure 6.8: Socket communication software architecture of a node

## 2. *Socket*:

An object of type *Socket* is created for every socket defined on any node in the system. This object can perform the following functions:

- (a) Accept incoming connections in case of a server socket.
- (b) Send data to remote hosts.
- (c) Receive data from remote hosts.

## 3. *SocketFactory*:

Only one object of type *SocketFactory* is defined for each node in the system. The main functionality of this object include:

- (a) Creating new sockets: This is done through the “create server” and “create client” functions implemented in the class *Node*.
- (b) Monitor all the sockets (on a node) in the same time using the *select()* Linux system call described in section 6.3.

Figure 6.8 illustrates the proposed socket communication software architecture of a typical node in the proposed distribution system analysis and control framework.

The two classes *DspfApp* and *ZcuApp*, described in chapter 3, section 3.4, are combined (using Inheritance concept in Object Oriented Programming (OOP)) with the aforementioned socket programming software node architecture (illustrated in Figure 6.8).

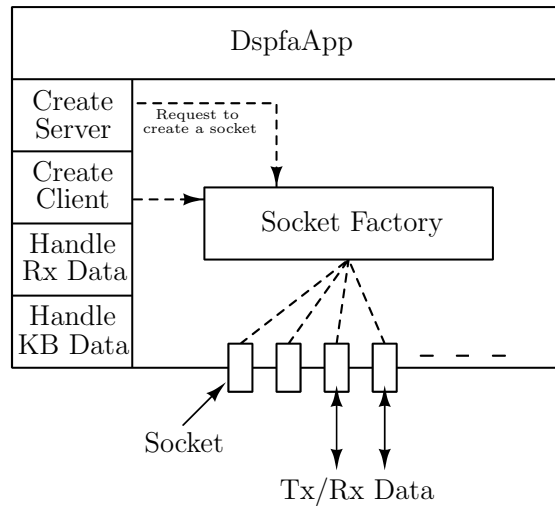


Figure 6.9: Software architecture of *DspfaNode*

This step completes the power and communication systems integration in the test bed in order to examine the distribution system analysis and control framework discussed in this thesis. Figures 6.9 and 6.10 illustrate the resulting software architecture of a regular node in the system *DspfaNode*, and of the Zone Control Unit (ZCU) node *ZcuNode*.

The resulting application *DspfaNode* is installed on every node in the system, except the ZCU, which has the application *ZcuNode* installed.

### 6.4.3 Test Bed Operation

In order to test the analysis and control framework for a particular distribution system, a binary file, “\*.bin”, containing the distribution system data is created using GNU-Octave. The distribution system data contained in this binary file are:

1. Peak load values.
2. Line impedance.
3. Shunt fixed and switched capacitors information.
4. DG information.

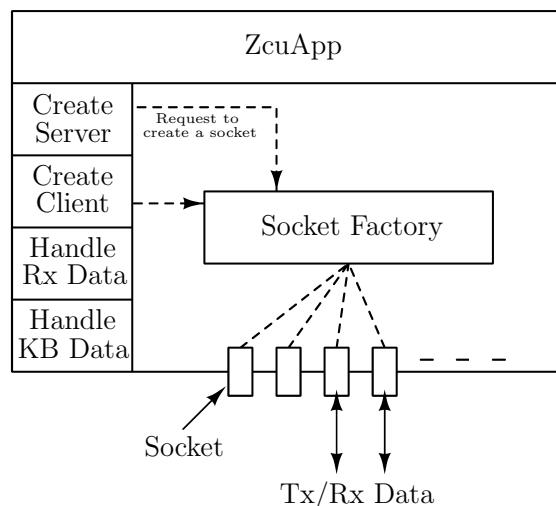


Figure 6.10: Software architecture of *ZcuNode*

5. Transformers and voltage regulator information.

The test bed operates in two modes:

1. The Preparation Mode (Setup Mode):

In this mode, the Octave-generated binary file is sent over the WiFi network to a specific Raspberry PI node designated as the “MasterNode”. This node has a special set of C++ scripts created to extract the distribution system data from the binary file, generate individual binary files containing the data pertaining to each individual node, and transfer the generated individual files to the respective nodes over the WiFi network.

For instance, the information pertaining to node *nn* is extracted into a new set of data files as follows:

(a) *node\_nn.data*:

This file contains the following information:

- i. Node ID.
- ii. Peak load value.
- iii. Number of children.
- iv. line impedance to the parent.

- v. The node's ID, IP address, and the listening port number.
  - vi. Children ID's, IP addresses, and the listening ports numbers.
  - vii. Parent ID, IP address, and the listening port number.
  - viii. The IP address and the port number of the ZCU.
  - ix. Initial voltage and the allowed voltage tolerance  $\epsilon$ .
- (b) ***node\_nn\_RegTrans.data***:  
This file contains information related to voltage regulating transformers connected to node ***nn***. This file type is used when the transformer has a fixed tap settings. This file include information such as:
- i. Whether node ***nn*** is the primary/secondary node.
  - ii. The fixed tap setting.
  - iii. The transformer's impedance referred to the primary side.
- (c) ***node\_nn\_Avr.data***:  
This file contains information about Automatic Voltage Regulators (AVR) connected to node ***nn***. The information contained in this file include:
- i. Whether node ***nn*** is the primary/secondary node.
  - ii. The transformer's impedance referred to the primary side.
  - iii. Information related to the automatic control of the voltage regulator using the Line Drop Compensation (LDR) method [11] such as the rating of the current transformer primary side  $CT_P$ , the potential transformer turns ratio  $N_{PT}$ , the  $R'$  and  $X'$  dial settings, etc.
- (d) ***node\_nn\_Dg.data***:  
Information pertaining to DG units (e.g. rated power, maximum and minimum power factor) connected to node ***nn*** is included in this file.
- (e) ***node\_nn\_CapBank.data***:  
Information related to switched capacitor banks (e.g. number of connected stages, KVAR of each stage) connected to node ***nn*** is included in this file.
- (f) ***node\_nn\_Load.data***:  
This file contains the load profile of node ***nn***, this load profile data is used to represent the readings acquired from the smart meters.

A set of the aforementioned files is created for each node in the distribution system, therefore each node has access to its own local information such as its parent ID/address, its children ID/address, line impedance to the parent and children, peak load value, load profile, and information pertaining to any connected devices.

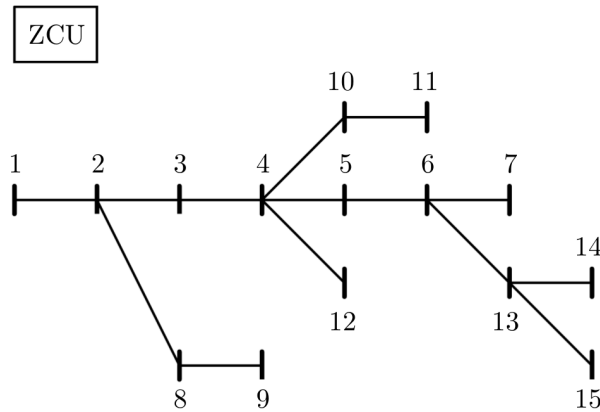


Figure 6.11: A 15-node radial distribution feeder

In this mode, updated versions of *DspfNode*, and *ZcuNode* can be transferred to the nodes over the WiFi network as well.

2. The Execution Mode (Operation Mode):

In this mode, the test bed, with its hardware and software components, executes the proposed distribution system analysis and control framework. Each individual node in the system utilizes the data provided during the preparation mode, communicate with its parent and children in order to perform power flow analysis, and to perform system control and coordination.

## 6.5 15-Node Distribution Feeder Results

A 15-node distribution feeder, shown in Figure 6.11, is employed in this section in order to examine the test bed implementation of the analysis and control framework. The line impedance, and the peak load values are given in Table 6.1. The base voltage is 23 kV, and the base power is 100 kVA. Five test cases are considered in this section:

### Test case 0:

In the preparation mode, the Octave-generated binary file corresponding to the 15-node distribution feeder as described in Table 6.1 is processed at the “MasterNode” in order to

Table 6.1: 15-node radial distribution system data

From node	To node	Impedance ( $\Omega$ )	Peak Load (MVA)
1	2	$0.5096 + j1.703$	$1.323 + j0.441$
2	3	$0.2191 + j0.0118$	$0.261 + j0.087$
2	8	$0.3485 + j0.3446$	0
8	9	$1.1750 + j1.0214$	$0.468 + j0.156$
3	4	$0.5639 + j0.5575$	$0.261 + j0.087$
4	5	$0.5530 + j0.4806$	0
4	12	$1.6625 + j0.9365$	$0.903 + j0.301$
4	10	$1.3506 + j0.76080$	0
10	11	$1.3506 + j0.7608$	$0.722 + j0.251$
5	6	$1.3259 + j0.7469$	$0.095 + j0.032$
6	7	$1.3259 + j0.74690$	0
6	13	$3.9707 + j2.2369$	$0.953 + j0.418$
13	14	$0.3432 + j0.3393$	$0.959 + j0.320$
13	15	$0.5728 + j0.4979$	$1.229 + j0.410$

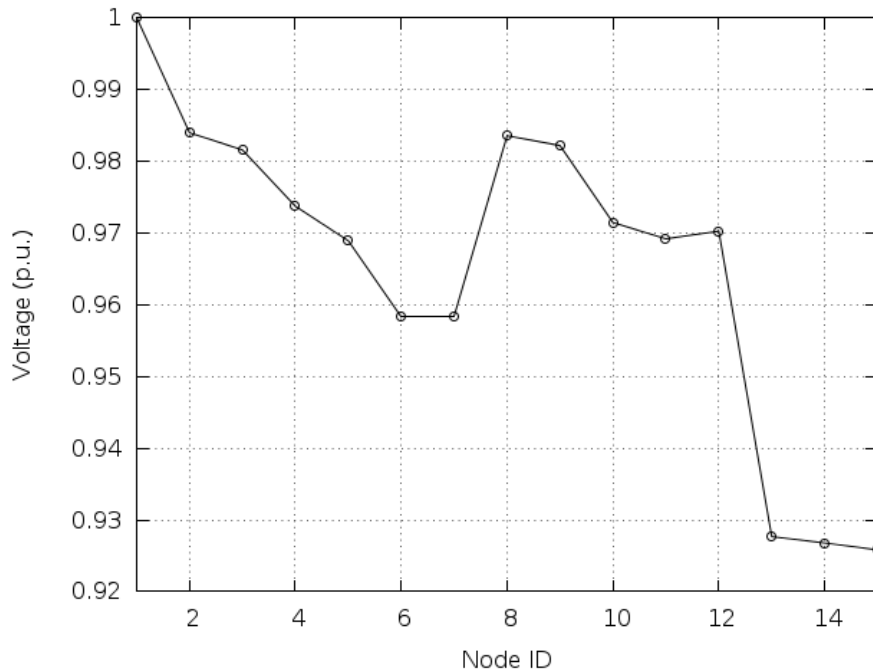


Figure 6.12: Voltage profile obtained through the collaboration of the 15 Raspberry PI nodes in the test bed for test case 0

generate the individual data files for each one of the 15 nodes in the system. These files are transferred to the respective nodes over the WiFi network.

In the execution mode, the analysis is triggered such that each node starts executing the analysis and control framework (*DspfaApp* C++ application running on each Raspberry PI node), utilizing the local information available, calculating its own voltage and current, and exchanging information with its parent and children.

In this test case, all the 15 Raspberry PI nodes in the test bed collaborate together such that each node calculates its own voltage, current, losses, and power flow. The voltage profile obtained through the node collaboration is shown in Figure 6.12, and the total system losses are 267.9 kW. The results obtained from the test bed are identical to those obtained from GNU-Octave simulations and from NS-3 simulations.

The 15 Raspberry PI nodes needed approximately 13 seconds to execute the distribution system analysis and obtain the voltage profile shown in Figure 6.12.



It is important to note the following:

1. This delay includes:

- (a) The time needed to process the data and execute the application *DspfaApp* running on the Raspberry PI node.
- (b) The WiFi communication network delays.

These two components of the delay are accumulated over the multiple iterations needed for the backward/forward sweep power flow analysis method to converge.

2. This delay is just for one run. To get the average execution time for this specific distribution system, the experiment must be run multiple times.

### Test case 1:

Starting from test case 0, three switched capacitor banks are installed at nodes 2, 5 and 13. Each capacitor bank has ten stages of 175 kVAR each.

The switched capacitor bank data is included in the preparation mode. Each node with a switched capacitor bank (i.e. nodes 2, 5 and 13) receives an additional data file describing the attached capacitor bank, its number of stages, the kVAR of each stage, etc. This information is utilized by the *DspfaNode* application running on each one of the nodes 2, 5 and 13 in order to execute the multiple switched capacitor bank control and coordination technique described in chapter 4, section 4.2.

In the execution mode, the analysis is triggered in the 15 Raspberry PI nodes such that they collaborate together to obtain a state for the three switched capacitor banks that reduce the total system losses.

Executing this test case resulted in a capacitor banks' state  $\alpha = [Q_2, Q_5, Q_{13}] = [1575, 525, 1225]$  kVAR, with a percentile rank of 99.925%, and the total system losses are 229.203 kW.

Table 6.2 shows the global optimal state (obtained from GNU-Octave exhaustive search) compared with the state obtained from the execution of the analysis and control framework on the test bed.

The execution of the analysis and control framework involves going through multiple intermediate iterations to achieve the final state given in Table 6.2, and the final voltage profile shown in Figure 6.13. Figure 6.14 shows the voltage profiles and the losses calculated during the intermediate iterations.

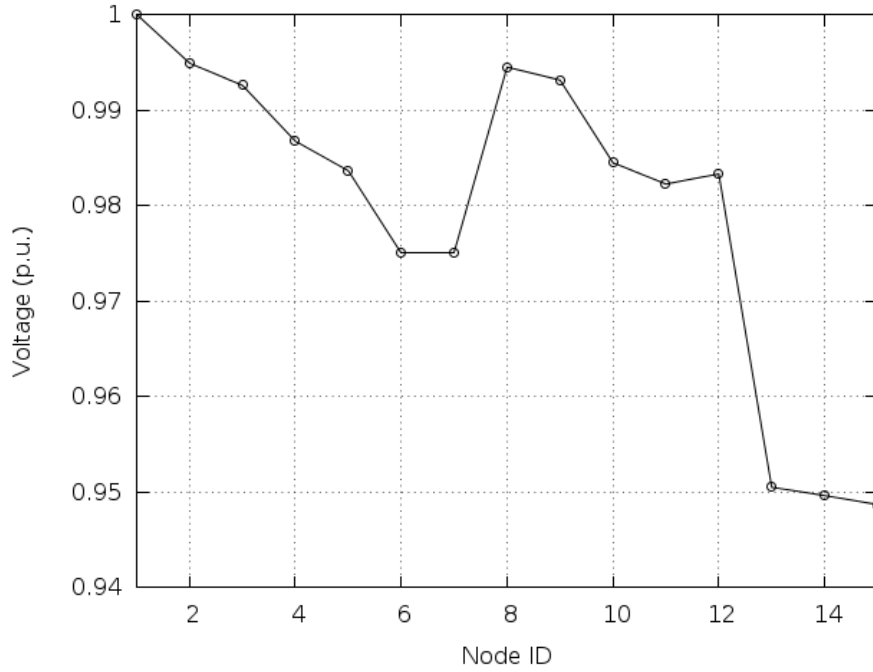


Figure 6.13: Voltage profile obtained through the collaboration of the 15 Raspberry PI nodes in the test bed for test case 1

Table 6.2: Optimal state vs. the state obtained from the test bed for the 15-node system with three switched capacitor banks (test case 1)

	Exhaustive Search Optimum State	Test Bed
$Q_2$ (kVAR)	1750	1575
$Q_5$ (kVAR)	525	525
$Q_{13}$ (kVAR)	1225	1225
Losses (kW)	229.190	229.203
Percentile Rank	—	99.925%
Convergence Time (minutes)	—	$\approx 3.8$

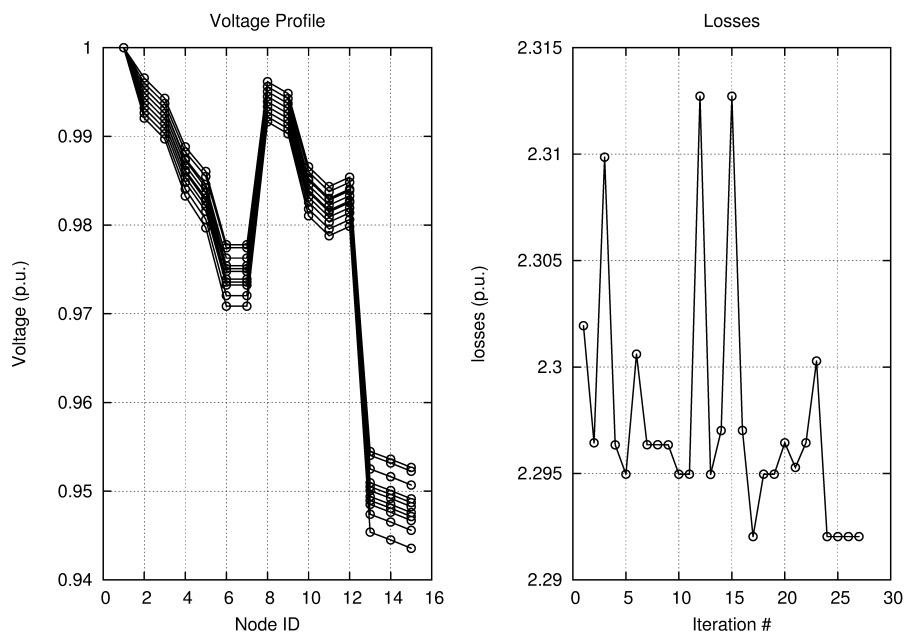


Figure 6.14: Voltage profiles and losses during the intermediate iterations for test case 1

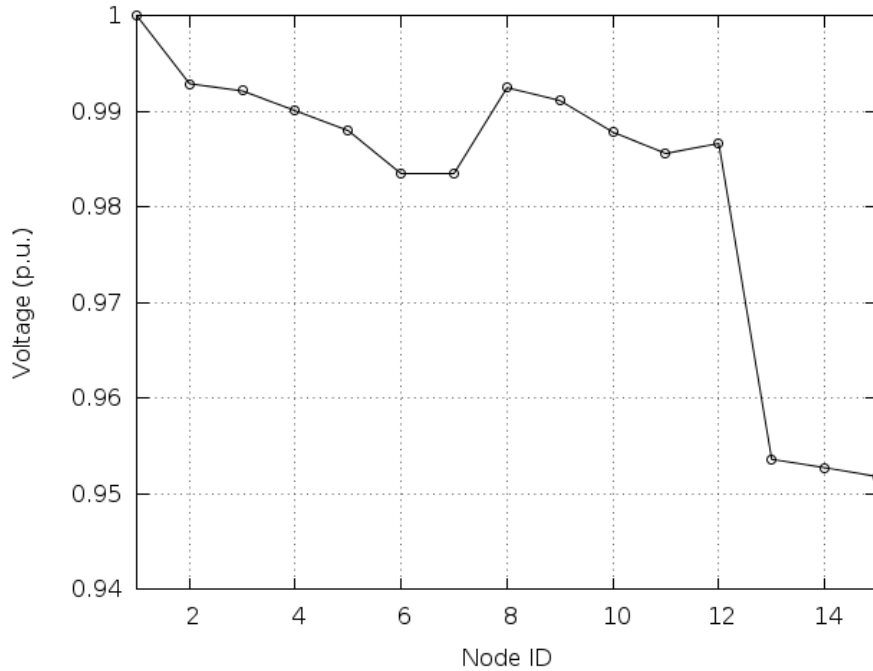


Figure 6.15: Voltage profile obtained through the collaboration of the 15 Raspberry PI nodes in the test bed for test case 2

### Test case 2:

Starting with the 15-node distribution system as described in test case 0, two DG units are installed at nodes 4 and 6 each with a rated power of 2 MVA.

In the preparation mode each node with a DG unit (i.e. nodes 4 and 6) receives an additional data file describing the data of the attached DG unit. This information is utilized by the *DspfANode* application running on each one of the nodes 4 and 6 in order to execute the multiple DG units control and coordination technique presented in chapter 4, section 4.3.

The analysis is triggered in the 15 Raspberry PI nodes in the execution mode to obtain a state for the two DG units in order to reduce the total system losses. The obtained state is  $\beta = [pf_4, pf_6] = [0.91, 0.95]$ , its percentile rank is 93.75%, and the total system losses are 128.44 kW.

Table 6.3: Optimal state vs. the state Obtained from the test bed for the 15-node system with two DG units (test case 2)

	Exhaustive Search Optimum State	Test Bed
$pf_4$	0.93	0.91
$pf_6$	0.93	0.95
Losses (kW)	128.31	128.44
Percentile Rank	—	93.75%
Convergence Time (minutes)	—	$\approx 3.5$

Table 6.3 compares the global optimal state (obtained from GNU-Octave exhaustive search) with the state obtained from the execution of the analysis and control framework on the test bed. Figure 6.16 shows the voltage profiles, and the losses calculated during the intermediate iterations encountered through the solution process before achieving the final state given in Table 6.3.

### Test case 3:

The three switched capacitors described in test case 1, and the two DG units described in test case 2 are added to the 15-node system. The “MasterNode” generate the individual data files, and move these files to the respective nodes over the WiFi network.

Figure 6.17 shows the voltage profile obtained from running test case 3 on the test bed. Table 6.18 compares the optimal state (obtained from GNU-Octave exhaustive search) with the state obtained from the test bed.

Figure 6.18 shows the voltage profiles and the system losses during the intermediate iterations.

### Test case 4:

The 15-node distribution system with three switched capacitor banks and two DG units described in test case 3 is used in this test case. The load level at each node in the

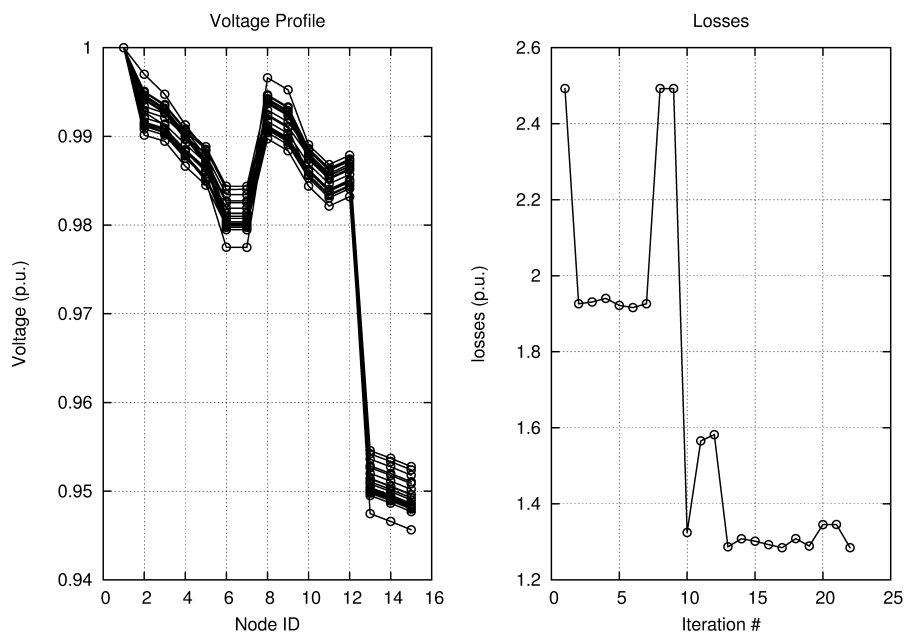


Figure 6.16: Voltage profile and losses during the intermediate iterations for test case 2

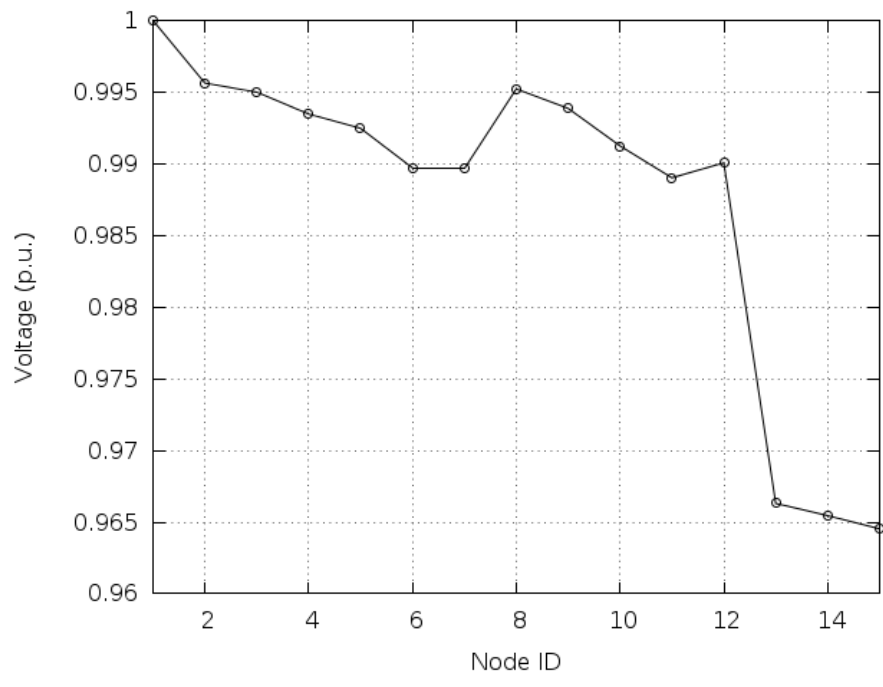


Figure 6.17: Voltage profile obtained through the collaboration of the 15 Raspberry PI nodes in the test bed for test case 3

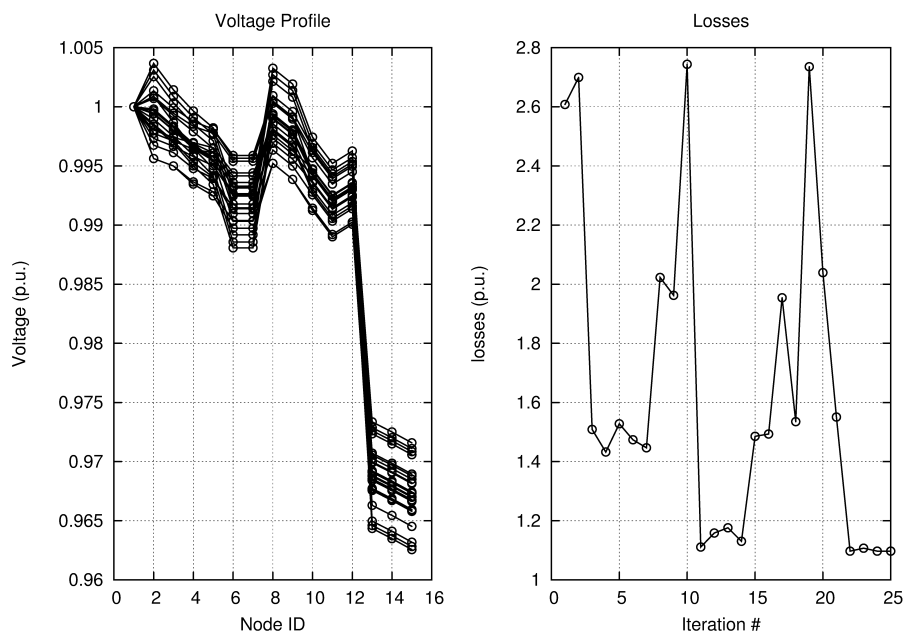


Figure 6.18: Voltage profile and losses during the intermediate iterations for test case 3



Table 6.4: Optimal state vs. the state obtained from the test bed for the 15-node system with three switched capacitor banks and two DG units (test case 3)

	Exhaustive Search Optimum State	Test Bed
$pf_4$	1	1
$pf_6$	1	0.99
$Q_2$ (kVAR)	1225	525
$Q_5$ (kVAR)	525	0
$Q_{13}$ (kVAR)	1225	1400
Losses (kW)	108.03	109.73
Percentile Rank	—	99.49%
Convergence Time (minutes)	—	$\approx 4$

distribution feeder is changed every hour in accordance with the load profile given in Figure 6.19 as a percentage of the peak load value. In the test bed implementation presented in this chapter, the hourly load values are used to represent the load information acquired from the smart meters.

Therefore, the load level at each node in the system changes every hour, and the test bed executes the analysis and control framework trying to select a state for all the switched capacitor banks and DG units that reduces the overall system losses based on the updated load values.

The voltage profiles and total system losses for each hour are shown in Figures 6.20 and 6.21 respectively.

As discussed previously, the analysis and control framework goes through multiple intermediate iterations before achieving the final state for each hour. Figures 6.22 and 6.23 show the voltage profiles and the total system losses for all the intermediate iterations for each hour of the 24 hour load profile.

This test case illustrates the ability of the analysis and control framework to utilize the information acquired from smart meters in order to control the distribution system.

The average execution time of the analysis and control framework (implemented on the test bed) for each one of the 24 load levels is approximately 3.7 minutes.

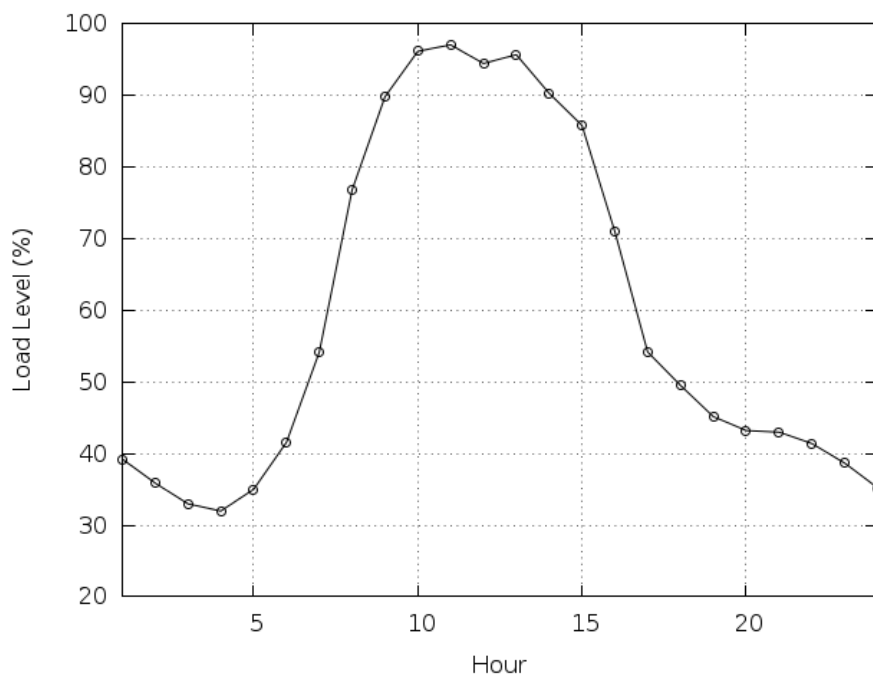


Figure 6.19: 24 Hour load profile

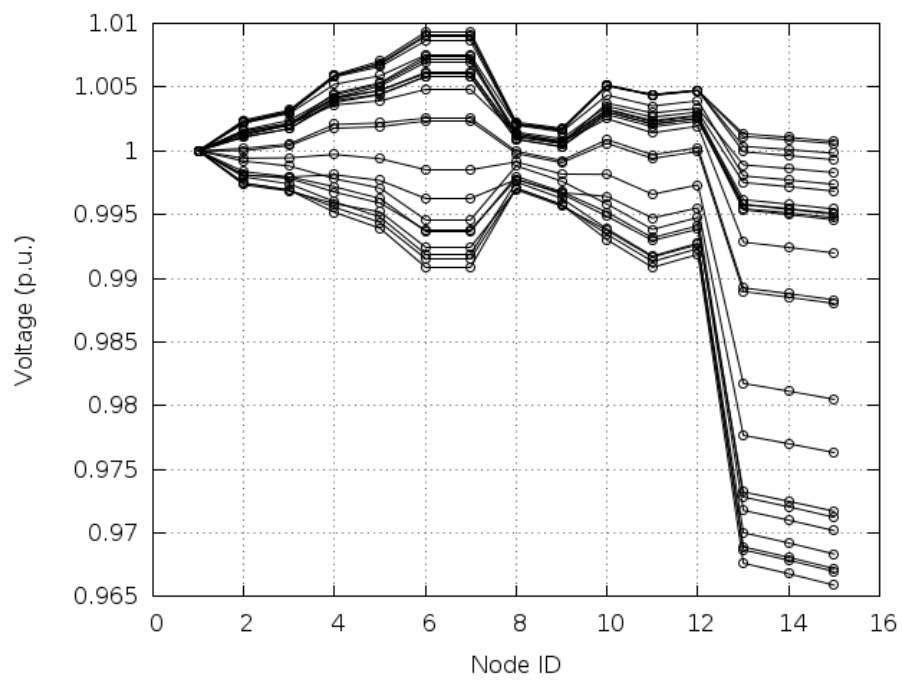


Figure 6.20: Voltage profiles for each hour of the 24-hour period investigated

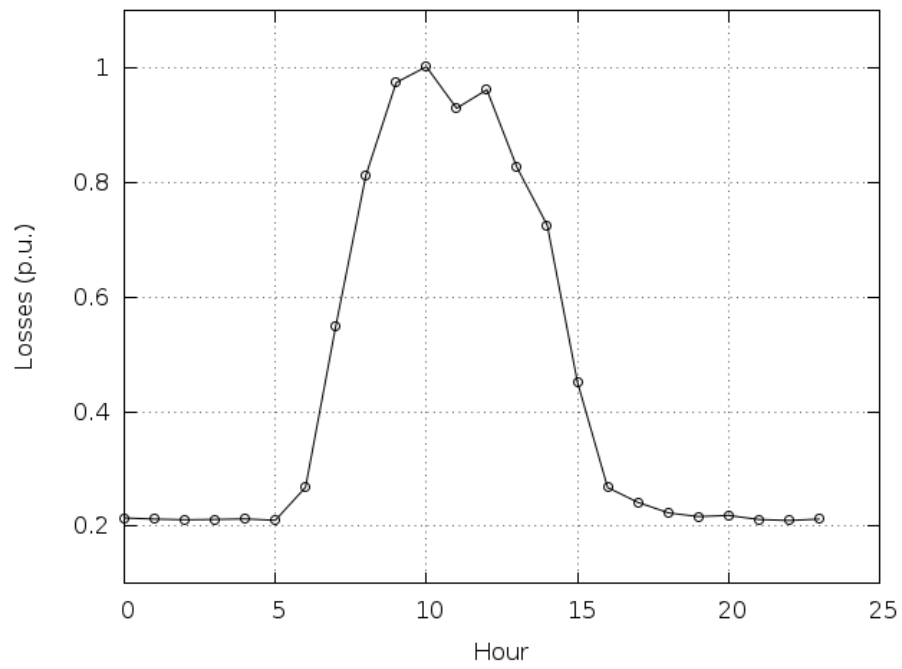


Figure 6.21: Total system losses for the 24-hour period investigated

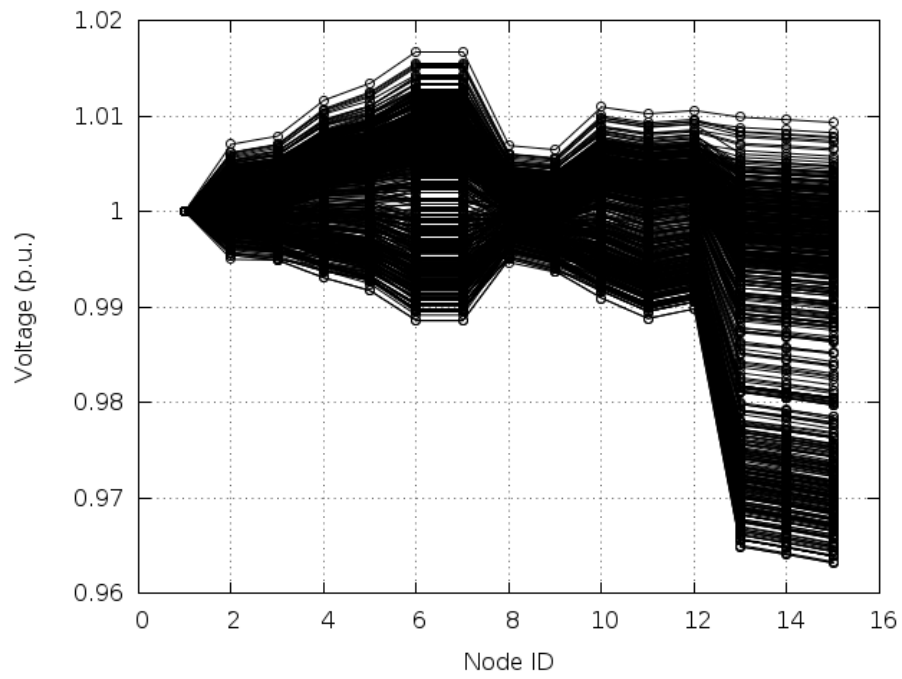


Figure 6.22: Voltage profiles for all intermediate iterations for the 24-hour period investigated

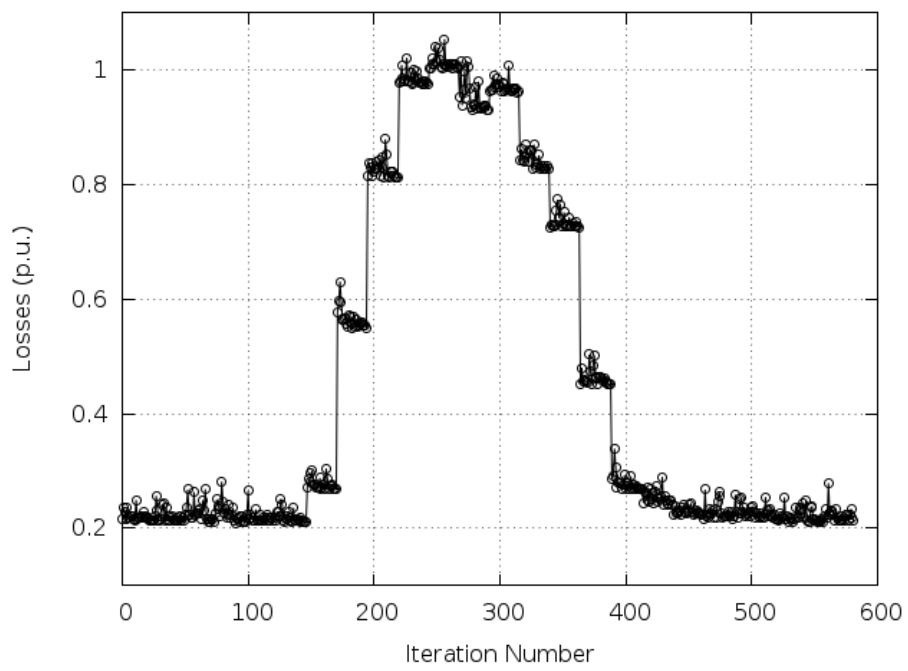


Figure 6.23: Total system losses for all intermediate iterations for the 24-hour period investigated

Figure 6.24 is a screen shot of the ZCU node showing the incoming connections from all the nodes in the system, while Figures 6.25 and 6.26 are another screen shots of the ZCU node showing a summary of all the connected nodes, and showing the end of the 24 load point analysis respectively.

A screen shot of the control logs of the capacitor bank at node 2 and the DG unit at node 4 are shown in Figures 6.27 and 6.28 respectively.

## 6.6 Conclusion

This chapter presents an experimental setup which is built and used as a test bed for the distribution system analysis and control framework. The hardware used to build the test bed includes 17 Raspberry PI computers equipped with WiFi network interface cards. The software running on each Raspberry PI computer is a C/C++ implementation of the analysis and control framework. Socket programming is used to provide the TCP data connectivity among the different Raspberry PI nodes.

Multiple test cases are used in this chapter to examine the test bed. The results are in close agreement to those obtained from GNU-Octave and NS-3 in terms of the voltage profiles, system losses, and the switched capacitor banks and DG units states.

In the last test case, the load level at each node is changed according to a 24-hour load profile. The test bed executes the analysis and control framework using the updated load values in order to reduce the total system losses. The 24-hour load profile is used to represent the load data acquired from smart meters.

The results obtained from the experimental setup clearly indicates that the framework proposed in this thesis can be implemented successfully in real systems.

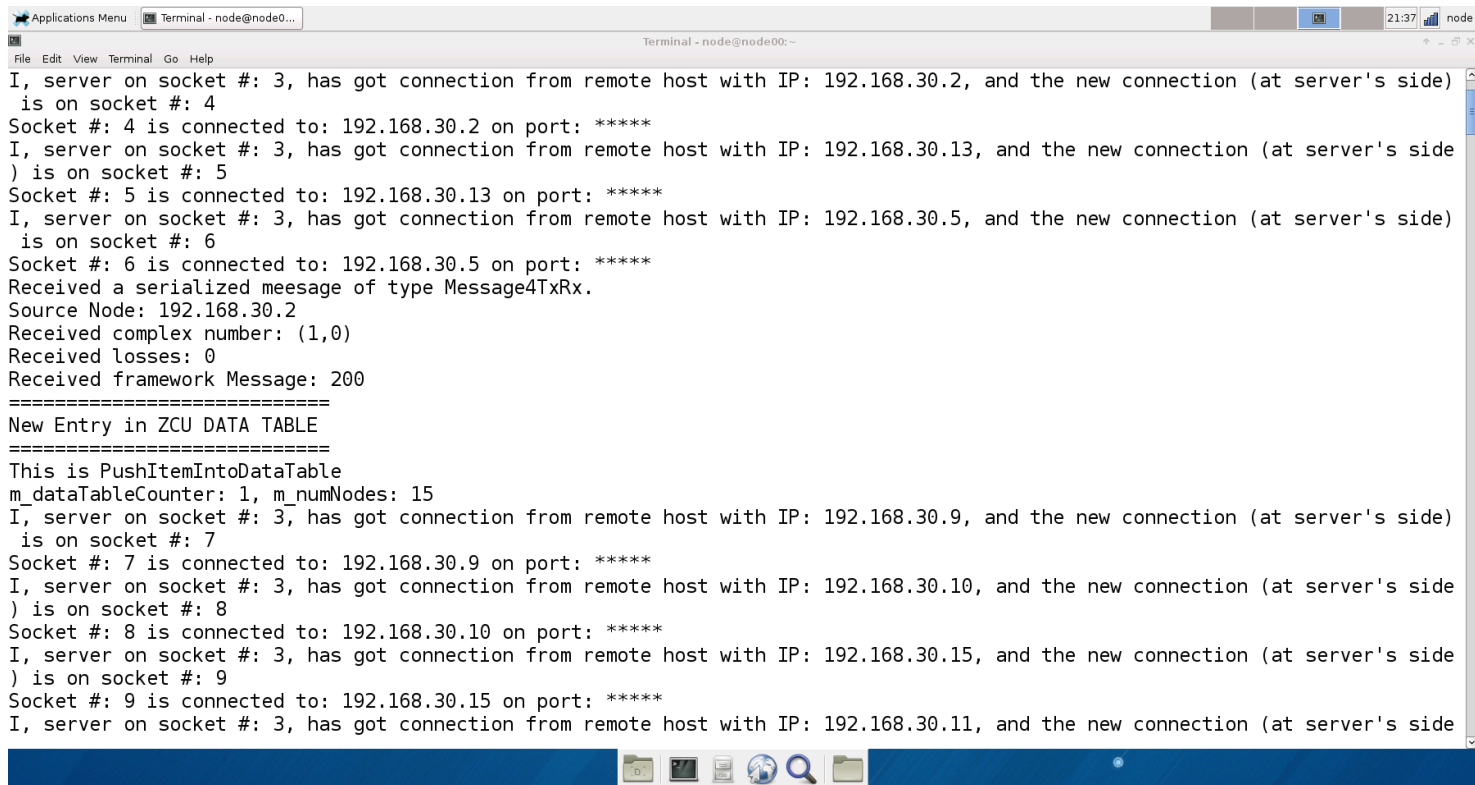
A terminal window titled 'Terminal - node@node00:~' showing a series of log messages. The messages indicate that a server on socket #3 is receiving connections from remote hosts with various IP addresses (192.168.30.2, 192.168.30.13, 192.168.30.5, 192.168.30.9, 192.168.30.10, 192.168.30.15, 192.168.30.11). Each connection is assigned a new socket number (4 through 9). The logs also show that a message of type 'Message4TxRx' was received from source node 192.168.30.2, with a complex number of (1,0) and 0 losses. A 'New Entry in ZCU DATA TABLE' is noted, with a counter of 1 and 15 nodes. The terminal window has a menu bar with 'File', 'Edit', 'View', 'Terminal', 'Go', and 'Help'. The system tray at the bottom shows icons for file manager, terminal, and search, along with the time 21:37 and the user 'node'.

Figure 6.24: Screen shot of the ZCU handling the incoming connections



The terminal window displays a table of connected nodes and subsequent log messages. The table has the following columns: Address, ID, Type, ConvFlag, PvConvFlag, DgConvFlag, and CapBankConvFlag. Below the table, there are three log entries, each starting with 'Received a serialized message of type Message4TxRx.' and followed by source node information, complex numbers, losses, and framework messages.

Address	ID	Type	ConvFlag	PvConvFlag	DgConvFlag	CapBankConvFlag
192.168.30.2	1	200	1	1	1	1
192.168.30.3	2	232	0	1	1	0
192.168.30.4	3	202	0	1	1	1
192.168.30.5	4	222	0	1	0	1
192.168.30.6	5	232	0	1	1	0
192.168.30.7	6	222	0	1	0	1
192.168.30.8	7	201	0	1	1	1
192.168.30.9	8	202	0	1	1	1
192.168.30.10	9	201	0	1	1	1
192.168.30.11	10	202	0	1	1	1
192.168.30.12	11	201	0	1	1	1
192.168.30.13	12	201	0	1	1	1
192.168.30.14	13	232	0	1	1	0
192.168.30.15	14	201	0	1	1	1
192.168.30.16	15	201	0	1	1	1

Received a serialized message of type Message4TxRx.  
Source Node: 192.168.30.3  
Received complex number: (0.99799,0.0047692)  
Received losses: 0.022857  
Received framework Message: 204  
Received a serialized message of type Message4TxRx.  
Source Node: 192.168.30.4  
Received complex number: (0.99875,0.0051204)  
Received losses: 0.017107  
Received framework Message: 204  
Received a serialized message of type Message4TxRx.  
Source Node: 192.168.30.9  
Received complex number: (0.99783,0.0046899)

Figure 6.25: Screen shot of the ZCU showing the connected nodes information

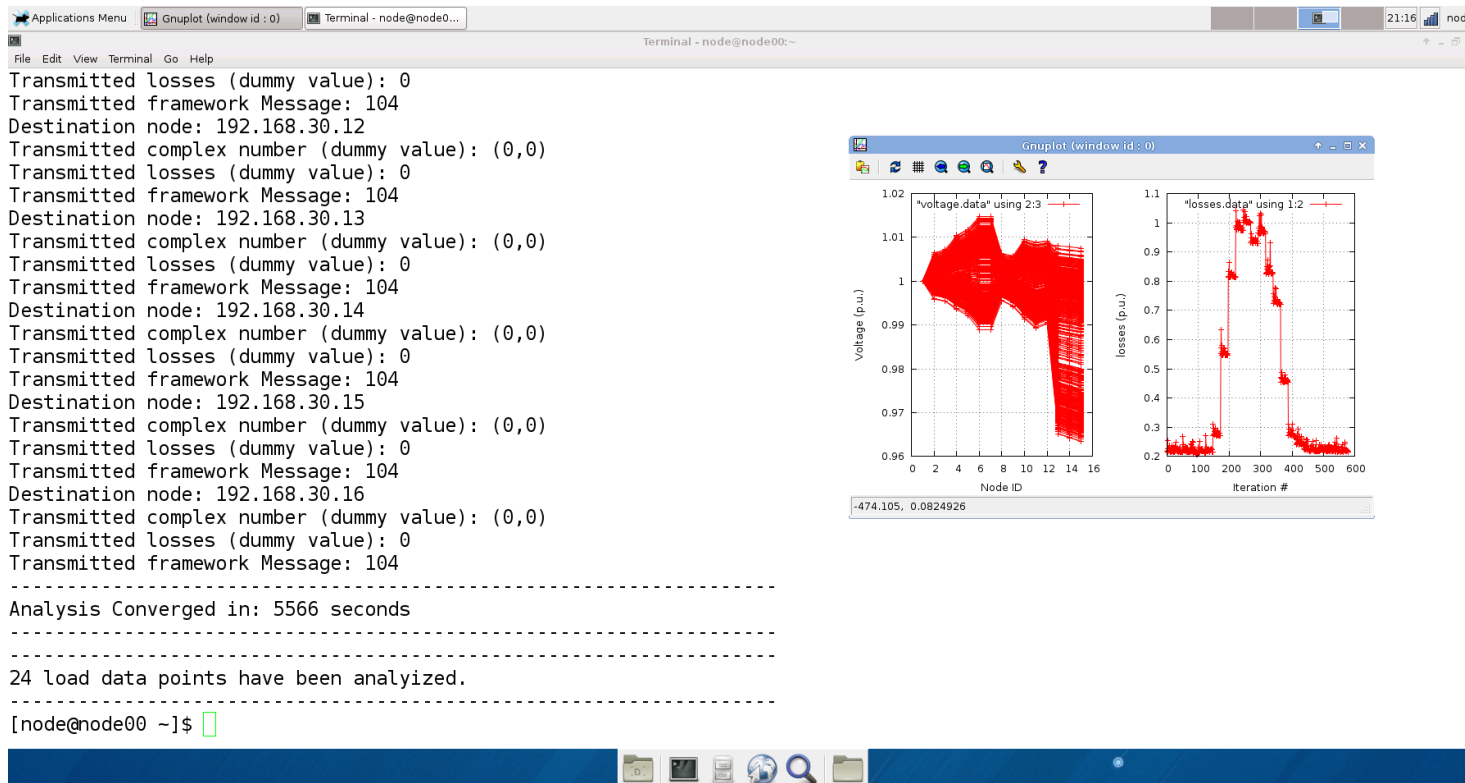


Figure 6.26: Screen shot of the ZCU showing the end of the analysis for the 24 load points

```
Applications Menu Terminal - node@node0... 19:56 node
Terminal - node@node02...
File Edit View Terminal Go Help
GNU nano 2.3.1 File: CapBankControlLog.data

CapBankControl - Mode 0
capBankSelector... 102
I am Node 192.168.30.3 with a capBank in Mode 0 and m_sCapBank will be (0,10.5) in the next iteration.
CapBankControl - Mode 0
capBankSelector... 102
I am Node 192.168.30.3 with a capBank in Mode 0 and m_sCapBank will be (0,0) in the next iteration.
CapBankControl - Mode 0
capBankSelector... 102
I am Node 192.168.30.3 with a capBank in Mode 0 and m_sCapBank will be (0,5.25) in the next iteration.
CapBankControl - Mode 0
capBankSelector... 102
I am Node 192.168.30.3 with a capBank in Mode 0 and m_sCapBank will be (0,5.25) in the next iteration.
CapBankControl - Mode 0
capBankSelector... 102
I am Node 192.168.30.3 with a capBank in Mode 0 and m_sCapBank will be (0,5.25) in the next iteration.
CapBankControl - Mode 0
capBankSelector... 105
I am Node 192.168.30.3 with a capBank in Mode 0 --> Mode 1 and m_sCapBank will be (0,7) in the next iteration
CapBankControl - MODE 1
GenerateRandomSign() returned ... 0
I am Node 192.168.30.3 with a capBank in Mode 1 --> Mode 2 and m_sCapBank will be (0,5.25) in the next iteration
CapBankControl - MODE 2
capBankSelector... 102
CapBankControl - MODE 2

[ Read 27191 lines ]
^G Get Help      ^O WriteOut     ^R Read File    ^Y Prev Page    ^K Cut Text     ^C Cur Pos
^X Exit          ^J Justify      ^W Where Is     ^V Next Page    ^U UnCut Text   ^T To Spell
```

Figure 6.27: Screen shot of node 2 showing a part of the capacitor bank control log

```
Applications Menu Terminal - node@node0... 19:59 node
Terminal - node@node04:~
File Edit View Terminal Go Help
GNU nano 2.3.1 File: DgMode2ControlLog.data

dgSelector: 102
DspfaApp::DgControl
DgControl - MODE 2
dgSelector: 102
DspfaApp::DgControl
DgControl - MODE 2
dgSelector: 105
+++++
m_dgData.pfVectorPtrHistory: 15
m_dgData.lossesVector: 0.216474
+++++
m_dgData.pfVectorPtrHistory: 11
m_dgData.lossesVector: 0.253096
+++++
GenerateRandomSign() returned ... -1
I am Node 192.168.30.5 with a DG in Mode 2 and m_dgData.pf will be 0.99 in the next iteration
DspfaApp::DgControl
DgControl - MODE 2
dgSelector: 102
DspfaApp::DgControl
DgControl - MODE 2
dgSelector: 102
DspfaApp::DgControl

^G Get Help      ^O WriteOut      ^R Read File     ^Y Prev Page     ^K Cut Text      ^C Cur Pos
^X Exit          ^J Justify       ^W Where Is     ^V Next Page     ^U UnCut Text    ^T To Spell
```

Figure 6.28: Screen shot of node 4 showing a part of the DG unit control log

# Chapter 7

## Conclusion and Future Work

This main purpose of the research presented in this thesis is to integrate distributed intelligence and wireless communication networks into the electrical power distribution system analysis and control.

This chapter summarizes the main ideas and concepts proposed in this thesis, provides some concluding remarks, and proposes some ideas and directions for the future work.

### 7.1 Summary and Conclusion

In this research, a novel approach to integrate distributed intelligence and wireless communication networks into the electrical power distribution system analysis and control is presented. We believe that this approach is one step toward the implementation of the smart grid notion in the distribution system.

As discussed in chapter 3, processing units with wireless communication transceivers are installed on each capacitor bank, DG unit, transformer, node with multiple children in the distribution system. These processing unit handle the information acquired from the Advanced Metering Infrastructure (AMI) in real-time, collaborate and exchange information with the neighboring nodes in order to perform distribution system analysis, the results of which are used to control and coordinate the different system components.

This proposed architecture of the analysis and control framework provides the following features:

1. The distribution system analysis is the base for all control actions, therefore resulting in a seamless coordination among the different system components. This also results in a unified framework where any system component can be included in the analysis and hence can be controlled accordingly without any conflicts with the other system components.
2. The AMI information is incorporated in the analysis and control framework as soon as they are acquired.
3. The system analysis and control is performed in a decentralized / distributed manner where each system component and each node contribute to the analysis and control calculations. So, having more nodes in the system means having more processing power.
4. Most of the processing units operate in parallel which can result in a scalable implementation of the framework.
5. The communication network is threaded into the distribution system analysis and control. Communication network helps the nodes to exchange information in order to reach a control decision rather than just transferring the final control decision.
6. The threading of communication network into the distribution system analysis and control results in a flexible framework because the distribution network topology is defined and maintained through the communication connectivity among the system nodes. Therefore, any change in system connectivity can be easily accounted for in the system analysis and control by simply changing the local information stored in each node such as the IP addresses of the parent and children.
7. Adding or removing components to the distribution system can be accommodated easily in the system analysis and control mainly due to the threading of the communication network and the distributed intelligence into the framework. This feature represents another side of the framework flexibility.
8. Based on the distribution system analysis, multiple control and coordination techniques can be integrated into the framework as presented in chapter 4.
9. The proposed analysis and control framework has the potential to be used to perform numerous tasks, one example is presented in chapter 5 where the proposed framework is used to perform Volt/VAR Control (VVC).

The proposed analysis and control framework represents an integrated design of power, communication and control systems. The performance of this framework is assessed throughout this thesis using three different approaches:

1. GNU-Octave simulations are used to evaluate the performance of the proposed analysis and control framework without the communication layer. The performance is evaluated in terms of the calculated losses, voltage profiles, and the optimality of the proposed control techniques. GNU-Octave simulation results are presented throughout the thesis in chapters 3, 4, and 5.
2. The network simulator NS-3 is used to simulate the proposed distribution system analysis and control framework along with the communication network supporting its operation. The framework is implemented as a set of C++ applications that are integrated into NS-3. Two wireless communication technologies are used in NS-3 simulations, namely WiMAX and LTE. The implementation details of the proposed framework for NS-3 is discussed in chapter 3, and the simulation results are presented in chapters 3, 4, and 5.
3. An experimental setup is created using 17 Raspberry PI computers equipped with WiFi interfaces in order to create a test bed that is used as a proof-of-concept for the proposed framework. chapter 6 discusses the hardware and software implementation of the test bed along with the results of some test cases.

It is important to emphasize that the term “real-time” is used in this thesis in the context of normal non-emergency operation of the distribution system where capacitors and OLTC transformers are switched few times per day therefore allowing enough time for the analysis and control framework to converge.

## 7.2 Future Work

The analysis and control framework presented in this thesis can be extended in order to accommodate new smart grid applications. For instance, the framework can be extended to control and operate microgrids which can be defined as a a controllable group of interconnected loads and DG units that connects and disconnects from the main grid to enable both grid-connected and island modes.

Some of the issues that can be included in the framework in order to accommodate the microgrid is the transition between the grid-connected and the islanded modes, the power

exchange between the microgrid and the main power grid in the grid-connected mode, and balancing the generated power from the DG units.

The increased level of DG installation complicates the system protection and requires dynamic coordination among the relays and circuit breakers, this is another possible extension of the research presented in this thesis is to include modules to operate and control the relays and circuit breakers in order to achieve a dynamic smart protection system.

Additional modules can be integrated into the proposed framework to enhance system reliability, reduce carbon emissions, or to manage the energy exchange among the customers with local generation, their neighbors, and the main power grid.



# APPENDICES



# Appendix A

## Random Search Algorithms

Random search algorithms are numerical techniques that work iteratively in order to find a minimum (or maximum) value of a function using some kind of randomness or probability in the definition of the algorithm.

Random search algorithms have been shown to have the potential to solve large-scale problems efficiently in a way that is not possible for deterministic optimization algorithms [105]. The authors of [106] report that using random search techniques require less time compared to using deterministic methods when applied to large problems. Another advantage of random search algorithms is that they are relatively easy to implement on complex problems [105].

Typically random search algorithms sacrifice a guarantee of optimality for finding a good solution quickly with high probability of being correct [105, 106]. Another disadvantage of these algorithms is that they need to be customized to each specific problem largely through trial and error [105].

### A.1 Generic Random Search

Random search techniques are used to obtain a solution for the general optimization problem defined as [105, 106, 107],

$$\min_{x \in S} f(x) \tag{A.1}$$

where  $x$  is a vector of  $n$  decision variables,  $S$  is an  $n$ -dimensional feasible region and assumed to be nonempty, and  $f$  is a real-valued function defined over  $S$ . The goal is to find a value for the vector  $x$  contained in the feasible region  $S$  that minimizes the function  $f$ .

Let the global optimal solution to this optimization problem be denoted by  $(x_*, y_*)$ , i.e.

$$x_* = \arg \min_{x \in S} f(x) \quad (\text{A.2})$$

and

$$y_* = f(x_*) = \min_{x \in S} f(x) \quad (\text{A.3})$$

The distribution system loss minimization problem presented in chapter 4, can be formulated in a similar manner where:

1. The problem dimensionality  $n$  is determined by the number of switched capacitor banks  $N_C$  as in section 4.2, the number of DG units  $N_{DG}$  as in section 4.3, or their sum  $N_C + N_{DG}$  as in section 4.7.
2. The  $n$ -dimensional decision variables vector  $x$  represents the capacitor banks tap settings ( $\alpha$ ) as discussed in section 4.2, the DG units power factors ( $\beta$ ) as discussed in section 4.3, or the combination of both as discussed in section 4.7.
3. The function  $f$  represents the total system losses obtained from the execution of the decentralized/distributed power flow analysis presented in chapter 3.
4. The  $n$ -dimensional feasible region  $S$  represents the set of all possible capacitor bank states, set of all possible DG units power factors, or the combination of both as illustrated in sections 4.2, 4.3, and 4.7 respectively.

The Volt/Var problem presented in chapter 5 can be formulated in the same manner with additional constraints on the maximum and minimum allowed voltage levels.

In Euclidean space the concept of neighborhood is typically defined by a ball of radius  $\delta$ ,  $\delta > 0$ , of points that are within a distance  $\delta$  of a point  $x \in S$  [106]. In the proposed control techniques in chapters 4 and 5 for switched capacitor banks, DG units, and OLTC

transformer, the feasible domain  $S$  is discrete <sup>1</sup> and the neighborhood of a vector  $x$  is defined through a list of the nearest neighbors. The proposed algorithms in chapters 4 and 5 select the next iterate from this list of the nearest neighbors.

A generic random search algorithm (called a sequential random search in [105]) can be described as follows [105, 106, 107]:

1. Initialize algorithm parameters and initial point  $X_0 \in S$  and set iteration index  $k = 0$ .
2. Generate a candidate point  $V_{k+1} \in S$  according to a specific generator.
3. Update the current point  $X_{k+1}$  based on the candidate point  $V_{k+1}$  and previous points.
4. If a stopping criteria is met, stop. Otherwise increment  $k$  and return to step 2.

Different methods can be used to initialize the random search algorithm, generate candidate points, update the current point, and terminate the algorithm.

### A.1.1 Generating Candidate Points

In pure random search the candidate points are generated by repeatedly sampling the feasible region  $S$ , typically according to a uniform sampling distribution.

Another common method to generate a candidate point is to use the current iterate  $X_k$  and take a step size in a vector direction [105, 106]. Step 2 of the algorithm can be expressed as

$$V_{k+1} = X_k + S_k D_k \tag{A.4}$$

where  $X_k$  is the current point,  $S_k$  is the step size, and  $D_k$  is the direction on iteration  $k$ .

---

<sup>1</sup>Switched capacitor banks and OLTC transformer has discrete tap positions. The DG power factor is allowed to change only in discrete steps  $\Delta pf$  between a maximum and minimum power factors,  $pf_{max}$  and  $pf_{min}$

The step size  $S_k$  can be either fixed or variable, and the direction  $D_k$  can be selected according to a uniform distribution on a hypersphere<sup>2</sup>[105, 106].

Among the different methods that can be used to select the step size and the direction, the proposed control algorithms in chapters 4, and 5 employ equation A.4 where the step size and the direction are selected using a uniform distribution among the nearest neighbors of the current iterate  $X_k$ .

### A.1.2 Updating the Current Iterate

There are two main approaches to updating the current iterate  $X_k$ , either to accept improving points only (known as strictly improving approach), or to accept non-improving points with a probability (e.g. as in simulated annealing) [105, 106].

The strictly improving approach can be expressed as follows

$$X_{k+1} = \begin{cases} V_{k+1} & \text{if } f(V_{k+1}) < f(X_k). \\ X_k & \text{otherwise.} \end{cases} \quad (\text{A.5})$$

The other approach accepts the candidate point  $V_{k+1}$  with a probability, the improving points are accepted with a probability one. For instance, in simulated annealing the candidate points are accepted with a probability that reflects a Boltzmann distribution [105, 106],

$$X_{k+1} = \begin{cases} V_{k+1} & \text{with probability } \min \left\{ 1, \exp \left( \frac{f(X_k) - f(V_{k+1})}{T_k} \right) \right\}. \\ X_k & \text{otherwise.} \end{cases} \quad (\text{A.6})$$

where  $T_k$  is the temperature parameter which can take different values for different iterations.

In the proposed control techniques in this thesis, the strictly improving approach is adopted to update the current iterate  $X_k$ .

---

<sup>2</sup>The  $n$ -hypersphere (often simply called the  $n$ -sphere) is a generalization of the circle and usual sphere to dimensions  $n \geq 4$ . The  $n$ -sphere is therefore defined as the set of  $n$ -tuples of points  $[x_1, x_2, \dots, x_n]$  such that  $x_1^2 + x_2^2 + \dots + x_n^2 = R^2$ , where  $R$  is the radius of the hypersphere.

### A.1.3 Stopping Criteria

The stopping criteria adopted in the proposed control algorithms in chapters 4, and 5 is to allow a maximum number of iterations  $N_{iter}$  as suggested in [107].

### A.1.4 Convergence in Probability

Multiple convergence proofs are reported in [105, 106] for general step size random algorithms with conditions on the generating the step length and direction. These conditions are simply that the method for generating the subsequent point does not consistently ignore any region.

Convergence means that, with probability one, the sequence  $f(X_k)$  converges to the global optimum as the iteration counter  $k$  tends towards infinity. This results in the anticipated trade-off between the probability of reaching the global optimum and the computational burden represented by the number of iterations.

The author of [106] also reports that using random search is often far more practical than running general algorithms until the mathematically proven stopping criteria are satisfied.

The performance of stochastic search algorithms is discussed in details in [105] and [107].





# References

- [1] Tropos Networks. Networking the smart grid. [http://www.tropos.com/pdf/whitepapers/SmartGridWP\\_A7.pdf](http://www.tropos.com/pdf/whitepapers/SmartGridWP_A7.pdf).
- [2] Z. Jiang, F. Li, W. Qiao, H. Sun, H. Wan, J. Wang, Y. Xia, Z. Xu, and P. Zhang. A vision of smart transmission grids. In *Power & Energy Society General Meeting, 2009. PES'09. IEEE*, pages 1–10. IEEE, 2009.
- [3] The Electricity Advisory Committee. Smart grid: Enabler of the new energy economy. <http://energy.gov/sites/prod/files/oeprod/DocumentsandMedia/final-smart-grid-report.pdf>, 2008.
- [4] GT Heydt. The next generation of power distribution systems. *Smart Grid, IEEE Transactions on*, 1(3):225–235, 2010.
- [5] S. Mohagheghi, M. Mousavi, J. Stoupiš, and Z. Wang. Modeling distribution automation system components using iec 61850. In *Power & Energy Society General Meeting, 2009. PES'09. IEEE*, pages 1–6. IEEE, 2009.
- [6] B. Saint. Rural distribution system planning using smart grid technologies. In *Rural Electric Power Conference, 2009. REPC'09. IEEE*, pages B3–B3. IEEE, 2009.
- [7] HE Brown and S. Suryanarayanan. A survey seeking a definition of a smart distribution system. In *North American Power Symposium (NAPS), 2009*, pages 1–7. IEEE.
- [8] H.A. Khan, Z. Xu, H. Iu, and V. Sreeram. Review of technologies and implementation strategies in the area of smart grid. In *Power Engineering Conference, 2009. AUPEC 2009. Australasian Universities*, pages 1–6. IEEE, 2009.

- [9] VK Sood, D. Fischer, JM Eklund, and T. Brown. Developing a communication infrastructure for the smart grid. In *Electrical Power & Energy Conference (EPEC), 2009 IEEE*, pages 1–7. Ieee, 2009.
- [10] T.A. Short. *Electric power distribution handbook*. CRC Press, 2004.
- [11] W.H. Kersting. *Distribution system modeling and analysis*. Electric power engineering series. CRC Press, 2002.
- [12] C-H Lo and Nirwan Ansari. Decentralized controls and communications for autonomous distribution networks in smart grid. 2013.
- [13] J. Northcote-Green and R. Wilson. *Control and automation of electric power distribution systems*. Power engineering. CRC/Taylor & Francis, 2006.
- [14] Anthony M Giacomoni, S Massoud Amin, and Bruce F Wollenberg. A control and communications architecture for a secure and reconfigurable power distribution system: An analysis and case study. In *IFAC World Congress*, 2011.
- [15] GNU Octave. <https://www.gnu.org/software/octave/>.
- [16] ns-3 project. <https://www.nsnam.org/>.
- [17] U.S. Department of Energy. The smart grid: An introduction. <http://energy.gov/oe/downloads/smart-grid-introduction-0>.
- [18] Michael Ibrahim and Magdy M. A. Salama. Smart distribution system volt-var control using distributed intelligence and wireless communication. Accepted for publication in the IET Generation, Transmission & Distribution Journal - Sept. 2014.
- [19] National Energy Technology Laboratory. Smart grid principal characteristic: Enables new products, services, and markets. [https://www.smartgrid.gov/sites/default/files/doc/files/Smart\\_Grid\\_Principal\\_Characteristics\\_Enables\\_New\\_Products\\_Se\\_201001.pdf](https://www.smartgrid.gov/sites/default/files/doc/files/Smart_Grid_Principal_Characteristics_Enables_New_Products_Se_201001.pdf), 2010.
- [20] National Energy Technology Laboratory. Smart grid principal characteristic: Provides power quality for the digital economy. [https://www.smartgrid.gov/sites/default/files/doc/files/Smart\\_Grid\\_Principal\\_Characteristics\\_Provides\\_Power\\_Quality\\_200906.pdf](https://www.smartgrid.gov/sites/default/files/doc/files/Smart_Grid_Principal_Characteristics_Provides_Power_Quality_200906.pdf), 2009.

- [21] National Energy Technology Laboratory. Smart grid principal characteristic: Optimized asset utilization and operate efficiently. [https://www.smartgrid.gov/sites/default/files/pdfs/optimizes\\_asset\\_utilization\\_and\\_operates\\_efficiently\\_10-2009.pdf](https://www.smartgrid.gov/sites/default/files/pdfs/optimizes_asset_utilization_and_operates_efficiently_10-2009.pdf), 2009.
- [22] National Energy Technology Laboratory. Smart grid principal characteristic: Anticipate and responds to system disturbances (self-heals). [https://www.smartgrid.gov/sites/default/files/pdfs/self\\_heals\\_final08312010.pdf](https://www.smartgrid.gov/sites/default/files/pdfs/self_heals_final08312010.pdf), 2010.
- [23] National Energy Technology Laboratory. Smart grid principal characteristic: Operate resiliently against attack and natural disaster. [https://www.smartgrid.gov/sites/default/files/pdfs/operates\\_resiliently\\_against\\_attack\\_and\\_natural\\_disaster\\_10-2009.pdf](https://www.smartgrid.gov/sites/default/files/pdfs/operates_resiliently_against_attack_and_natural_disaster_10-2009.pdf), 2009.
- [24] H. Shateri and S. Jamali. Load flow method for distribution networks with multiple source nodes. In *Electric Power Conference, 2008. EPEC 2008. IEEE Canada*, pages 1–5. IEEE.
- [25] S. Jamali and H. Shateri. Some trouble-making aspects of load flow analysis in distribution systems and their solutions. In *Electricity Distribution, 2005. CIREN 2005. 18th International Conference and Exhibition on*, pages 1–5. IET.
- [26] S. Khushalani and N. Schulz. Unbalanced distribution power flow with distributed generation. In *Transmission and Distribution Conference and Exhibition, 2005/2006 IEEE PES*, pages 301–306. IEEE, 2006.
- [27] WH Kersting. A method to teach the design and operation of a distribution system. *Power Apparatus and Systems, IEEE Transactions on*, (7):1945–1952, 1984.
- [28] GW Chang, SY Chu, and HL Wang. An improved backward/forward sweep load flow algorithm for radial distribution systems. *Power Systems, IEEE Transactions on*, 22(2):882–884, 2007.
- [29] RC Dugan, RF Arritt, TE McDermott, SM Brahma, and K. Schneider. Distribution system analysis to support the smart grid. In *Power and Energy Society General Meeting, 2010 IEEE*, pages 1–8. IEEE, 2010.
- [30] Nokhum Markushevich and Wenpeng Luan. Achieving greater vvo benefits through ami implementation. In *Power and Energy Society General Meeting, 2011 IEEE*, pages 1–7. IEEE, 2011.

- [31] PA Parikh and TD Nielsen. Transforming traditional geographic information system to support smart distribution systems. In *Power Systems Conference and Exposition, 2009. PSCE'09. IEEE/PES*, pages 1–4. IEEE, 2009.
- [32] S. Magazine. Challenges for smart distribution systems: Data representation and optimization objectives. In *2010 12th International Conference on Optimization of Electrical and Electronic Equipment (OPTIM)*, pages 1236–1244, 2010.
- [33] Q. LiJun, W. Ying, H. Cuijuan, and L. Meng. Multi-agent system wide area protection considering distributed generation impact. In *Advanced Power System Automation and Protection (APAP), 2011 International Conference on*, volume 1, pages 549–553. IEEE, 2011.
- [34] Mohamed E Elkhatib, RE Shatshat, and Magdy MA Salama. Decentralized reactive power control for advanced distribution automation systems. *Smart Grid, IEEE Transactions on*, 3(3):1482–1490, 2012.
- [35] G. Acampora, V. Loia, and A. Vitiello. Exploiting timed automata based fuzzy controllers for voltage regulation in smart grids. In *Fuzzy Systems (FUZZ), 2011 IEEE International Conference on*, pages 223–230. IEEE, 2011.
- [36] V. Loia and A. Vaccaro. A decentralized architecture for voltage regulation in smart grids. In *Industrial Electronics (ISIE), 2011 IEEE International Symposium on*, pages 1679–1684. IEEE, 2011.
- [37] S. Toma, T. Senjyu, Y. Miyazato, A. Yona, K. Tanaka, and C.H. Kim. Decentralized voltage control in distribution system using neural network. In *Power and Energy Conference, 2008. PECon 2008. IEEE 2nd International*, pages 1557–1562. IEEE, 2008.
- [38] C.H. Lin, H.J. Chuang, C.S. Chen, C.S. Li, and C.Y. Ho. Fault detection, isolation and restoration using a multiagent-based distribution automation system. In *Industrial Electronics and Applications, 2009. ICIEA 2009. 4th IEEE Conference on*, pages 2528–2533. IEEE.
- [39] T. Nagata and H. Sasaki. A multi-agent approach to power system restoration. *Power Systems, IEEE Transactions on*, 17(2):457–462, 2002.
- [40] I.S. Baxevanos and D.P. Labridis. Implementing multiagent systems technology for power distribution network control and protection management. *Power Delivery, IEEE Transactions on*, 22(1):433–443, 2007.

- [41] A. Saleem, K. Heussen, and M. Lind. Agent services for situation aware control of power systems with distributed generation. In *Power & Energy Society General Meeting, 2009. PES'09. IEEE*, pages 1–8. IEEE, 2009.
- [42] J. See, W. Carr, and S.E. Collier. Real time distribution analysis for electric utilities. In *Rural Electric Power Conference, 2008 IEEE*, pages B5–B5. IEEE, 2008.
- [43] D. Shirmohammadi, W.H.E. Liu, K.C. Lau, and H.W. Hong. Distribution automation system with real-time analysis tools. *Computer Applications in Power, IEEE*, 9(2):31–35, 1996.
- [44] N.I. Santoso and O.T. Tan. Neural-net based real-time control of capacitors installed on distribution systems. *Power Delivery, IEEE Transactions on*, 5(1):266–272, 1990.
- [45] T.I.I. Cadırcı, Y. Akkaya, S. Bilgen, and M. Ermis. Nationwide real-time monitoring system for electrical quantities and power quality of the electricity transmission system. 2011.
- [46] M. Kleinberg, K. Miu, and C. Nwankpa. A study of distribution power flow analysis using physically distributed processors. In *Power Systems Conference and Exposition, 2006. PSCE'06. 2006 IEEE PES*, pages 518–521. IEEE, 2006.
- [47] M. Kleinberg, K. Miu, and C. Nwankpa. Radial distribution power flow studies in a remotely distributed environment. In *Circuits and Systems, 2006. ISCAS 2006. Proceedings. 2006 IEEE International Symposium on*. IEEE, 2006.
- [48] M. Kleinberg, K. Miu, and C. Nwankpa. Network modeling for distributed simulations of unbalanced power systems. In *Proceedings of the 2007 summer computer simulation conference*. Society for Computer Simulation International, 2007.
- [49] M. Kleinberg and K. Miu. A study of distributed capacitor control for electric power distribution systems. In *North American Power Symposium (NAPS), 2011*, pages 1–6. IEEE, 2011.
- [50] Thomas Ackermann, Göran Andersson, and Lennart Söder. Distributed generation: a definition. *Electric power systems research*, 57(3):195–204, 2001.
- [51] Mohammad Shahidehpour and Yaoyu Wang. *Communication and control in electric power systems: applications of parallel and distributed processing*, chapter 11. John Wiley & Sons, 2004.

- [52] VH Méndez Quezada, J Rivier Abbad, and T Gomez San Roman. Assessment of energy distribution losses for increasing penetration of distributed generation. *Power Systems, IEEE Transactions on*, 21(2):533–540, 2006.
- [53] Konstantin Turitsyn, Petr Sulc, Scott Backhaus, and Michael Chertkov. Options for control of reactive power by distributed photovoltaic generators. *Proceedings of the IEEE*, 99(6):1063–1073, 2011.
- [54] Ferry A Viawan and Daniel Karlsson. Voltage and reactive power control in systems with synchronous machine-based distributed generation. *Power Delivery, IEEE Transactions on*, 23(2):1079–1087, 2008.
- [55] Alberto Borghetti, Mauro Bosetti, Samuele Grillo, Stefano Massucco, Carlo Alberto Nucci, Mario Paolone, and Federico Silvestro. Short-term scheduling and control of active distribution systems with high penetration of renewable resources. *Systems Journal, IEEE*, 4(3):313–322, 2010.
- [56] Mesut E Baran and Ismail M El-Markabi. A multiagent-based dispatching scheme for distributed generators for voltage support on distribution feeders. *Power Systems, IEEE Transactions on*, 22(1):52–59, 2007.
- [57] Luis F Ochoa, Andrew Keane, and Gareth P Harrison. Minimizing the reactive support for distributed generation: Enhanced passive operation and smart distribution networks. *Power Systems, IEEE Transactions on*, 26(4):2134–2142, 2011.
- [58] S Srikanth, Murugesu Pandian, and Xavier Fernando. Orthogonal frequency division multiple access in wimax and lte: a comparison. *Communications Magazine, IEEE*, 50(9):153–161, 2012.
- [59] Morris J Chang, Zakhia Abichar, and Chau-Yun Hsu. Wimax or lte: Who will lead the broadband mobile internet? *IT professional*, 12(3):26–32, 2010.
- [60] Zakhia Abichar, Yanlin Peng, and J Morris Chang. Wimax: The emergence of wireless broadband. *IT professional*, 8(4):44–48, 2006.
- [61] 3rd generation partnership project. <http://www.3gpp.org/>.
- [62] David Astély, Erik Dahlman, Anders Furuskar, Ylva Jading, Magnus Lindstrom, and Stefan Parkvall. Lte: the evolution of mobile broadband. *Communications Magazine, IEEE*, 47(4):44–51, 2009.

- [63] Jeffrey G Andrews, Arunabha Ghosh, and Rias Muhamed. *Fundamentals of WiMAX: understanding broadband wireless networking*. Pearson Education, 2007.
- [64] Leonhard Korowajczuk. *LTE, WiMAX and WLAN network design, optimization and performance analysis*. John Wiley & Sons, 2011.
- [65] Wimax forum. <http://www.wimaxforum.org/>.
- [66] Christopher Cox. *An introduction to LTE: LTE, LTE-advanced, SAE and 4G mobile communications*. John Wiley & Sons, 2012.
- [67] Maxime Pelcat, Slaheddine Aridhi, Jonathan Piat, and Jean-François Nezan. *Physical Layer Multi-Core Prototyping: A Dataflow-Based Approach for LTE eNodeB*, volume 171. Springer, 2012.
- [68] ns-3 project. ns-3 manual. <http://www.nsnam.org/docs/release/3.19/manual/ns-3-manual.pdf>.
- [69] ns-3 project. ns-3 tutorial - release ns-3.19. <https://www.nsnam.org/docs/release/3.19/tutorial/ns-3-tutorial.pdf>, 2013.
- [70] Oracle. Anatomy of the client/server model. [http://docs.oracle.com/cd/E13203\\_01/tuxedo/tux71/html/intbas3.htm](http://docs.oracle.com/cd/E13203_01/tuxedo/tux71/html/intbas3.htm).
- [71] Cisco. TCP/IP Overview. <http://www.cisco.com/c/en/us/support/docs/ip/routing-information-protocol-rip/13769-5.html#intro>.
- [72] Information Sciences Institute, University of Southern California. Transmission control protocol - darpa internet program - protocol specification. <http://www.ietf.org/rfc/rfc793.txt>.
- [73] Thomas F Herbert. *The Linux TCP/IP Stack: Networking for Embedded Systems*. Charles River Media, 2004.
- [74] H Shateri, M Ghorbani, AA Amjadi, and AH Mohammad-Khani. Load flow method for distribution networks with series voltage regulator. In *Universities Power Engineering Conference (UPEC), 2010 45th International*, pages 1–6. IEEE, 2010.
- [75] MMA Salama and AY Chikhani. A simplified network approach to the var control problem for radial distribution systems. *Power Delivery, IEEE Transactions on*, 8(3):1529–1535, 1993.

- [76] Mesut E Baran and Felix F Wu. Optimal capacitor placement on radial distribution systems. *Power Delivery, IEEE Transactions on*, 4(1):725–734, 1989.
- [77] Reza Khorram-Nia, Aliasghar Baziar, and Abdollah Kavousi-Fard. A novel stochastic framework for the optimal placement and sizing of distribution static compensator. *Journal of Intelligent Learning Systems & Applications*, 5(2), 2013.
- [78] M.E. Baran and F.F. Wu. Network reconfiguration in distribution systems for loss reduction and load balancing. *Power Delivery, IEEE Transactions on*, 4(2):1401–1407, 1989.
- [79] Masoud Aliakbar Golkar. Reactive power control in distribution systems by using advanced techniques. In *Energetics (IYCE), Proceedings of the 2011 3rd International Youth Conference on*, pages 1–6. IEEE, 2011.
- [80] Hannele Holttinen. Impact of hourly wind power variations on the system operation in the nordic countries. *Wind Energy*, 8(2):197–218, 2005.
- [81] Bob Uluski. Volt/var control and optimization concepts and issues. <http://cialab.ee.washington.edu/nwess/2012/talks/uluski.pdf>.
- [82] Bob Uluski. Integrated volt-var control. [http://wiki.powerdistributionresearch.com/images/f/f0/DATutorial08Chap5\\_SlidesRURRevised.pdf](http://wiki.powerdistributionresearch.com/images/f/f0/DATutorial08Chap5_SlidesRURRevised.pdf).
- [83] Y-Y Hsu and H-C Kuo. Dispatch of capacitors on distribution system using dynamic programming. In *IEE Proceedings C (Generation, Transmission and Distribution)*, volume 140, pages 433–438. IET, 1993.
- [84] YM Deng and XJ Ren. Optimal capacitor switching with fuzzy load model for radial distribution systems. *IEE Proceedings-Generation, Transmission and Distribution*, 150(2):190–194, 2003.
- [85] Jong-young Park, Soon-ryul Nam, and Jong-keun Park. Control of a ultc considering the dispatch schedule of capacitors in a distribution system. *Power Systems, IEEE Transactions on*, 22(2):755–761, 2007.
- [86] Hu Zechun, Wang Xifan, and Chen Haoyong. Time-interval based volt/var control in distribution systems. In *Power System Technology, 2002. Proceedings. PowerCon 2002. International Conference on*, volume 1, pages 81–85. IEEE, 2002.



- [87] Zechun Hu, Xifan Wang, Haozhong Chen, and GA Taylor. Volt/var control in distribution systems using a time-interval based approach. In *Generation, Transmission and Distribution, IEE Proceedings-*, volume 150, pages 548–554. IET, 2003.
- [88] A Ulinuha, M.A.S. Masoum, and S.M. Islam. Optimal dispatch of ltc and shunt capacitors in the presence of harmonics using genetic algorithms. In *Power Systems Conference and Exposition, 2006. PSCE'06. 2006 IEEE PES*, pages 733–740. IEEE, 2006.
- [89] S Auchariyamet and S Sirisumrannukul. Optimal dispatch of ultc and capacitors for volt/var control in distribution system with harmonic consideration by particle swarm approach. In *Sustainable Power Generation and Supply, 2009. SUPERGEN'09. International Conference on*, pages 1–7. IEEE, 2009.
- [90] S Auchariyamet and S Sirisumrannukul. Volt/var control in distribution systems by fuzzy multiobjective and particle swarm. In *Electrical Engineering/Electronics, Computer, Telecommunications and Information Technology, 2009. ECTI-CON 2009. 6th International Conference on*, volume 1, pages 234–237. IEEE, 2009.
- [91] MB Liu, Claudio A Cañizares, and W Huang. Reactive power and voltage control in distribution systems with limited switching operations. *Power Systems, IEEE Transactions on*, 24(2):889–899, 2009.
- [92] Sumit Paudyal, Claudio A Canizares, and Kankar Bhattacharya. Optimal operation of distribution feeders in smart grids. *Industrial Electronics, IEEE Transactions on*, 58(10):4495–4503, 2011.
- [93] William H Kersting. *Distribution system modeling and analysis*. CRC press, 2012.
- [94] Raspberry PI Foundation. <http://www.raspberrypi.org/>.
- [95] [http://en.wikipedia.org/wiki/Raspberry\\_Pi](http://en.wikipedia.org/wiki/Raspberry_Pi).
- [96] [http://elinux.org/RPi\\_Low-level\\_peripherals#I2C](http://elinux.org/RPi_Low-level_peripherals#I2C).
- [97] <http://www.raspbian.org/>.
- [98] <http://pidora.ca/>.
- [99] Geoff Friesen. *Beginning Java 7*. Springer, 2011.

- [100] Jan Graba and Jan Graba. *An Introduction to Network Programming with Java*. Springer, 2006.
- [101] Beej Jorgensen. Beej's guide to network programming, using internet sockets. [http://beej.us/guide/bgnet/output/print/bgnet\\_USLetter.pdf](http://beej.us/guide/bgnet/output/print/bgnet_USLetter.pdf).
- [102] David Mertz. Programming linux sockets, part 1: Using tcp/ip, creating an echo server and client. <https://www.ibm.com/developerworks/linux/tutorials/1-sock/1-sock-pdf.pdf>.
- [103] IBM. Example: Non-blocking i/o and select(). <https://publib.boulder.ibm.com/infocenter/iserics/v5r3/index.jsp?topic=%2Frzab6%2Frzab6xnnonblock.htm>.
- [104] select(2) - linux man page. <http://linux.die.net/man/2/select>.
- [105] Zelda B Zabinsky. *Stochastic adaptive search for global optimization*, volume 72. Springer, 2003.
- [106] Zelda B Zabinsky. Random search algorithms. *Wiley Encyclopedia of Operations Research and Management Science*, 2009.
- [107] Anatoly Zhigljavsky and Antanas Žilinskas. *Stochastic global optimization*. Springer, 2007.